

RO ADIOLOGY AND NCOLOGY



December 1999
Vol. 33 No. 4
Ljubljana

ISSN 1318-2099

Ω

*preprosto
neboleče*

*Napolnjene injekcijske brizge
za samoaplikacijo*

volumen (ml)	jakost (I.E.)
1	EPOMAX [™] 4000
0,5	EPOMAX [™] 2000
0,5	EPOMAX [™] 1000



EPOMAX[™]



EPOETIN OMEGA

lek
v sodelovanju z
Eplanar

Podrobnejše informacije o zdravilu dobite pri proizvajalcu.

RADIOLOGY AND ONCOLOGY



Editorial office

Radiology and Oncology

Institute of Oncology

Vrazov trg 4

SI-1000 Ljubljana

Slovenia

Phone: +386 61 1320 068

Phone/Fax: +386 61 1337 410

E-mail: gsera@onko-i.si

December 1999

Vol. 33 No. 4

Pages 257-329

ISSN 1318-2099

UDC 616-006

CODEN: RONCEM

Aims and scope

Radiology and Oncology is a journal devoted to publication of original contributions in diagnostic and interventional radiology, computerized tomography, ultrasound, magnetic resonance, nuclear medicine, radiotherapy, clinical and experimental oncology, radiobiology, radiophysics and radiation protection.

Editor-in-Chief

Gregor Serša

Ljubljana, Slovenia

Editor-in-Chief Emeritus

Tomaž Benulič

Ljubljana, Slovenia

Executive Editor

Viljem Kovač

Ljubljana, Slovenia

Editor

Uroš Smrdel

Ljubljana, Slovenia

Editorial board

Marija Auersperg

Ljubljana, Slovenia

Nada Bešenski

Zagreb, Croatia

Karl H. Bohuslavizki

Hamburg, Germany

Haris Boko

Zagreb, Croatia

Nataša V. Budihna

Ljubljana, Slovenia

Marjan Budihna

Ljubljana, Slovenia

Malte Clausen

Hamburg, Germany

Christoph Clemm

München, Germany

Mario Corsi

Udine, Italy

Christian Dittrich

Vienna, Austria

Ivan Drinković

Zagreb, Croatia

Gillian Duchesne

Melbourne, Australia

Béla Fornet

Budapest, Hungary

Tullio Giraldi

Trieste, Italy

Andrija Hebrang

Zagreb, Croatia

László Horváth

Pécs, Hungary

Berta Jereb

Ljubljana, Slovenia

Vladimir Jevtič

Ljubljana, Slovenia

H. Dieter Kogelnik

Salzburg, Austria

Jurij Lindtner

Ljubljana, Slovenia

Ivan Lovasić

Rijeka, Croatia

Marijan Lovrenčić

Zagreb, Croatia

Luka Milas

Houston, USA

Metka Milčinski

Ljubljana, Slovenia

Maja Osmak

Zagreb, Croatia

Branko Palčić

Vancouver, Canada

Jurica Papa

Zagreb, Croatia

Dušan Pavčnik

Portland, USA

Stojan Plesničar

Ljubljana, Slovenia

Ervin B. Podgoršak

Montreal, Canada

Jan C. Roos

Amsterdam, Netherlands

Slavko Šimunić

Zagreb, Croatia

Lojze Šmid

Ljubljana, Slovenia

Borut Štabuc

Ljubljana, Slovenia

Andrea Veronesi

Aviano, Italy

Živa Zupančič

Ljubljana, Slovenia

Publishers

*Slovenian Medical Association - Slovenian Association of Radiology, Nuclear Medicine Society,
Slovenian Society for Radiotherapy and Oncology, and Slovenian Cancer Society
Croatian Medical Association - Croatian Society of Radiology*

Affiliated with

*Societas Radiologorum Hungarorum
Friuli-Venezia Giulia regional groups of S.I.R.M.
(Italian Society of Medical Radiology)*

Copyright © Radiology and Oncology. All rights reserved.

Reader for English

*Olga Shrestha
Mojca Čakš*

Key words

Eva Klemenčič

Secretaries

*Milica Harisch
Betka Savski*

Design

Monika Fink-Serša

Printed by

Imprint d.o.o., Ljubljana, Slovenia

Published quarterly in 750 copies

Bank account number 50101 679 901608

Foreign currency account number

50100-620-133-900-27620-978-515266/6

NLB - Ljubljanska banka d.d. - Ljubljana

Subscription fee for institutions \$ 100 (16000 SIT), individuals \$ 50 (5000 SIT)

The publication of this journal is subsidized by the Ministry of Science and Technology of the Republic of Slovenia.

Indexed and abstracted by:

BIOMEDICINA SLOVENICA

CHEMICAL ABSTRACTS

EMBASE / Excerpta Medica

This journal is printed on acid-free paper

Radiology and Oncology is available on the internet at: <http://www.onko-i.si/radiolog/rno.htm>



CONTENTS

RADIOLOGY

- How reliable is classic chest radiography in the diagnosis of small pleural effusions**
Kocijančič I, Vidmar K 257

- Computer system for determination of hip joint contact stress distribution from antero-posterior pelvic radiograph**
Iglič A, Kralj-Iglič V 263

ULTRASOUND

- Ultrasound in diagnosis and treatment of anal fistulas**
Košorok P 267

COMPUTERIZED TOMOGRAPHY

- Acute subarachnoid haemorrhage: detection of aneurysms of intracranial arteries by computed tomographic angiography**
Milošević Z 275

NUCLEAR MEDICINE

- Indium-111-DTPA-octreotide scintigraphy in patients with carcinoid tumor**
Težak S, Ostojić R, Perković Z, Rustemović N, Car N, Papa B, Poropat M, Dodig D 283
-

ONCOLOGY

Adenocarcinoma skin metastases treated by electrochemotherapy with cisplatin combined with radiation

Serša G, Čemažar M, Rudolf Z, Fras AP

291

Reorganization of microtubules in V-79 cells after treatment with cytohalasin B

Iglič A, Batista U, Veranič P

297

Comparison of colorimetric MTT and clonogenic assays for irradiation and cisplatin treatment on murine fibrosarcoma SA-1 cells

Čemažar M, Marolt D, Lavrič M, Serša G

303

RADIOPHYSICS

Comparison of four models for calculation of collimator scatter factors of linac photon beams

Faj D, Bistrovic M

309

SLOVENIAN ABSTRACTS

315

NOTICES

321

REVIEWERS IN 1999

325

AUTHOR INDEX 1999

325

SUBJECT INDEX 1999

328

How reliable is classic chest radiography in the diagnosis of small pleural effusions

Igor Kocijančič¹, Ksenija Vidmar²

¹Department of Radiology, Institute of Oncology Ljubljana, Slovenia

²Institute of Radiology, Clinical Centre, Ljubljana, Slovenia

Purpose. To evaluate the usefulness of expirium lateral decubitus views in the radiological diagnosis of small pleural effusions.

Materials and methods. Patients referred to abdominal sonography for different reasons were routinely checked for possible pleural effusion. From November 1994 till May 1996, 36 such patients were found to have pleural effusion not exceeding 15 mm and were included in the study. Patients were examined radiologically in erect PA and lateral projections and, after 5 min. in decubitus position, in inspiratory - expiratory lateral decubitus projections with 10° hip elevation and central beam on the lateral chest wall.

Results. In 22 out of 36 patients (61%), the pleural fluid was not visible on erect PA and lateral chest radiogram. However, the fluid was visible in 35/36 patients (97%) in expirium from lateral decubitus view. The average thickness of fluid from lateral decubitus views in inspirium and expirium was 4.3 and 7.9 mm, respectively. In 31 out of 36 patients (86%), the thickness of the fluid layer as measured in expirium and inspirium was different. In 16%, the fluid was not visible on inspirium lateral decubitus projections.

Conclusions. Radiography turned out to be almost as sensitive as sonography in detection of small pleural effusions. Lateral decubitus views taken in expirium contributed essentially to the diagnostic sensitivity in our study.

Key words: pleural effusion-radiology; thoracic radiography-methods; diagnosis

Introduction

A small pleural effusion may be an important finding, sometimes leading, via thoraco-

Received 19 October 1999

Accepted 18 November 1999

Correspondence to: Igor Kocijančič, MD, MSc, Department of Radiology, Institute of Oncology, Zaloška 2, SI - 1000 Ljubljana, Slovenia. Phone: + 386 61 13 21 195, Fax: + 386 61 13 14 180, E-mail: rtg@onko-i.si

centesis, to a definitive diagnosis of pleural carcinomatosis, infection or transudate. The data on the smallest detectable amount of pleural fluid vary considerably, but they are essentially within the same range whether CT, sonography or X-ray examination are used.¹⁻¹³

Rigler¹⁴ was the first to use lateral decubitus views for radiological diagnosis of small pleural effusions. Others^{1,3,15}, who further

developed the technique, detected, working on cadavers,¹ as small amounts as 5 ml of pleural fluid.

No valid comparison has been made between the thickness of the pleural effusion, as seen on X-ray or sonography, and the amount of aspirated fluid. A small amount of fluid (5-10 ml) is often present in the pleural space of a healthy person.² There is probably some residual fluid after thoracocentesis. These two circumstances would, in our view, severely limit the reliability of „exact“ quantitative studies of small pleural effusions. We have therefore tried to assess the clinical usefulness of the method.

The aim of our study was to assess:

- whether lateral decubitus views are really more effective in detecting small pleural effusions than erect PA and lateral projections only;
- and, more important, whether the use of inspiratory-expiratory views can further improve the results.

Patients and methods

Patients, referred to abdominal sonography for different reasons, were routinely checked for possible unsuspected pleural effusion.

From November 1994 till May 1996 thirty-six such patients, in whom the thickness of the pleural effusion in sonography did not exceed 15 mm, were included into the study. Of these 36 patients, 27 were males and 9 females, their age ranging between 28 - 80 years, with a mean age of 54.8 years.

Their condition was clinically diagnosed as:

Lung cancer	14
Metastasis to the lung	6
Pulmonary TB	5
Cardiac failure	4
Systemic connective tissue disease	4
Liver cirrhosis	2
Chest trauma	1

Abdominal sonography was performed first. The patient was then put for 5 minutes into lateral decubitus position. Then the sonography of the lower pleural space, followed, first, with the patient leaning on his/her elbow, and second, in a sitting position. It was performed by a Toshiba SAL 38-B ultrasound unit with a 5 MHz large radius convex transducer. The findings were recorded on Polaroid films.

Radiological examination was performed only if sonography had shown any small pleural effusion. Erect PA and lateral projections were obtained for other indications. Written consent was obtained from the patients for additional, simultaneous lateral decubitus views.

A 140 kV Siemens unit was used, with 2 m F-F distance for the erect views of the chest, and 1.5 m F-F distance for lateral decubitus views. For these, the patient was put into lateral decubitus position for 5 minutes, with 10 deg. hip elevation. Exposures were taken in both, inspirium and expirium, with the central beam aimed at the lateral chest wall and the patient slightly rotated onto his/her back. An experienced radiologist was always present at the examination. The films were evaluated independently by two experienced radiologists with no previous knowledge of findings.

The criteria for determining the presence of pleural fluid were:

Sonography^{8,16-18}

- a non-echogenic zone between the parietal and the visceral pleura, changing between expirium and inspirium as well as changing with different positions of the patient,
 - fluttering of the pulmonary edge during respiration,
 - moving hyperechogenic particles within the fluid.
- X ray^{3,19}
- from a lateral decubitus view, the minimum thickness of the horizontal fluid layer should be 3 mm,

- costophrenic angle density with meniscus sign on erect views.

Matching pairs T-test was used for the analysis of differences in measurements on the same individual.

Results

In 22 out of 36 patients (61%) the pleural fluid was not visible on erect PA and lateral chest radiogram.

The average thickness of the visible fluid on lateral decubitus views was 4.3 mm in inspirium and 7.9 mm in expirium, the difference of 3.6 mm being statistically significant ($p < 0,005$).

In 6 out of 36 patients (16%), the fluid was not visible from lateral decubitus views in inspirium. In 5 of these, the fluid level was visible in expirium, its thickness being 4 - 8 mm (Table 1). In one patient, the fluid was only visible on sonography, proved by thoracocentesis.

In 31 out of 36 patients (86%), there was a difference in the thickness of the fluid layer as measured in expirium and inspirium from lateral decubitus views.

In 5 patients (14%), the layer was unchanged in inspirium and expirium.

Discussion and conclusions

Rigler¹⁴ was the first to use lateral decubitus views for the demonstration of pleural fluid. He did not use exposure in expirium, nor did he aim the central beam at the lateral chest wall, parallel to the expected fluid level. The latter technical improvement was introduced by Hessen³ together with the elevation of the patient's hip, while the exposure in expirium is mentioned in the work of Müller and Löfstedt¹⁵ but apparently without gaining wider acceptance.

Table 1. Thickness of pleural fluid layer on lateral decubitus views

Thickness of fluid	Number of patients in	
	inspirium	expirium
0 mm	6 (16%)	1 (3%)
3-5 mm	17 (48%)	8 (22%)
6-10 mm	12 (33%)	18 (50%)
11-15 mm	1 (3%)	9 (25%)

The amounts of pleural fluid detectable this way were assessed in cadaver experiments¹ and were as little as 5 ml in experimental conditions. This is probably less reliable in practice due to the unaccurate results of thoracocentesis.

With the advent of sonography it was shown that very small amounts of pleural fluid can be demonstrated this way.⁴⁻⁸

In the literature, we couldn't find any exact quantitative definition of small pleural effusions. So, our term of small pleural effusions includes clinically silent effusions which are usually unexpected findings on X-ray and/or sonography examinations for different reasons.

In the course of our study we have achieved comparable results using sonography and radiography. Interestingly, the main sign, allowing the demonstration of the smallest effusions, was similar in both modalities: the changing of the fluid layer during inspirium - expirium.

Obviously, a thicker fluid level, as is more often seen in expiratory views, would tend to facilitate the diagnosis (Figure 1, 2). Another advantage of using this criterion was our increased ability to recognise artefacts such as skin folds, sheets, subcutaneous fat and the like.

Since both sonography and „classical“ radiography seem to be sensitive methods for demonstrating small pleural effusions, there should not be any overwhelming reason to use CT as the first choice for this purpose, especially since the results of CT do not seem superior in this respect.^{9,13,20}

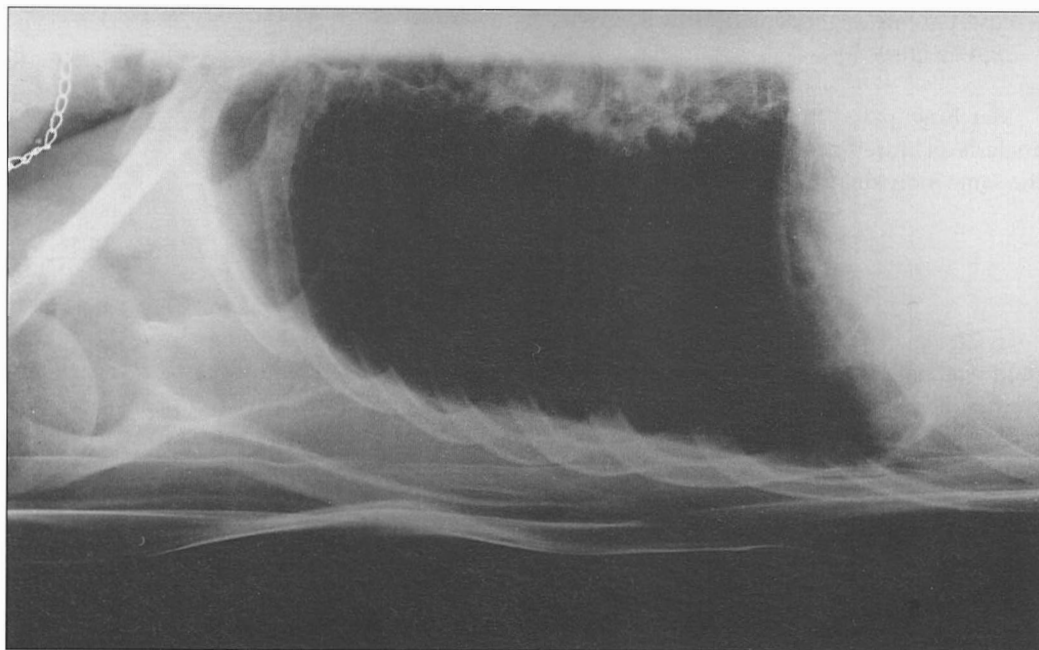


Figure 1. Inspiratory lateral decubitus projection showing about 5 mm wide layer of pleural fluid in 30 years old male patient with TBC pleuritis.

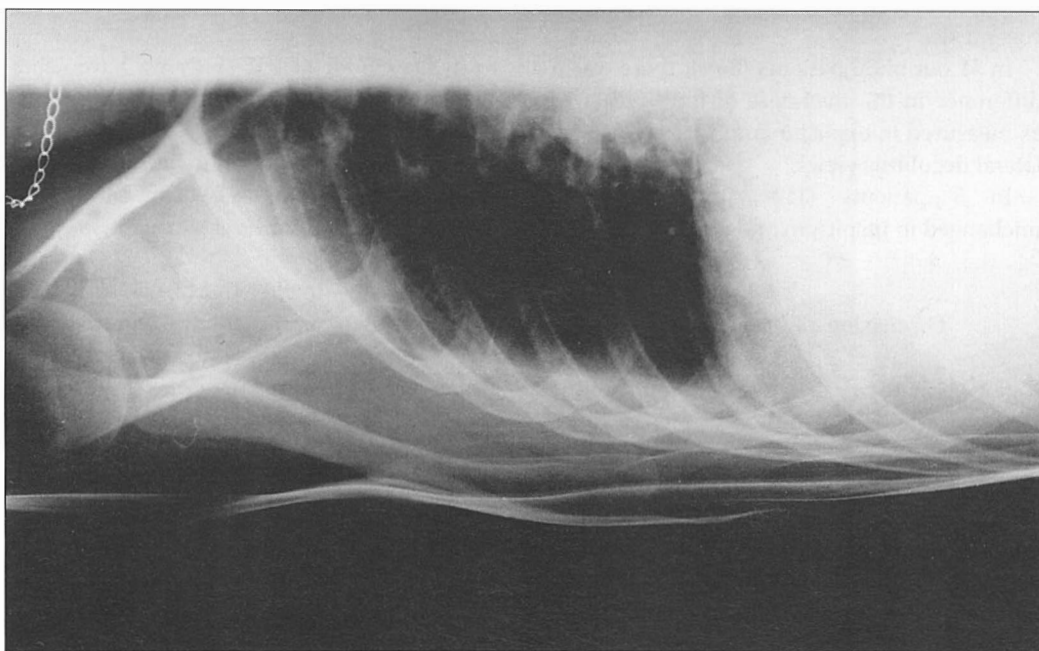


Figure 2. Expiratory lateral decubitus projection in the same patient showing much thicker fluid level (about one cm), which tends to facilitate the diagnosis.

For satisfactory results, meticulous adherence to the technique described may be an advantage. Lateral decubitus views taken in expirium contributed essentially to the diagnostic sensitivity of radiological examination in our study.

Reference

1. Moskowitz H, Platt RT, Schachar R, Mellus H. Roentgen visualization of minute pleural effusion. *Radiology* 1973; **109**: 33-5.
2. Felson B. *Chest rentgenology*. Philadelphia: W.B. Saunders; 1973. p. 352.
3. Hessen I. Roentgen examination of pleural fluid. A study of the localisation of free effusions, the potentialities of diagnosing minimal quantities of fluid and its existence under physiological conditions. *Acta Radiol* 1951; **86 Suppl 1**: 1-80.
4. Grymiski J, Krakowa P, Lypacewicz G. The diagnosis of pleural effusion by ultrasonic and radiologic techniques. *Chest* 1976; **70**: 33-7.
5. Lipscomb DJ, Flower CDR. Ultrasound in the diagnosis and management of pleural disease. *Br J Dis Chest* 1980; **74**: 353-61.
6. Von Eibenberger K, Dock W, Metz V, Weinstabl C, Haslinger B, Grabenwöger F. Wertigkeit der thorax bettaufnahmen zur diagnostik und quantifizierung von pleuraergüssen - überprüfung mittels sonographie. *RöFo* 1991; **155**: 323-6.
7. Lorenz J, Börner N, Nikolaus HP. Sonographische volumetrie von pleuraergüssen. *Ultraschall* 1988; **9**: 212-5.
8. Mathis G. *Lungen und pleurasonographie*. Berlin: Springer - Verlag; 1992. p. 11.
9. Mc Loud TC, Flower CDR. Imaging of the pleura: Sonography, CT and MR imaging. *AJR* 1991; **156**: 1145-53.
10. Mikloweit P, Zachgo W, Lörcher U, Meier-Sydow J. Pleuranage lungenprozesse: diagnostische wertigkeit sonographie versus CT. *Bildgebung* 1991; **58**: 127-31.
11. Leung AN, Muller NL, Miller RR. CT in the differential diagnosis of pleural disease. *AJR* 1990; **154**: 487-92.
12. Maffesanti M, Tommasi M, Pellegrini P. Computed tomography of free pleural effusions. *Eur J Radiol* 1987; **7**: 87-90.
13. Flower CDR. CT and ultrasound in the management of pleural disease. In: The Fleischner Society, editor. 21st annual symposium on chest disease, 1991 May 23-25; Interlaken, Switzerland, 1991. p. 445-8.
14. Rigler LG. Roentgen diagnosis of small pleural effusions. *JAMA* 1931; **96**: 104-8.
15. Müller R, Löfstedt S. Reaction of pleura in primary tuberculosis of the lungs. *Acta Med Scand* 1945; **122**: 105-33.
16. Targhetta R, Bourgeois JM, Marty-Double C, et al. Vers une autre approche du diagnostic des masses pulmonaires périphériques. *J Radiol* 1992; **73**: 159-64.
17. Marks WM, Filly RA, Callen PW. Real-time evaluation of pleural lesions: New observations regarding the probability of obtaining free fluid. *Radiology* 1982; **142**: 163-4.
18. Brant WE. US of the thorax. In: Rumack CM, Wilson SR, Charboneau JW, editors. *Diagnostic ultrasound*. St. Louis: Mosby-Year Book; 1991. p. 413-28.
19. Raasch BN, Carsky EW, Lane EJ, O'Callaghan JP, Heitzman ER. Pleural effusion: Explanation of some typical appearances. *AJR* 1982; **139**: 889-904.
20. Stark P. The pleura. In: Taveras JM, Ferrucci JT, editors. *Radiology, diagnosis, imaging, intervention*. Philadelphia: J.B. Lippincott comp.; 1995. Chapter 80. p. 3.

Computer system for determination of hip joint contact stress distribution from antero-posterior pelvic radiograph

Aleš Iglič¹ and Veronika Kralj-Iglič²

¹Laboratory of Applied Physics, Faculty of Electrical Engineering, Ljubljana, Slovenia

²Institute of Biophysics, Medical Faculty, Ljubljana, Slovenia

Background. A computer system HIPSTRESS is described. The system can be used for the determination of the contact stress distribution in the hip joint for a known body weight and some characteristic pelvic and hip geometrical parameters which can be determined directly from the standard antero-posterior radiograph. **Conclusions.** The system can be applied in clinical practice to predict an optimal stress distribution in different operative interventions in the hip.

Key words: antero-posterior radiograph, hip joint contact stress, pelvis

Introduction

The studies of the distribution of the contact stress¹⁻⁴ in the hip joint are important to explore the pathomechanics of the degenerative joint diseases⁴⁻⁶ as well as to predict an optimal stress distribution after certain operative interventions in order to improve their efficiency.^{2,6,7}

In this work, we describe the computer system HIPSTRESS which can be used for the determination of the hip joint contact stress distribution for individual patients^{2,3,8,9}. The system needs, as the input data, the body weight of the patient and some characteristic geometrical parameters of the pelvis and hip which can be determined from the antero-pos-

terior (AP) radiograph of the pelvis with both hips.¹⁰⁻¹²

Material and methods

The system HIPSTRESS^{2,3,8,9} is suitable to use on any personal computer with installed TURBO PASCAL. The system consists of two programs; one for the determination of the hip joint contact stress distribution^{2,3} and the other for the determination of resultant hip joint force **R**.^{8,9}

The hip joint contact stress distribution can be calculated by solving a relatively simple single non-linear algebraic equation.^{2,3} The program for the determination of the hip joint contact stress distribution^{2,3} requires, as the input data, the magnitude and the direction of the resultant hip joint force **R**, the center-edge angle of Wiberg (ϑ_{CE}) and the radius of the hip joint articular surface (r) (Figure1).

Received 4 October 1999

Accepted 15 October 1999

Correspondence to: Assist. Prof. Aleš Iglič, Ph.D., Laboratory of Applied Physics, Faculty of Electrical Engineering, Tržaška 25, SI-1000 Ljubljana, Slovenia.

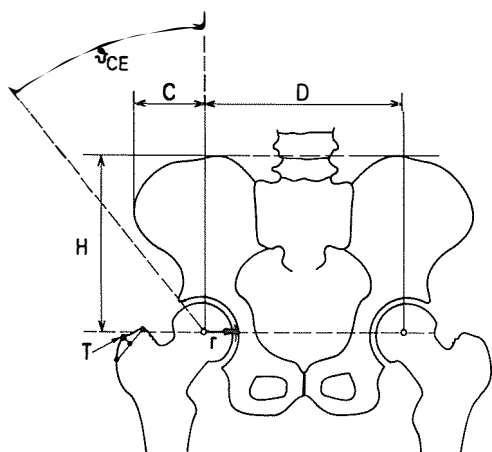


Figure 1. Schematic presentation of the pelvic and hip geometrical parameters that are used in corrections of the reference coordinates of the model muscle attachment points and in calculation of the contact stress distribution in the hip joint articular surface.

The resultant hip joint force R is calculated by the program based on the mathematical model of the hip joint in the one-legged stance body position^{8,9,13-15} which requires, as the input data, the distance between the two femoral head centers (D), the coordinates of the greater trochanter (point T), the height of the pelvis (H), the horizontal distance between the most lateral point on the crista iliaca and the femoral head center (C) (Figure 1) and the body weight. The values of the model muscle attachment points are adapted for each patient individually where the measured values of D , H and C and the position of the greater trochanter (point T) from AP radiographs for each patient are taken into account. The reference values of the model muscle attachment points were taken from Dostal and Andrews.¹⁶

The described geometrical parameters of the pelvis and the hip (D , H , C , point T , ϑ_{CE} , r) can be determined directly from the AP radiographs or by computer systems.^{11,17,18} The magnification rate should be taken into account. The computer systems HIJOMO¹⁷ and ANXRAY¹⁸ use a digitized profile of standard AP radiograph of the pelvis and both proxi-

mal femurs as input data. The curves that represent the head of the prosthesis and the femoral head were fitted by the circles using the least squares method.¹⁷

Results and conclusions

Figure 2 shows the calculated hip joint contact stress distribution in the female hip (age 76). The AP radiograph was taken from the archives of the authors.

Due to the simplifications in the mathematical models^{2,3} we cannot accurately predict the contact stress in the hip joint in detail or give an absolute stress distribution. However, the model predicts global averages which are in accordance with the relevant experimental in vivo data in the literature.¹⁹⁻²¹

In order to establish the clinical relevance of the determination of the hip joint contact stress distribution the computer system should be applied to various populations of patients where the correlation between the clinical status and the hip stress should be studied.

Recently, the system HIPSTRESS has been used in order to determine the peak contact stress in the articular surface of the hip joint from standard AP radiographs for 37 male and 44 female healthy hips of patients subject to trauma of the other hip.¹² It was shown that the peak contact stress is considerably higher (cca 20%) in the female population than in the male population. The results are in favor of the hypothesis that the increased hip joint contact stress in the female population could contribute to greater incidence of arthrosis in the female population relative to the male population.

To conclude, the described computer system HIPSTRESS can be used for the determination of the contact stress distribution from standard AP radiographs. The system can be applied in clinical practice to predict an optimal stress distribution in different operative

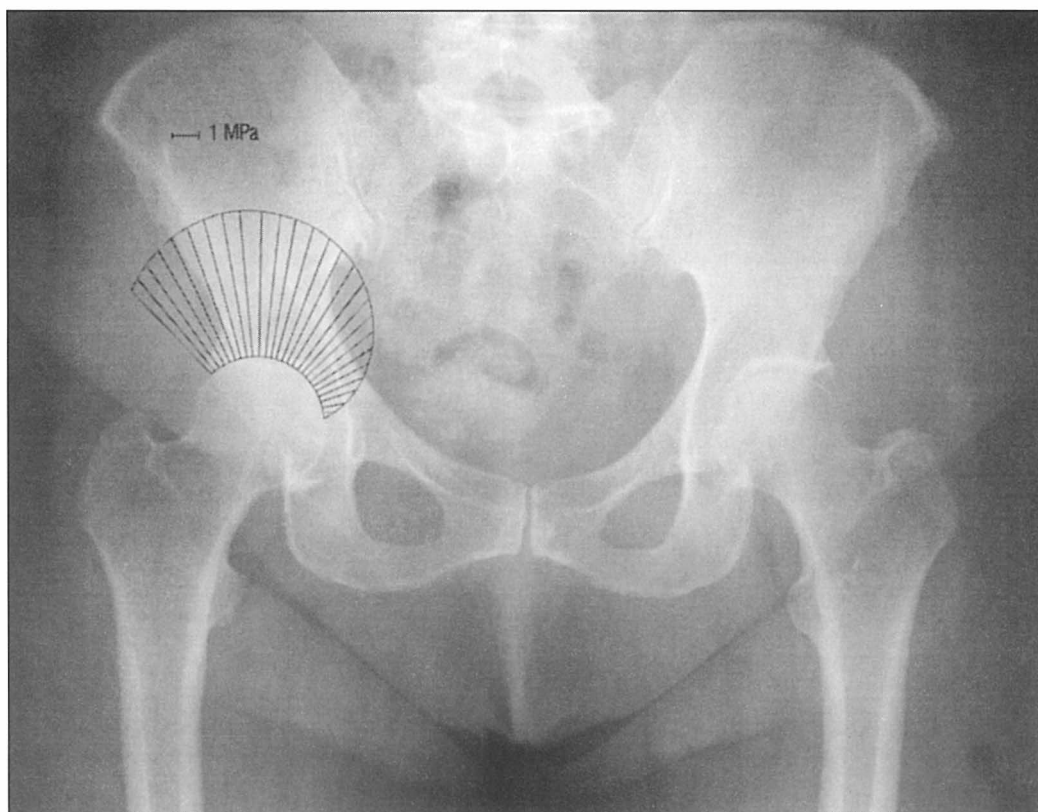


Figure 2. The hip joint contact stress distribution of the 76 year old female person (body weight 800 N, $\vartheta_{CE} = 44^\circ$, $r = 2.27$ cm) determined by the computer system HIPSTRESS.

interventions in the hip and to analyze the short and long term outcome of treatment of various conditions of the hip.

Acknowledgments

The computer system HIPSTRESS is available from the authors only to be used for scientific purposes and according to ethical principles.

References

1. Genda E, Konishi N, Hasegawa Y, Miura T. A computer simulation study of normal and abnormal hip joint contact pressure. *Arch Orthop Trauma Surg* 1995; **114**: 202-6.
2. Iglič A, Kralj-Iglič V, Antolič V, Srakar F, Stanič U. Effect of the periacetabular osteotomy on the stress on the human hip joint articular surface. *IEEE Trans Rehab Engr* 1993; **1**: 207-12.
3. Ipavec M, Brand RA, Pedersen DR, Mavčič B, Kralj-Iglič V, Iglič A. Mathematical modelling of stress in the hip during gait. *J Biomechanics* 1999; **32**: 1229-35.
4. Pauwels F. *Biomechanics of the normal and diseased hip*. Berlin, Heidelberg, New York: Springer; 1976.

5. Brinckmann P, Frobin W, Hierholzer E. Stress on the articular surface of the hip joint in healthy adults and persons with idiopathic osteoarthritis of the hip joint. *J Biomechanics* 1981; **14**: 149-56.
6. Kummer B. Die klinische Relevanz biomechanischer Analysen der Hüftregion. *Z Orthop* 1991; **129**: 285-94.
7. Baker KJ, Brown TD, Brand RA. A finite-element analysis of intertrochanteric osteotomy on stresses in femoral head osteonecrosis. *Clin Orthop* 1989; **249**: 183-98.
8. Iglič A, Srakar F, Antolič V, Kralj Iglič V, Batagelj V. Mathematical analysis of Chiari osteotomy. *Acta Orthop Jugosl* 1990; **20**: 35-9.
9. Iglič A, Srakar F, Antolič V. Influence of the pelvic shape on the biomechanical status of the hip. *Clin Biomech* 1993; **8**: 223-4.
10. Antolič V, Srakar F, Iglič A, Kralj-Iglič V, Zaletel-Kragelj L, Maček-Lebar A. Changes in configuration of the hip due to Chiari osteotomy. *Orthopedics* 1996; **4**: 183-6.
11. Kersnič B, Iglič A, Kralj-Iglič V, Srakar F, Antolič V. Increased incidence of arthrosis in female population could be related to femoral and pelvic shape. *Arch Orthop Trauma Surg* 1996; **116**: 345-7.
12. Smrke D, Jaklič A, Stankovski V, Iglič A, Kralj-Iglič V. Peak contact stress in articular surface of healthy hip joint in male and female population - a comparative study. *Arch Orthop Trauma Surg*; (in print).
13. Srakar F, Iglič A, Antolič V, Herman S. Computer simulation of the periacetabular osteotomy. *Acta Orthop Scand* 1992; **63**: 411-2.
14. Iglič A, Antolič V, Srakar F. Biomechanical analysis of various operative hip joint rotation center shifts. *Arch Orthop Trauma Surg* 1993; **112**: 124-6.
15. Iglič A, Antolič V, Srakar F, Kralj-Iglič V, Maček-Lebar A, Brajnik D. Biomechanical study of various greater trochanter positions. *Arch Orthop Trauma Surg* 1995; **114**: 76-8.
16. Dostal WF, Andrews JG. A three-dimensional biomechanical model of the hip musculature. *J Biomechanics* 1981; **14**: 803-12.
17. Jaklič A, Pernuš F. Morphometric analysis of AP pelvic and hip radiographs. In : Zajc B and Solina F, editors. *Proceedings of the third Slovenian electro-technical and computer science conference*. Ljubljana; 1994. p. 352-5.
18. Stankovski V, Smrke D, Kocjančič B, Kralj-Iglič V, Iglič A. Quantitative determination of geometrical parameters of the human femur and pelvis. *Med Biol Eng Comput* 1999; **37 Suppl 1**: 189-90.
19. Hodge WA, Fijan RS, Carlson KL, Burgess RG, Harris WH, Mann RW. Contact pressures in the human hip joint measured in vivo. *Proc Natl Acad Sci USA* 1986; **83**: 2879-83.
20. Hodge WA, Carlson KL, Fijan RS, Burgess RG, Riley PO, Harris WH, et al. Contact pressures from an instrumented hip endoprosthesis. *J Bone Joint Surg* 1989; **71A**: 1378-2883.
21. Krebs DE, Elbaum L, Riley PO, Hodge WA, Mann RW. Exercise and gait effects on in vivo hip contact pressures. *Phys Ther* 1991; **71**: 301-9.

Ultrasound in diagnosis and treatment of anal fistulas

Pavle Košorok

IATROS Medical Centre, Ljubljana, Slovenia

Background. Endoanal ultrasound (EUS) is helpful in the diagnosis of anorectal fistulas and abscesses due to its high resolution image quality and anatomical orientation using a radial scanning echoprobe. This type of information is essential in monitoring the response to treatment. Initial EUS examination prior to treatment, is mandatory in order to compare the results before and after treatment. Intraoperative EUS may also be helpful if the lesion is deep beyond the pelvic floor muscle which may not be seen during surgery. Better results in EUS imaging of perianorectal fistulas can be obtained using hydrogen peroxide as a contrast medium.

Concomitant advantage of hydrogen peroxide ultrasound was the detection of suspected or unsuspected sphincter defects.

However, interobserver reliability has to be taken into account together with the learning curve of a particular observer.

Conclusions. Endoanal US is a safe, economic, and reliable procedure for the assessment of fistula-in-ano, and is superior to physical examination.

Key words: rectal fistula - ultrasonography; rectal diseases - ultrasonography; abscess

Introduction

The history of ultrasound in medicine started immediately after the end of World War II on the basis of experiences in marine warfare with the detection of submarines. In early 50's, a breakthrough was accomplished with the introduction of transrectal ultrasound by Wild.¹ But it took more than two decades for the technology to be refined and introduced into clinical practice. Thereafter, investigators

from major centres in Europe, Japan, and the United States reported that transcolorectal endosonography could provide accurate diagnosis and staging of gastrointestinal diseases.^{2,3}

Anal endosonography - basic principles

Ultrasound scanner is used with a rotating rectal probe providing a 360° image. All images are oriented in the way that the anterior is on the right and recorded.

As the probe is withdrawn down the anal canal, the images of the puborectalis muscle, external anal sphincter, internal anal sphincter, longitudinal muscle, superficial transverse

Received 12 October 1999

Accepted 21 October 1999

Correspondence to: Assist. Prof. Pavle Košorok, M.D., Ph.D., IATROS Medical Centre, Parmova 51B, 1000 Ljubljana, Slovenia. Phone: +386 61 13 66 190; Fax: +386 61 13 66 194.

perineal muscle and ischiocavernosus muscles are recorded. The presence of other structures, such as the central point of the perineum and the anococcygeal ligament are also documented. Prints of the images are made at four levels (Figure 1) and the thickness of the puborectalis, longitudinal muscle, internal and external anal sphincter is measured in the midcoronal plane on both sides. The external sphincter measurements are made from the outer border of the internal sphincter to the outer edge of the external sphincter and include the longitudinal muscle, as in many females these structures could not be separated sonographically. The longitudinal muscle is also measured only when identified separately.

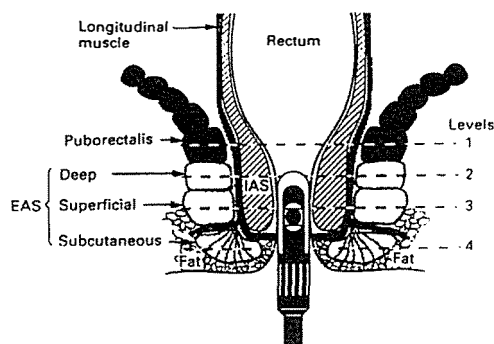


Figure 1. Schematic representation of the anal canal with a probe in situ illustrating the various levels at which measurements of muscle thicknesses are taken. Level 1, Puborectalis muscle; level 2, deep (proximal) external anal sphincter (EAS; level 3, superficial (mid) EAS; level 4, subcutaneous (distal) EAS.

The subepithelial tissues and internal sphincter are clearly defined in all patients. The longitudinal muscle is hyperechoic relative to the external sphincter in males and, so, identifiable as a separate structure. The same applied to 40% of females, but in the remainder, the longitudinal muscle and external sphincter were of similar echogenicity and, therefore, indistinguishable.

The morphology of the anal structures at the four levels is described in the study of Sultan et al.¹

(I) Puborectalis muscle

The puborectalis muscle is seen consistently as a hyperechoic diverging "U"-shaped muscle in all patients.

(II) External anal sphincter (EAS)

The deep aspect of the EAS is in continuity with the puborectalis posteriorly in both sexes. The anterior part differed between males and females. In females, the postero-lateral muscle bundles sloped infero-medially to unite anteriorly into an intact anterior ring lower down in the anal canal. Imaging just above this level showed an apparent anterior defect in all but one female. By contrast, the EAS is symmetric at all levels in males.

In general, the deep EAS is usually annular in both sexes, otherwise it is conical, tapered posteriorly to insert into the anococcygeal ligament.

(III) Longitudinal muscle

Where the EAS is hypoechoic, the longitudinal muscle layer is clearly distinguishable as a hyperechoic layer. This pattern of echogenicity is present in all males but only in 40% of the females. The longitudinal muscle is thicker postero-laterally and less prominent anteriorly.

(IV) Internal anal sphincter

This layer appears homogeneously hypoechoic and is identified in all subjects.

(V) Mucosa and subepithelial tissues

The hyperechoic submucosa (subepithelium) is seen in all subjects. The mucosa is not distinguishable as a separate sonographic structure.

(VI) Anococcygeal ligament

This structure is inferred from the presence of a triangular hypoechoic structure, the apex of

which merges into a posterior conical deformity of the EAS. It is more prominent and also more often in males (76%) than in females (49%).

(VII) Perineal body

The perineal body is not a clearly defined sonographic structure. However, the central point of the perineum, where the superficial transverse perinei, deep external sphincter and bulbospongiosus (bulbocavernosus) muscles appear to meet, is seen in some subjects, particularly in males.

(VIII) Ischiocavernosus muscle

The ischiocavernosus muscle is not identified in females but is seen in 43% of males as a hypoechoic structure parallel to the pubic rami.

(IX) Muscle thicknesses

The puborectalis and deep superficial external sphincter is significantly thicker in males. A similar trend is seen in the subcutaneous external sphincter, but is not statistically significant. The males, however, are significantly heavier than the females, with a significant positive correlation between their body weight and the mean thickness of the combined components of the external sphincter, as well as the mean thickness of the puborectalis muscle.

The mean internal sphincter and longitudinal muscle thicknesses are not significantly different between males and females.^{1,3}

A better understanding of the normal sonographic anatomy of the anal sphincter should lead to more precise diagnosis.

Ultrasound in diagnosis and treatment of anorectal disorders

Perianorectal fistulas and abscesses are often found in patients with inflammatory bowel

disease. Rectal digital examination, rectosigmoidoscopy, CT and MRI are the standard procedures in diagnosing fistulas and abscesses. The results, however, are often unsatisfactory. Recently, magnetic resonance imaging (MRI) has been reported to be accurate in the diagnosis of fistulas and of the sinus tract especially in patients with Crohn's disease.^{4,5}

Different studies select the use of transcolorectal EUS as the most practical tool in clinicians' hands for the diagnosis and staging of perianorectal fistulas and abscesses.

A concomitant advantage of EUS and specially hydrogen peroxide US was the detection of suspected or unsuspected sphincter defects (recurrent fistulas; parous women), which have been shown to be present in a significant number of patients.⁶

Investigative technique

The investigative technique is similar to that in rectosigmoidoscopy, with the patient lying in a left lateral decubitus position after a phosphate enema. Rectal digital examination is necessary to palpate the probable pain area, which may be related to the site of the lesion. Careful visual inspection of the perianal skin is helpful in detecting the opening of an abscess or fistula. After this, the echoprobe, which is routinely covered with a water-filled balloon, is carefully inserted as deeply as possible. Introducing an echoendoscope, the insertion has to be endoscopically controlled to avoid any perforation. The instrument is withdrawn gradually under sonographic image control. Symmetric imaging of the left and right quadrants should be obtained to compare the anatomical structure. In this way, abnormalities can readily be found. Intravenous sedation may be indicated if the patient experiences any discomfort.

Indications for EUS examinations

1. Suspicious finding of fistula or abscess by rectal digital examination, endoscopy, barium enema, or CT.
2. Recurrent fever and anal pain suspicious for inflammatory bowel disease.
3. Ileoanal pouch for ulcerative colitis to find out pouch related complications.
4. Follow-up after the surgery for fistulas or abscesses, or both.

EUS criteria

A *fistula* is visualised as a hypoechoic ductlike structure adjacent to the colorectal lumen, with or without destruction of the pelvic floor musculature.

An *abscess* is visualised as an anechoic or hypoechoic cavity in the perirectal tissue, protruding into the colorectal lumen. Communication between an abscess and a fistulous tract, or between an abscess or a fistulous tract and the surrounding structures such as the skin, vagina, bladder, scrotal, or labial region, can be seen.

EUS is helpful in the diagnosis of perianorectal fistulas and abscesses due to its high-resolution image quality and easy anatomical orientation by using a radial scanning echoprobe. This type of information is essential in monitoring the response to treatment. Initial EUS examination prior to treatment, however, is mandatory in order to compare the results before and after treatment. In general, it can be stated that a reduction in the number or size of lesions found initially can be considered as partial remission. Disappearance of initial lesions is indicative of complete remission. Intraoperative EUS may also be helpful if the lesion is deep beyond the pelvic floor muscle which may not be seen during surgery. Perianorectal fistulas and abscesses, however, may often relapse. Interestingly, the comparisons between EUS and electromyogra-

phy have been carried out to evaluate external sphincter muscle defects.⁶ The three-dimensional imaging capabilities, high soft-tissue contrast, and lack of ionizing irradiation provided by MRI have been reported as advantageous features over CT in showing the exact extension of fistulas and sinus tract in patients with Crohn's disease.^{4,5} EUS is superior to CT and MRI for the reasons mentioned above. Studies comparing EUS, CT and MRI should be carried out to determine the accuracy and limitations of various modalities.

Gastroenterologists and surgeons are using EUS in designing treatment strategies to manage these difficult diseases. The examination is less complicated than upper gastrointestinal endosonography, and is well tolerated by patients.

The conventional surgical treatment of a fistula-in-ano is to lay open the fistulous tract and to heal by secondary intention (fistulotomy). Fecal incontinence is a feared complication, and even division of a low fistula has been associated with continence disorders in up to 34% of patients.⁷⁻⁹

Surgical techniques that preserve the anal sphincters, such as the mucosal advancement flap, seem promising in preserving continence and might be of use, especially in fistulas with an increased risk for continence disorders, e.g., anterior fistulas in women, high fistulas (supra, extra, and high transsphincteric), and recurrent fistulas.¹⁰ Preoperative radiologic assessment of fistulous tract anatomy may be of assistance in planing surgical strategy (fistulography, CT, MRI). Transanal ultrasound (US) is an excellent modality for imaging internal and external anal sphincters,¹¹ but the results of localising fistulas varied significantly.¹²

Imaging of fistulous tract

Different substances can be used to visualise fistulous tract (indigo blue, milk, hydrogen peroxide).

Hydrogen peroxide (HP) as a contrast medium might improve the reliability of ultrasonographic imaging of fistula-in-ano. Accuracy of hydrogen peroxide-enhanced transanal ultrasound (HPUS) in assessing a fistulous tract anatomy and the additive value obtained with this technique in comparison with physical examination and conventional US was evaluated in a special study described by Poen et al., considering the operative findings as the criterion standard.¹³

Twenty-one patients underwent surgery for fistula-in-ano. Patients without an external fistulous opening were excluded from the study. All fistulas, except one, were of cryptoglandular origin. Eight patients had a recurrent fistula. Evaluation consisted of physical examination, conventional US, and HPUS. With all investigations, the fistulous tract was classified according to Parks et al.¹⁴ as intersphincteric, transsphincteric, extrasphincteric or suprasphincteric. Furthermore, the site of the internal opening (if present) was noted, and secondary extensions were described (intersphincteric, ischiorectal supraleatory, and horseshoe).

Physical examination

After the visualisation of the external opening, the palpation of the subcutaneous induration, followed by rectal examination and careful probing of the fistula, was performed. During rectal examination, the presence of the internal opening (induration) and palpation of the tip of the passing probe was noted. Proctoscopy was performed to exclude proctitis and any malignancy of the anus.

Hydrogen peroxide ultrasound

Ultrasound is using a diagnostic ultrasound system with a rotating endoprobe covered by a water-filled hard sonolucent cone producing a 360° view. The endoprobe is introduced

into the rectum, and serial radial images and video recordings of the distal part of the rectum, the puborectal muscle, and the anal canal are taken. A fistulous tract could be seen as a tube-like hypoechoic lesion. A sphincter defect is seen as a hypoechoic interruption in the sphincter complex. After conventional US is performed, HP (3%) is introduced into the fistulous tract with a flexible intravenous cannula (Venflon). Hereafter, US is repeated as described above. By infusion of HP, which generated formation of small hyperechoic air bubbles, the fistulous tract turned from hypoechoic to bright hyperechoic. The comparison of the images with and without HP identifies the course of the fistula and its extensions and allows a distinction between active fistulas and fibrotic tissue in patients who had previously been operated on. The site of the internal opening, secondary extensions of the fistula, and the presence of defects in one or both sphincters are also carefully recorded. Evidence that the internal opening is present is defined as a hypoechoic (conventional US) or a echogenic (HPUS) breach at the level of the submucosa.

Surgery

The surgeon has to be familiar with ultrasonographic findings. Under anaesthesia, careful digital examination with a probe is performed. The fistula is classified according to Parks et al.¹⁴, by assessing of the amount of sphincter tissue to be divided and the direction of the probe, relative to the longitudinal axis of the anal canal. In the case of a low fistula, the probe will meet the axis of the anal canal close to a right angle, whereas with a high fistula the angle is more oblique. The presence of an internal opening is evaluated. Based on preoperative classification and operative findings, the appropriate surgical treatment is chosen (Fistulotomy, mucosal advancement flap and excision of the sinus).

Primary tract

In the Poen's study, 8 intersphincteric, 11 transsphincteric and 2 sinus tracts (without internal opening) were found on surgery. The classification was not possible in 13 of 21 patients by physical examination, because of pain or mechanical resistance during probing, whereas 8 patients (38%) were adequately classified as having a low (intersphincteric or transsphincteric) fistula. With US, fistulas appeared as hypoechoic lesions. A correct classification of the fistula in relation to the sphincters was possible in 12 patients (57%). In nine patients, classification was impossible, the main reason being the inability to distinguish active fistulas from fibrotic tissue in previously operated on patients. After the infusion of hydrogen peroxide, which was easily tolerated in all patients, active fistulas became visible by turning from hypoechoic to bright hyperechoic. Subsequently, with HPUS, the fistula was classified correctly in 20 patients, the overall concordance with surgery being 95% , representing very good agreement.

Internal opening

During surgery, 19 internal openings were found in 21 patients. Most of the internal openings could also be found by physical examination, by probing, or by digital palpation (a small induration in the dentate line). Proctoscopy was not helpful in identifying the internal openings. Moreover, it was difficult to identify internal openings with US and HPUS. The number of internal openings found on physical examination did not differ significantly from the number found on surgery.

Secondary extensions

With HPUS, one or more secondary extensions were found in seven patient. Although there was reasonable concordance between HPUS and surgery (71%), two secondary extensions shown with HPUS in two patients

were not found during surgery. Both patients developed a recurrent fistula.

Sphincter defects

Sphincter defects were seen by US and HPUS in eight patients (in 6 patients with a recurrent fistula and in 2 patients after obstetric trauma). In four cases, the sphincter defect was not suspected during digital palpation.

Additive value of HPUS

HPUS added important information in ten patients (48%). This information was helpful in facilitating correct classification of the fistula and revealing unsuspected secondary tracts or unsuspected sphincter defects. In patients with a recurrent fistula, HPUS added significant information. Based on a combination of clinical and endosonographic findings, in five of these patients, an endorectal advancement flap repair was performed instead of routine fistulotomy. In two patients, both having an extrasphincteric sinus, the excision of the sinus could be performed without damaging the sphincter complex. In the remaining three patients, the type of surgery was not altered by additional information from HPUS and a routine fistulotomy was performed.

Discussion

Surgical treatment for fistula-in-ano is based on healing of the fistula and preserving continence. Therefore, it is important to know the anatomy of the primary tract, the site of the internal opening, and secondary extensions. Personal experience and skills are of great importance in the treatment of fistula-in-ano. Fistulography and CT have very limited value in the assessment of perianal fistulas.¹⁵ There are several articles on the use of US in the assessment of fistulous tracts.¹⁶ Deen et al.¹⁰

found US and surgery to correlate in 17 of 18 patients (94%). In contrast, Choen et al.,¹⁷ demonstrated no additional value of US compared with digital examination and probing under anaesthesia. Also, US could not reveal any primary superficial tracts and high fistulous extensions (supraleatory) and could not differentiate between the scar tissue and an active fistula. In none of these studies, HP was used. Because of these disappointing results, most centers have been focusing on the use of magnetic resonance imaging (MRI).^{4,5} This modality, with either external or enteroanal coils, has been proven to detect perianal fistulas accurately, the concordance rates with surgery of the primary tract varying from 64 to 86 percent.¹³ Both Lunniss et al.¹¹ and Hussain et al.¹² found MRI significantly more accurate in the detection of fistulous tracts than US, although no HP was used. However, MRI is expensive and the special software required to obtain clear images of the anal canal is not widely available, which justifies any attempt to search for alternative diagnostic tools.

HPUS and its potential benefits were originally described by Cheong et al.¹³ in case report. In two patients with recurrent complex perianal fistula, HPUS demonstrated accurately the fistulous tract anatomy, which was confirmed during surgery. The same group presented very recently a larger retrospective study of HPUS in 65 patients with perianal fistulas. Thirty-eight patients had surgery, the concordance of HPUS with intraoperative findings being 92 percent regarding the primary fistula tract. Besides the high accuracy in classifying primary fistulous tracks, HPUS was a sensitive method to demonstrate secondary extensions. Identification of the internal opening, however, was difficult. In Poen's study, on HPUS, the number of correctly identified internal openings rose to 48 percent, which was considered still insufficient. However, together with HPUS, proctologic examination was

always performed, the number of internal openings found was 71%, which is not significantly different from the amount found on surgery.

A concomitant advantage of HPUS was the detection of suspected or unsuspected sphincter defects (recurrent fistulas, parous women), which have been shown to be present in a significant number of patients.⁶

In view of these results, HPUS is supposed to be a safe, economic, and reliable technique in the assessment of fistula-in-ano. It helps the surgeon in delineating the fistula tract anatomy and provides information about the presence of anal sphincter defects. In this way, HPUS may be of value in planning the therapeutic strategy and may consequently reduce the risk of fecal incontinence and recurrence. In case of a complex or "at risk" fistula, e.g., fistulas that tend to develop post-operative fecal incontinence (recurrent fistulas, (anterior) fistulas in women, high fistulas, and all fistulas in patients with chronic diarrhoea or impaired sphincters),¹⁶ a mucosal advancement flap instead of fistulotomy should be chosen. Moreover, HPUS enables the surgeon to inform patients in advance about the type of surgery that will be performed and its possible complications.

During the operation, the surgeon classifies the fistula by localising the internal opening, directing the probe during rectal examination, and by assessing the sphincter mass to be divided. Considering the approximate value of classification of fistulas during the operation, the question arises as to which of the two methods, surgery or HPUS, will become the criterion standard for classification of fistulas in the future.

Conclusions

Endoanal US is a safe, economic, and reliable procedure for the assessment of fistula-in-ano, being superior to physical examination.

HPUS, particularly, assists in delineating the anatomic course of perianal fistulas and may, therefore, be of value in planning surgical strategy.

A concomitant advantage of HPUS is detection of suspected or unsuspected sphincter defects which have been shown to be present in a significant number of patients.

However, personal experience, together with the learning curve of particular observer, and interobserver reliability, has to be taken into account.

References

1. Sultan AH, Kamm MA, Hudson CN, Nicholls JR, Bartram CI. Endosonography of the anal sphincters: normal anatomy and comparison with manometry. *Clin Radiol* 1994; **49**: 368-74.
2. Bartram CI. Anal endosonography. *Ann Gastroenterol Hepatol* 1992; **28**: 185-9.
3. Solomon MJ, Mcleod RS, Cohen EK, Simons ME, Wilson S. Reliability and validity studies of endoluminal ultrasonography for anorectal disorders. *Dis Colon Rectum* 1994; **37**: 546-51.
4. Koelbel G, Schmiedl U, Majer MC, Weber P, Jenss H, Kueper K, et al. Diagnosis of fistulae and sinus tracts in patients with Crohn disease: value of MR imaging. *Am J R Roentgenol* 1989; **152**: 999-1003.
5. Jenss H, Starlinger M, Skaleij M. Magnetic resonance imaging in perianal Crohn's disease [letter]. *Lancet* 1992; **340**: 8830.
6. Felt-Bersma RJ, van Baren R, Koorevaar M, Strijers RL, Cuesta MA. Unsuspected sphincter defects shown by anal endosonography after anorectal surgery: a prospective study. *Dis Colon Rectum* 1995; **38**: 249-53.
7. Cotte L, Pujol B, Valette PJ, Grandjean JP, Sonquet JC. Complicated perianorectal fistula: contribution of endosonography. *Gastroenterol Clin Biol* 1990; **14**: 510-1.
8. Law PJ, Talbot RW, Bartram CI, Northover J. Anal endosonography in the evaluation of perianal sepsis and fistula in ano. *Br J Surg* 1989; **76**: 752-5.
9. Eckart VF, Jung B, Fischer B, Lierse W. Anal endosonography in healthy subject and patients with idiopathic fecal incontinence. *Dis Colon Rectum* 1994; **37**: 235-42.
10. Deen KI, Williams JG, Hutchinson R, Keighley M, Kumar D. Fistulas in ano: endoanal ultrasonographic assessment assists decision making for surgery. *Gut* 1994; **35**: 391-4.
11. Lunniss PJ, Barker PG, Sultan AH, Armstrong P, Reznick RH, Bartram CI, et al. magnetic resonance imaging of fistula-in-ano. *Dis Colon Rectum* 1994; **37**: 708-18.
12. Hussain S, Stoker J, Schouten W, Hop W, Lameris J. Fistula in ano: endoanal sonography versus endoanal MR imaging in classification. *Radiology* 1996; **200**: 475-81.
13. Poen AC, Felt-Bersma RJF, Eijssbouts QAJ, Cuesta MA, Meuwissen SGM. Hydrogen peroxide-enhanced ultrasound in the assessment of fistula-in-ano. *Dis Colon Rectum* 1998; **41**: 147-152.
14. Parks A, Gordon P, Hardcastle J. A classification of fistula-in-ano. *Br J Surg* 1976; **63**: 1-12.
15. Iroatulam AJN, Nogueras JJ, Chen HH, Weiss EG, Potenti FM, Alabaz O, et al. Accuracy of endoanal ultrasonography in evaluating anal fistula. *Gastroenterology* 1997; **112**(Suppl): A1450.
16. Tio TL, Kallimanis GE. Endoscopic Ultrasonography of Perianorectal Fistulas. *Endoscopy* 1994; **26**: 813-5.
17. Choen S, Burnett S, Bartram CI, Nicholls RJ. Comparison between anal endosonography and digital examination in the evaluation of anal fistulae. *Br J Surg* 1991; **78**: 445-7.

Acute subarachnoid haemorrhage: detection of aneurysms of intracranial arteries by computed tomographic angiography

Zoran Milošević

Clinical Radiology Institute, University Medical Centre Ljubljana, Slovenia

Background. We wanted to determine the diagnostic accuracy, sensitivity and specificity of computed tomographic angiography (CTA) of intracranial vessels, and to establish the advantages and disadvantages of CTA compared to digital subtraction angiography (DSA) as the "gold standard" in patients with acute subarachnoid haemorrhage (SAH).

Patients and methods. We prospectively studied 52 patients with acute SAH. Confirmation of the haemorrhage by a conventional computed tomography (CT) scan was immediately followed by intracranial CTA. DSA was performed after the CTA examination and so did not influence the interpretation of CTA images. The sensitivity, specificity and diagnostic accuracy of CTA were determined by comparing the results with the data from DSA and with the surgical findings. Cases where the CTA and DSA results did not match were analysed, and the advantages and disadvantages of intracranial CTA were determined.

Results. The diagnostic accuracy of CTA was 95%, its sensitivity was 93%, and its specificity was 98%. False-negative results were obtained in three patients who harboured small aneurysms, two in the region of the cavernous sinus and one at the division of pericallosal and callosomarginal arteries. In one patient with a false-positive result, DSA showed an infundibular widening of the posterior communicating artery. In all seven patients who underwent operations on the basis of CTA results, the surgical findings confirmed the presence of aneurysms as well as the intracranial vessel anatomy demonstrated by CTA.

Conclusions. Intracranial CTA is a fast and minimally invasive method with a high diagnostic accuracy, sensitivity and specificity, which has an important place in the detection and preoperative evaluation of intracranial aneurysms in patients with acute SAH.

Key words: subarachnoid haemorrhage - diagnosis; cerebral aneurysm - diagnosis; tomography, x-ray computed; computed tomographic angiography, digital subtraction angiography

Introduction

Acute subarachnoid haemorrhage (SAH) resulting from a ruptured aneurysm of intracranial arteries carries a poor prognosis, and the mortality in untreated patients may be as high as 45%.¹ The risk of rebleeding, which can be fatal for the patient, is highest

Received 9 August 1999

Accepted 7 September 1999

Correspondence to: Zoran Milošević, MD, Clinical Radiology Institute, University Medical Centre Ljubljana, Zaloška 2, 1525 Ljubljana, Slovenia. Phone +386 61 143 1530; Fax: +386 61 133 1044; E-mail: zoran.milosevic@kclj.si

in the first 24-48 hours.^{2,3} Therefore, prompt exclusion of the ruptured aneurysm from the circulation is essential. Emergency computed tomography (CT) of the head is the first neuroradiological investigation in patients with suspected SAH. A negative CT scan is followed by a lumbar puncture.⁴ If SAH is demonstrated, the aneurysm must be visualised by angiography as soon as possible and its features must be defined.

Intraarterial digital subtraction angiography (DSA) (Figure 1) of all four cerebral arteries still represents the "gold standard" for the detection of intracranial aneurysms.⁴⁻⁷ DSA is an invasive investigation with complications encountered in 1% of patients, while 0.5% develop permanent neurological deficits.⁸ Therefore non-invasive magnetic resonance angiography (MRA) and minimally invasive computed tomographic angiography (CTA) have been used increasingly over the past few years.^{9,10}

MRA is a non-invasive investigation, providing three-dimensional visualisation of intracranial vessels in various projections without the use of contrast media or ionising radiation (Figure 2).^{10,11} Its main disadvantages in patients with acute SAH are the long examination time (up to 30 min) and difficult

patient monitoring.^{12,13} MRA cannot depict clearly small aneurysms or partially thrombosed aneurysms with a low flow.^{12,13} It is contraindicated in patients with ferromagnetic implants.

The spiral technique of CT, in which scanning is performed while the CT table with the

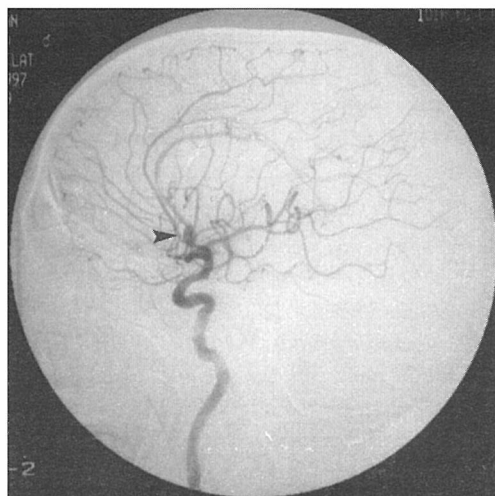


Figure 1b. Anteroposterior digital subtraction angiography view after right internal carotid injection demonstrates an anterior communicating artery aneurysm (arrow).



Figure 1a. Lateral digital subtraction angiography view after right internal carotid injection demonstrate an anterior communicating artery aneurysm (arrows).



Figure 2a. Digital subtraction angiogram of left internal carotid artery, lateral view, demonstrates posterior communicating artery aneurysm (arrow).



Figure 2b. Three-dimensional magnetic resonance angiographic image, posterolateral view, also clearly demonstrates the same aneurysm (arrows).

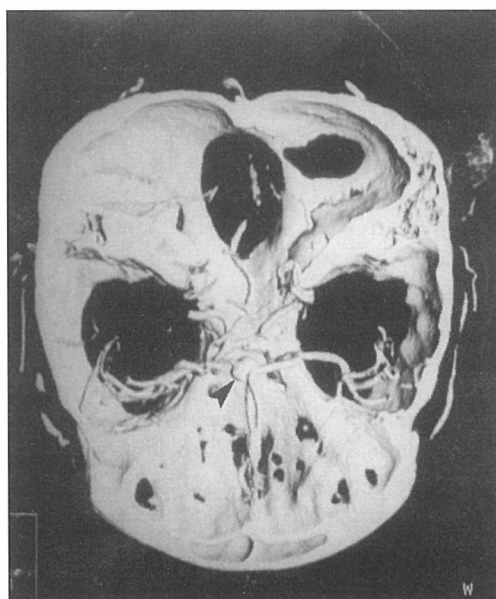


Figure 3a. Three-dimensional computed tomographic angiographic image, superior view, demonstrates a 9-mm-diameter anterior communicating artery aneurysm (arrow).

patient is drawn through the gantry, along with accurate timing of intravenous injections of contrast medium, has made it possible to obtain a three-dimensional display of intracranial arteries also with the use of CT (Figure 3).

The aims of our study were to assess the diagnostic value, advantages and disadvantages of intracranial CTA as compared to DSA

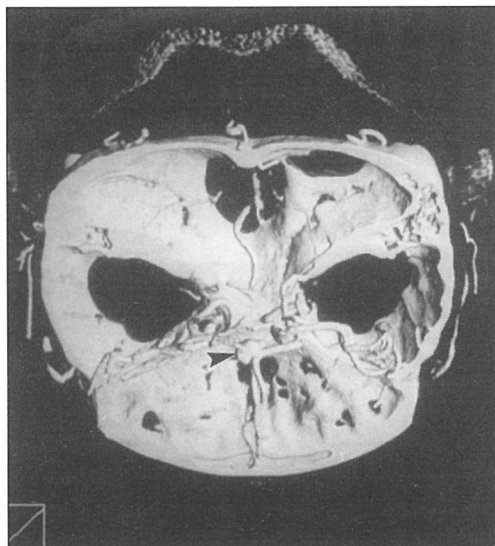


Figure 3b. Three-dimensional computed tomographic angiographic image, posterior view, demonstrates a 9-mm-diameter anterior communicating artery aneurysm (arrow).

in patients with ruptured aneurysms of intracranial arteries, and to define the criteria for proceeding with neurosurgical intervention on the basis of CTA results alone.

Patients and methods

From the introduction of CTA in November 1997 until February 1999, a total of 174 intracranial CTA examinations were performed at the Institute of Radiology in Ljubljana. The present prospective study included 52 patients (22 males and 30 females, aged between 32 and 81 years, average 51.7 years) in whom conventional CT confirming the presence of SAH was immediately followed by intracranial CTA performed on the same scanner (Figure 4). DSA was carried out subsequently, so that its results did not influence the interpretation of the CTA findings.

The CTA examinations were performed with a Siemens Somatom Plus 4 CT scanner, using the following protocol: slice thickness 1

mm, flow rate of contrast medium 2.5 ml/s, volume of contrast medium 120 ml, field of view 50 mm from the level of the posterior inferior cerebellar arteries to the level of the pericallosal arteries. The intracranial arteries were analysed in axial CT images and in three-dimensional reconstructions produced

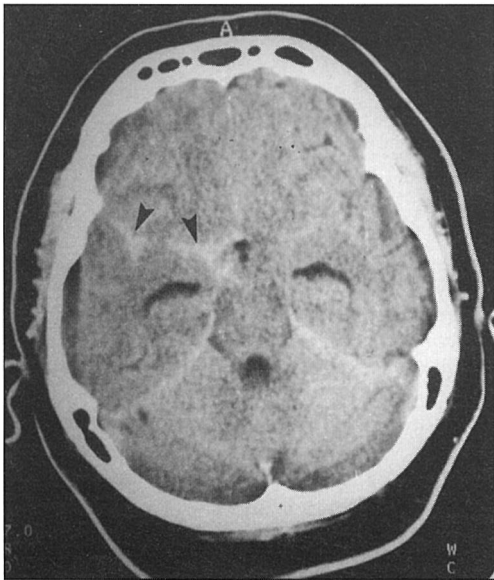


Figure 4a. Patient with subarachnoid haemorrhage from a ruptured aneurysm of the middle cerebral artery. Conventional axial CT shows blood in the basal cisterns and in the right Sylvian fissure (arrows).

on a Sienet Magicview 31 VA workstation.

In 45 of the 52 patients, a four-vessel DSA study of intracranial arteries was performed on a Philips Integris 2000 system within 12 hours of the CTA examination. In September 1998, the first patient was operated upon on the basis of the CTA results only; afterwards, six further operations were undertaken solely on the basis of CTA.

We evaluated the technical success of CTA and determined the time from the start of the examination until the definitive diagnostic images were produced.

The CTA findings were prospectively compared with the DSA results and for patients undergoing surgical intervention also with the surgical findings. In the seven patients who underwent surgery on the basis of positive CTA findings alone, the CTA result was compared with the neurosurgical result. In this way we were able to estimate the diagnostic value, sensitivity and specificity of intracranial CTA. Patients whose CTA results did not agree with the DSA findings were analysed separately.

We identified the cases where CTA used for the detection and preoperative evaluation of intracranial aneurysms provided sufficient information to allow neurosurgical intervention to be undertaken without DSA.

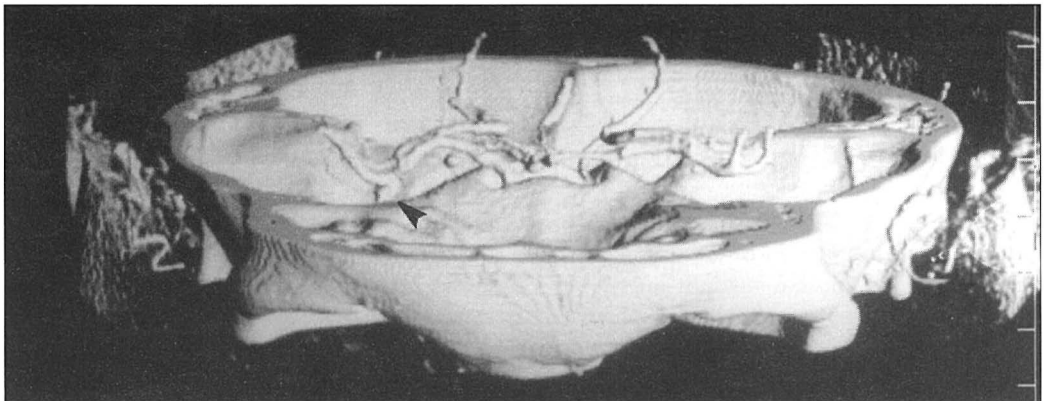


Figure 4b. Patient with subarachnoid haemorrhage from a ruptured aneurysm of the middle cerebral artery. Intracranial CTA performed immediately after conventional CT clearly demonstrates the small aneurysm of the middle cerebral artery (arrow).

Results

Of the 52 CTA studies, 50 (96%) were technically successful. In two studies the image quality was poor because the patients were restless, and so the examination had to be repeated.

The time from the start of the examination until the final elaboration of diagnostic films ranged from 35 to 60 min.

One or more aneurysms were present in 42 of the 52 patients studied. In all seven patients who underwent neurosurgical operations solely on the basis of positive CTA results, the presence and position of the aneurysm as seen on CTA was confirmed at surgery. The results for the remaining 45 patients, in whom the CTA examinations were followed by DSA, are presented in Table 1.

Table 1. Number of patients with acute SAH and number of aneurysms detected in these patients with CTA and/or DSA

	Positive DSA	Negative DSA
Positive CTA	32 patients 35 aneurysms	1 patient 1 aneurysm
Negative CTA	3 patients 3 aneurysms	9 patients

Both investigations were positive in 32 patients, in whom a total of 35 aneurysms were detected. One patient had two aneurysms and another had three. For all the

aneurysms visualised by CTA and DSA, the presence and position of the lesions were confirmed at neurosurgical operation.

In 10 patients the cause of the acute SAH was not found and so an operation was not undertaken.

In three patients, DSA detected an aneurysm that was not visible on CTA (false-negative results of CTA). In one patient, a small aneurysm measuring 2 mm was located at the bifurcation of the callosomarginal and

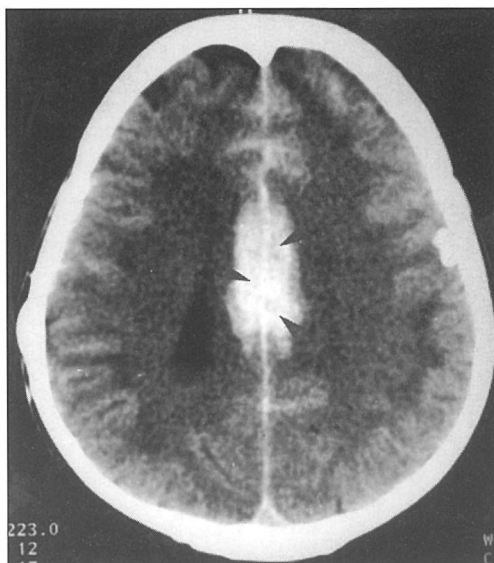


Figure 5a. Conventional CT shows blood in subarachnoid spaces and in the interhemispheric fissure (arrows).

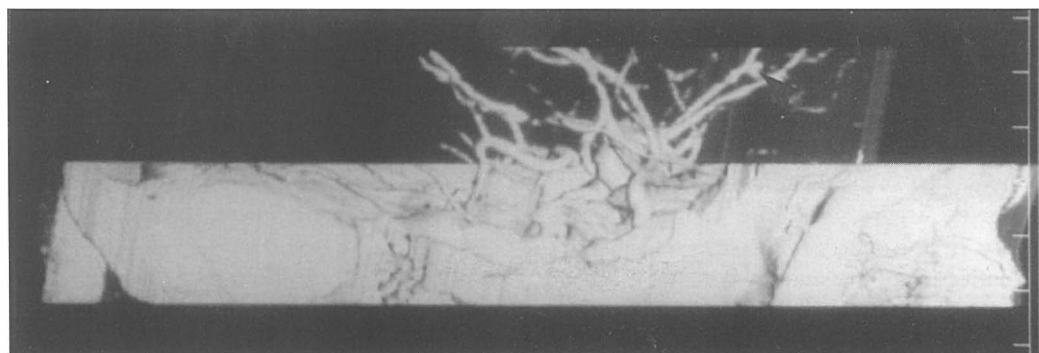


Figure 5b. This small aneurysm at the bifurcation of the callosomarginal and pericallosal arteries on the right side was missed on CTA images because of its small size and unusual position (arrow).

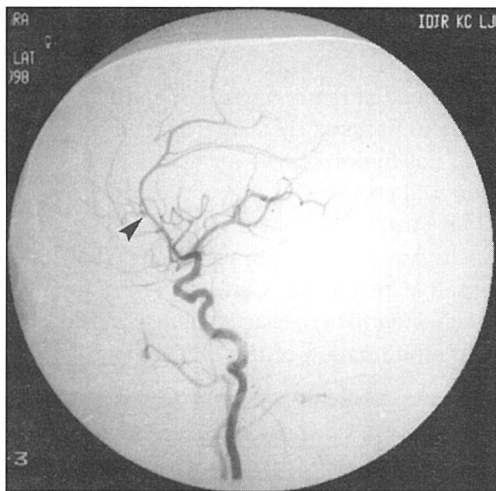


Figure 5c. DSA image, lateral projection, demonstrates this small aneurysm (arrow).

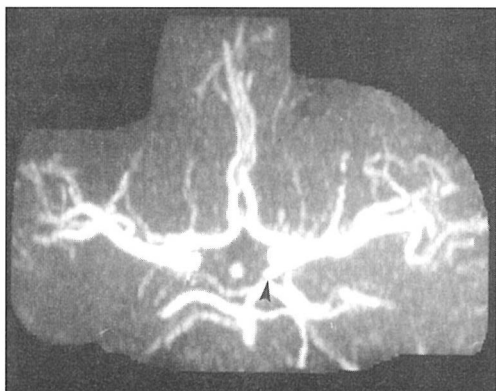


Figure 6a. On CTA images an infundibular widening of the posterior communicating artery (arrow) was misinterpreted as an aneurysm.

pericallosal arteries on the right side. The lesion was seen on CTA but could not be identified as an aneurysm because of its small size and position (Figure 5). Two other patients had small aneurysms, 3 and 4 mm in diameter, arising from the internal carotid artery in the area of the cavernous sinus; opacification of the sinus by contrast medium obscured the boundary between the sinus and the aneurysm. In one patient, an infundibular widening of the posterior communicating artery was erroneously interpreted

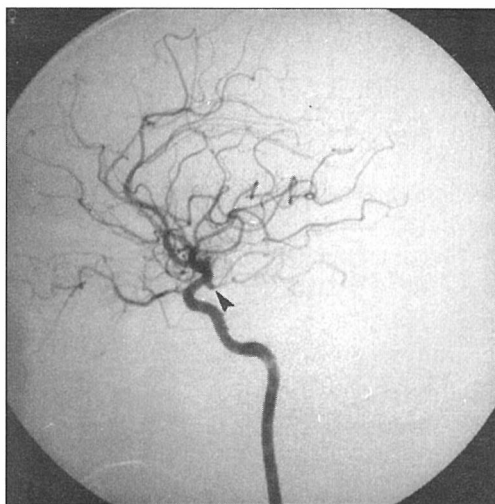


Figure 6b. DSA clarified the situation (arrow), and an operation was not undertaken.

ed as an aneurysm (a false-positive result of CTA); DSA clarified the situation, and an operation was not undertaken (Figure 6).

Comparison of the results of CTA with those of DSA and surgery showed that CTA in our patients had a sensitivity of 93%, a specificity of 98%, and a diagnostic accuracy of 95%.

Discussion

Intracranial CTA is the most recent neuroradiological angiographic examination method. Several authors have evaluated the diagnostic accuracy, sensitivity and specificity of intracranial CTA as compared to DSA^{4,7,9} and recently also to neurosurgical findings.^{16,17} Most of these studies have shown CTA to be highly accurate, sensitive and specific. This is confirmed also by our present results.

CTA has the following advantages over DSA:

1. It is a minimally invasive examination because contrast material is injected through an intravenous cannula.
2. It can be performed on the same scanner as conventional CT directly after the demonstra-

tion of SAH by a conventional CT scan. Therefore it gives results more rapidly than DSA, for which the patient must be transported to the apparatus and the team, which is constantly on call, must be assembled.

3. In a CTA study, three-dimensional reconstructions can be examined in any projection, but with DSA, the number of projections is limited.

4. CTA is able to define more accurately the relationship of the aneurysm to skeletal structures, and depict a thrombus within the aneurysm or calcifications within its wall, which is important in preoperative evaluation (Figure 7).

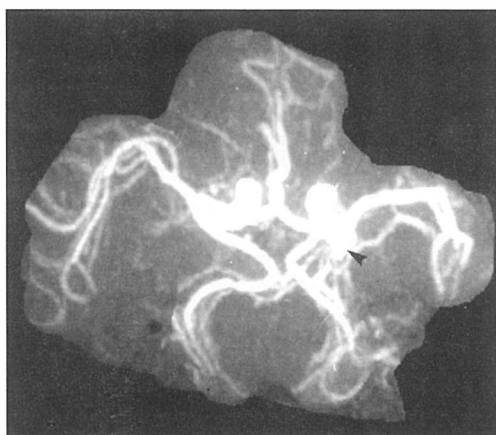


Figure 7a. Inferior view CT angiogram (maximum intensity projection) demonstrates left posterior communicating artery aneurysm and calcifications within the neck of this aneurysm (arrow).

Compared to DSA, CTA also has several disadvantages, which must be considered:

1. Because of lower image resolution, CTA carries a higher probability of false-negative results for small aneurysms measuring less than 3 mm.

2. CTA has a lower diagnostic accuracy in areas where the intracranial arteries border on skeletal structures or the cavernous sinus.

3. CTA requires a greater volume of contrast medium than DSA.

4. CTA is capable of displaying large intracranial arteries but is unable to depict clearly small peripheral arteries; therefore a negative CTA examination must be followed by DSA.

Since the two examinations are in most cases complementary, their combination often provides more data than would be obtained with each of them separately.

When CTA depicts clearly an aneurysm that appears to be the source of haemorrhage, considering the distribution of blood in the subarachnoid spaces, and when the intracranial vessels are distinctly visible from the level of the origin of the posterior inferior cerebellar artery to the level of pericallosal arteries, neurosurgical intervention can be undertaken on the basis of the CTA findings alone. Intracranial CTA has a high diagnostic accuracy, sensitivity and specificity. It can play an important part in the management of patients with acute SAH because the results are acquired rapidly and in a minimally invasive way.

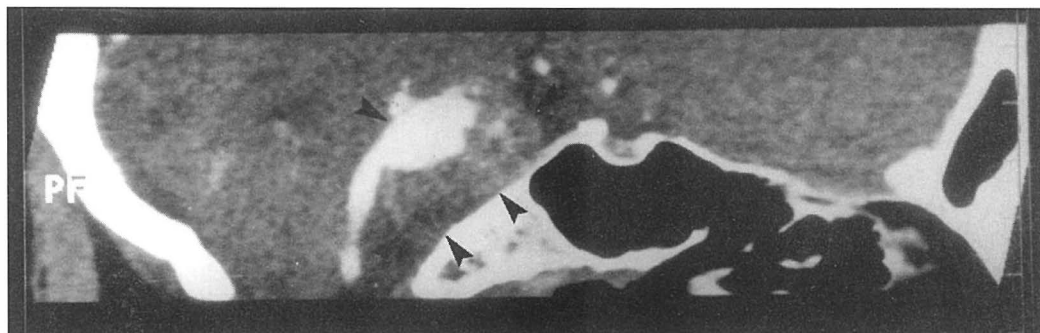


Figure 7b. Multiplanar reconstruction (MPR) in sagittal plane in another patient demonstrate a giant, partially thrombosed basilar artery aneurysm (arrows).

References

1. Hop JW, Rinkel GJE, Algra A, van Gijn J. Case fatality rates and functional outcome after subarachnoid hemorrhage: a systematic review. *Stroke* 1997; **28**: 660-4.
2. Inagawa T, Kamiya K, Ogasawara H, Yano T. Rebleeding of ruptured intracranial aneurysms in the acute stage. *Surg Neurol* 1987; **28**: 93-9.
3. Inagawa T. Ultra-early rebleeding within six hours after aneurysmal rupture. *Surg Neurol* 1994; **42**: 130-4.
4. Alberico RA, Patel M, Casey S, Jacobs B, Maguire W, Decker R. Evaluation of circle of Willis with three-dimensional CT angiography in patients with suspected intracranial aneurysms. *Am J Neuroradiology* 1995; **16**: 1571-8.
5. Zouaoui A, Sahel M, Marro B, Clemenceau S, Dargent N, Bitar A, et al. Three-dimensional CT angiography in detection of cerebral aneurysms in acute subarachnoid hemorrhage. *Neurosurgery* 1997; **41**: 125-30.
6. Velthuis BK, Rinkel GJ, Ramos LM, Witkamp TD, van der Sprenkel JW, Vandertop WP, et al. Subarachnoid hemorrhage: aneurysm detection and preoperative evaluation with CT angiography. *Radiology* 1998; **208**: 423-30.
7. Korogi Y, Takahashi M, Imakita S, Abe T, Utsunomiya H, Ochi M, et al. Diagnostic accuracy of three-dimensional CT angiography in screening evaluation of intracranial aneurysms. *Int J Neuroradiol* 1998; **4**: 373-9.
8. Heiserman JE, Dean BL, Hodak JA, Floam RA, Bird CR, Drayer BP, et al. Neurologic complications of cerebral angiography. *Am J Neuroradiology* 1994; **15**: 1401-7.
9. Katz DA, Marks MP, Napel SA, Bracci PM, Roberts SR. Circle of Willis: evaluation with CT angiography, MR angiography and conventional angiography. *Radiology* 1995; **195**: 445-9.
10. Harrison MJ, Johnson BA, Gardner GM, Welling BG. Preliminary results on management of unruptured intracranial aneurysms with MR angiography and CT angiography. *Neurosurgery* 1997; **40**: 947 - 57.
11. Heinz ER. Aneurysms and MR angiography. *Am J Neuroradiol* 1995; **14**: 974-7.
12. Korogi Y, Takahashi M, Mabuchi N, Miki H, Fujiwara S, Horikawa J, et al. Intracranial aneurysms: Diagnostic accuracy of three-dimensional, Fourier transform, time of flight MR angiography. *Radiology* 1994; **193**: 181 -186.
13. Huston J, Rufenacht DA, Ehman RL, Wiebers DO. Intracranial aneurysms and vascular malformations: Comparison of time of flight and phase contrast MR angiography. *Radiology* 1991; **181**: 721-30.
14. Klucnik NP, Carrier DA, Pyka R, Haid RW. Placement of a ferromagnetic intracerebral aneurysm clip in a magnetic field with a fatal outcome. *Radiology* 1993; **187**: 855-6.
15. Napel S, Marks M, Rubin GD, Dake MD, McDonnell CH, Song SM, et al. CT angiography with spiral CT and maximum intensity projection. *Radiology* 1992; **185**: 607-10.
16. Brown HJ, Lustrin ES, Lev MH, Ogilvy CS, Taveras JM. Characterisation of intracranial aneurysms using CT angiography. *AJR* 1997; **169**(3): 889-93.
17. Preda L, Gaetani P, Rodriguez RB, Di Maggio EM, La Fianza A, Dore R, et al. Spiral CT angiography and surgical correlations in evaluation of intracranial aneurysms. *Eur Radiol* 1998; **8**: 739 -45.

Indium-111-DTPA-octreotide scintigraphy in patients with carcinoid tumor

Stanko Težak¹, Rajko Ostojić², Zdravko Perković², Nadan Rustemović²,
Nikica Car³, Branko Papa⁴, Mirjana Poropat¹, Damir Dodig¹

¹Department of Nuclear Medicine and Radiation Protection, and

²Department of Internal medicine, University Hospital Rebro, ³Institute "Vuk Vrhovac",

⁴Department of Internal Medicine, University Hospital "Merkur", Zagreb, Croatia

Background. The aim of the study was the evaluation of clinical utility and comparison of ¹¹¹In-DTPA-octreotide receptor scintigraphy (SRS) with conventional imaging modalities (CIM) in the detection of carcinoid tumor.

Patients and methods. Fourteen patients with pathohistologically proven diagnosis of carcinoid tumor and one patient with clinical suspicion of carcinoid tumor were investigated by SRS. SRS was performed for localization of primary tumor, recurrence or estimation of spread of the disease after CIM had been completed.

Whole body scans and single photon emission computed tomography (SPECT) were acquired 6 and 24 h after the application of radiopharmaceutical. The intensity of nonspecific radiopharmaceutical uptake in the bowel was assessed semiquantitatively by a score using whole body scans.

Results. The evaluation was done for patients and for tumor sites. The sensitivity, specificity, and positive and negative predictive values for patient evaluation were 89%, 100%, 100% and 80%, respectively for both CIM and SRS, whereas for tumor sites, these parameters were 69%, 100%, 100% and 82% for CIM, and 88%, 100%, 100% and 92% for SRS. Intensity score of nonspecific ¹¹¹In-octreotide bowel accumulation was 0.92 and 2.01 for 6 and 24 h scans respectively ($p < 0.01$).

Conclusion. ¹¹¹In-octreotide scintigraphy should be included in the diagnostic algorithm for the patients with clinical suspicion of carcinoid and for the assessment of patients with proven carcinoid tumor.

Key words: carcinoid tumor-radionuclide imaging; indium radioisotopes, octreotide, DTPA; ¹¹¹In-octreotide scintigraphy, diagnosis; nonspecific bowel accumulation

Introduction

Indium-111-DTPA-octreotide (^{111}In -pentetreotide) is a radiolabeled octapeptide somatostatin analogue. It binds to somatostatin receptors in normal tissues and in a variety of tumors and inflammatory diseases.¹ Of five known somatostatin receptor subtypes, ^{111}In -octreotide exerts the highest affinity to the receptor subtype II and to a much lesser extent to the receptor subtype V.² A high percentage of carcinoid tumors express somatostatin receptors in vitro, specifically the subtype II, enabling their visualization by ^{111}In -octreotide scintigraphy (SRS) in patients.³⁻⁵ The rationale for introducing SRS into clinical practice is a relatively low sensitivity of conventional imaging modalities (CIM) for extrahepatic sites of carcinoid tumors.⁶ SRS adds diagnostic and therapeutic information to conventional imaging modalities and laboratory procedures in carcinoid patients.⁷ Indeed, several factors influence the sensitivity of SRS, including the density and subtype of the receptor expressed by the tumor, radioligand receptor affinity and tumor size.⁸ Unspecific bowel activity due to the biliary excretion of radiopharmaceutical may affect tumor to background ratio in imaging setting.^{9,10} Clinical utility and comparison of SRS with CIM in the detection of carcinoid tumor are evaluated. Semiquantitative assessment of changing intensity of unspecific bowel accumulation during scanning procedure is addressed, too.

Patients and methods

Patients

Fifteen patients (7 male and 8 female) mean age 49 years (range 23-70) were referred to SRS for clinical suspicion of carcinoid tumor, recurrence, assessment of spread of disease or in vivo estimation of somatostatin receptor activity. All patients except one had patho-

hologically proven diagnosis of carcinoid tumor either of primary site or of metastasis. On the basis of knowledge of primary site of carcinoid tumor prior to scintigraphy, the patients were divided into Group A: 10 patients with known primary site; and Group B: 5 patients with unknown primary site.

Two patients were on somatostatin therapy which was not withdrawn before scintigraphy.

Methods

Whole body scans in anterior and posterior projection and a single photon emission computed tomography (SPECT) of the abdomen, and the thorax when appropriate, were obtained 4-6 and 24 h after i.v. application of 111-145 MBq ^{111}In -octreotide on large, rectangular field of view by gamma camera equipped with high energy collimator and linked to an appropriate computer. The pulse height analyzer windows with a width of 20% were centered over 172 keV and 245 keV photon peaks of ^{111}In . For whole body scintigrams, the scanning speed was 10 cm/min and the data were collected in 128 word matrix. A 360° rotation ECT in steps of 6° lasting for 60 s was performed using 128 word matrix. Back projection algorithm applying a ramp filter was used on prefiltered data with Butterworth filter of order 5 and cut-off frequency 0.50 to 0.25.

The presence of unspecific uptake of radiopharmaceutical in the small and large intestine on anterior whole body scans was assessed by an intensity score; 0 for its absence, 1 for intensity smaller than the liver, 2 for intensity equal to the liver and 3 for intensity bigger than the liver (Figure 1).

CT of the abdomen was performed in all patients, whereas abdominal ultrasound, upper gastrointestinal series, bowel enema, CT of the thorax, bronchoscopy, bronchial lavage and bone x-ray were performed in some only.

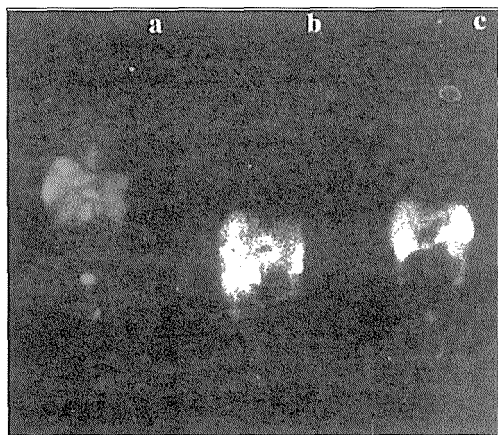


Figure 1. Intensity of nonspecific ^{111}In -octreotide bowel accumulation. **a:** Grade 0-1. **b:** Grade 2. **c:** Grade 3. Multiple pathologic hepatic and extrahepatic ^{111}In -octreotide accumulation in **a** and **b**. Physiologic ^{111}In -octreotide accumulation in **c**.

For both imaging modalities, 3 categories of lesions were searched for: the primary site of carcinoid, liver metastases and extrahepatic metastases. Liver metastases, regardless the number, were considered as single lesion.

Biological markers of tumor metabolism were not systematically investigated.

For statistical analysis of scintigraphy scores, a paired t-test was applied. For the evaluation of a diagnostic test, usual formulas were used.¹¹

Results

Group A

Results of CIM

All 10 patients had pathohistologically proven primary tumor, and in 9, the primary tumor was surgically removed. In the remaining patient, an unresectable carcinoid of the pancreatic head was found on operation. Five patients had liver metastases and only one patient had extrahepatic metastasis in the spleen. Extrahepatic lesions were detected by

conventional imaging in 3 patients: in one, an enlargement of right suprarenal gland was observed, the second had a thyroid nodule and a renal cyst and the third had a renal cyst (Table 1).

Table 1. Site of primary tumor and liver metastases detected by conventional imaging modalities (CIM) in Group A patients

Site	No. of patients	No. of patients with liver metastases
bronch	2	2
gastric polyp	3	0
ascending colon	1	1
appendix	2	0
caecum	1	1
pancreas	1	1

Results of SRS

^{111}In -pentetreotide scintigraphy revealed a carcinoid of the pancreas head in the patient with inoperable tumor. In other 9 patients, scintigraphy was negative at the site of the primary tumor. In 4 of 5 patients who had liver metastases scintigraphy was positive. The known spleen metastasis was visualized by scintigraphy. In 3 patients, scintigraphy revealed 3 additional lesions nonvisualized by conventional imaging: periaortic lymph nodes (Figure 2), mediastinal lymph nodes and a left clavicular metastasis.

Group B

Results CIM

Four patients in this group had proven liver metastases. In one of these patients, CT revealed an enlargement of the left suprarenal gland. Another patient had bilateral adnexectomy and omentectomy for metastatic carcinoid tumor. The patient with clinical suspicion of carcinoid syndrome had negative work up by conventio-

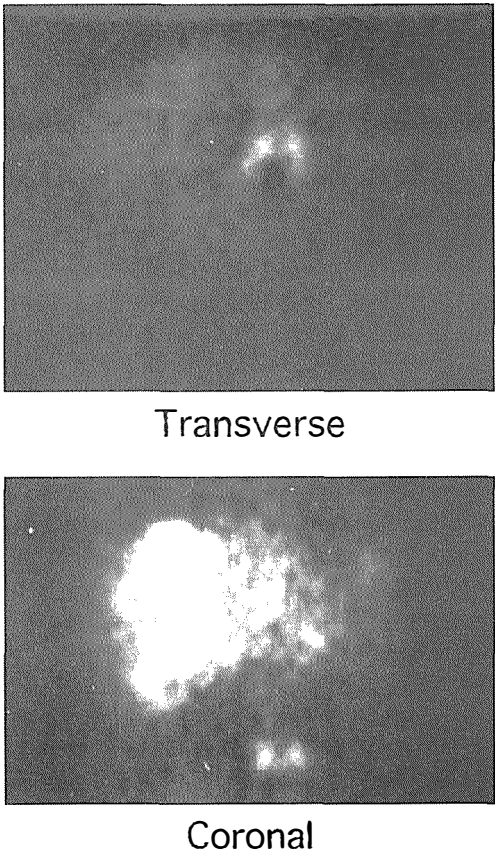


Figure 2. ¹¹¹In-octreotide SPECT of abdomen. Unsuspected paraaortic lymph node metastases in patient with liver metastases from coecal carcinoid. a. transversal and b. coronal slice.

nal imaging modalities except for elevated 5-hydroxyindol-acetic acid in one urine specimen.

Results of SRS

One out of 4 patients with liver metastases had scintigraphy after extirpation of a solitary liver metastasis. In the remaining 3 patients, the liver metastases were visualized by scintigraphy. In all 4 patients, SRS revealed 4 sites of extrahepatic accumulation, of which 2 were in the thorax and 2 in the abdomen; one carcinoid was removed from small intestine (Figure 3) and a tumor of the thymus was found on repeated CT. The remaining two

sites in 2 patients have not been characterized yet, but the scintigraphic pattern suggests a tumor uptake.

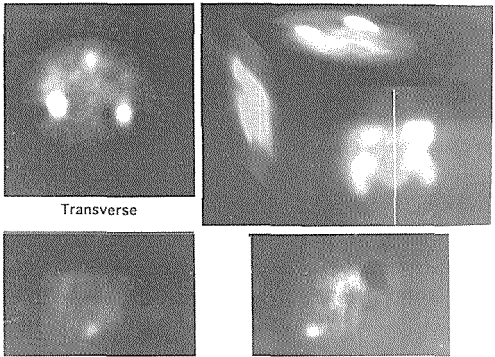


Figure 3. ¹¹¹In-octreotide SPECT of abdomen. Small intestine carcinoid.

In both groups, none of the extrahepatic solid lesions detected by CIM has demonstrated any uptake of radiopharmaceutical on scintigraphy, and none has yet been proven to represent a metastasis of carcinoid tumor. The comparison and summary of CIM and SRS findings are given in Table 2 and Table 3.

In 5 patients included in the final analysis (1 group A, 4 groups B), the primary tumor was not removed or its site was unknown prior to SRS. In all 5 patients, the uptake of

Table 2. Comparison of conventional imaging modalities (CIM) findings and corresponding ¹¹¹In-octreotide accumulation on scintigraphy (SRS) in Groups A and B

	CIM	SRS
primary site	1	5*
liver metastasis	8	7
spleen metastasis	1	1
lymph node metastasis	0	2
bone metastasis	0	1
renal cyst	2	0
thyroid nodule	1	0
suprarenal mass	2**	0

* 2 sites not confirmed by CIM or surgery
** unknown etiology

^{111}In -pentetreotid was present on possible sites of primary tumor. In 3 out of these 5 patients, the primary site of tumor has been confirmed by surgery or CT. Due to a proportionally small number of patients with primary tumor in the study population, primary tumors were evaluated together with extrahepatic lesions.

In 13 patients, 39 sites could be confirmed to bear carcinoid or to be free of tumor. Nine patients and 16 sites were tumor-bearing, 4 patients and 23 sites were tumor-free. On the basis of these data, sensitivity, specificity, and predictive positive and negative values of conventional imaging modalities and ^{111}In -pentetreotid scintigraphy were calculated.

The sensitivity, specificity, positive and negative predictive values of CIM for detection of disease in a patient were 89% 100%, 100% and 80% respectively. The same parameters of CIM for detection of a single lesion were 69%, 100%, 100% and 82%, respectively. The sensitivity, specificity, positive and negative predictive values of SRS for the detection of disease in a patient were 89%, 100%, 100% and 80%, respectively whereas, for the detection of a single lesion, these parameters were 88%, 100%, 100% and 92%, respectively (Table 4).

In 2 of 13 (15%) patients, the treatment strategy was changed on the basis of positive scintigraphic findings.^{12,13} The primary tumor was removed in a patient with liver metastases from group B and a contemplated liver transplantation was rejected for unsuspected extrahepatic spread in a group A patient (Figure 3).

Intensity of unspecific bowel accumulation was significantly higher ($p < 0.01$) on whole body scans at 24 h p.i. than after 6 h p.i. (score 2.01 vs. 0.93 respectively).

Discussion

In this study, the sensitivity, specificity, positive and negative predictive values were equal for both CIM and SRS, when considering the presence of the disease in a patient (Table 4). The result of sensitivity for CIM, which is in the range of 71%-91%,^{14,15} in our case can be explained on the basis of inclusion criteria. In 14 out of 15 patients, the diagnosis was established before scintigraphy. On the other hand, at the time of presentation, 50% of patients had liver metastases which were diagnosed by CT or ultrasound. CIM missed a patient with

Table 3. Summary of ^{111}In -octreotide scintigraphy and conventional imaging modalities (CIM) results in Groups A and B

	CIM			^{111}In		
	Group A	Group B	Total	Group A	Group B	Total
primary site	1	0	1	1	4	5
liver metastasis	5	3	8	4	3	7
extrahepatic lesion	5	1	6	4	0	4

Table 4. Evaluation of conventional imaging modalities and ^{111}In -octreotide scintigraphy in carcinoid tumor

	per patient		per lesion	
	CIM	In-111	CIM	In-111
sensitivity	89%	89%	69%	88%
specificity	100%	100%	100%	100%
positive predictive value	100%	100%	100%	100%
negative predictive value	80%	80%	82%	92%

clinical suspicion of carcinoid in whom SRS revealed a mediastinal accumulation, subsequently confirmed by repeated CT as mediastinal tumor, presumably thymoma. The sensitivity of SRS was in the expected range of 73% to 89% for the patients with carcinoid tumors.^{8,9,14} SRS missed a liver metastasis.

SPECT was positive in 7 of 8 patients with liver metastases (sensitivity 88%). This is in accordance with a recent report¹⁶ and supported by previous studies indicating the superiority of SPECT (Figure 4.) over planar imaging in detecting liver metastases.^{15,17}

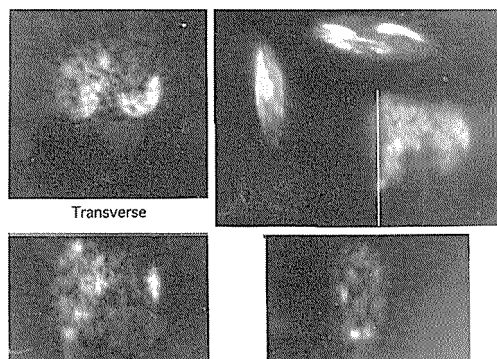


Figure 4. ¹¹¹In-octreotide SPECT of the liver. Transversal, coronal and sagittal slices. Multiple liver metastases in patient with bronchial carcinoid.

The sensitivity and negative predictive value for the detection of a single lesion were in favor of scintigraphy, on the account of detecting more primary and solid extrahepatic lesions (Tables 2 and 3). These SRS results are comparable to the results of previous studies.^{14,16,18} Factors affecting relatively low sensitivity of SRS for primary carcinoid sites are discussed elsewhere,^{15,16,19} adding to them site or even origin of carcinoid tumor. In vitro studies of carcinoid tumor receptor affinity for radiolabeled somatostatin analogues revealed that greater proportion of bronchial carcinoids had lower affinity for radioligand examined in comparison to carcinoids of midgut origin.⁵ Further, in vivo sensitivity for primary carcinoid site in the studies where

patients with carcinoids of foregut and midgut origin were included detection was about 50%.^{16,19} Indeed, in the studies enrolling only patients with carcinoids of midgut origin the sensitivity for the detection of primary site of carcinoids ranged from 70% to 87%.^{18,20}

In 2 patients, scintigraphy was performed under somatostatin treatment, which did not preclude the detection of liver and extrahepatic metastases. This contradicts the report of Schillaci^{5,21} and supports the observations that somatostatin treatment in carcinoid patients indeed enhances the tumor to background ratio.^{22,23}

The specificity of SRS can be compromised by nonspecific bowel accumulation due to biliary excretion, the intensity of which significantly increases on 24 h scintigrams making patients preparation with laxatives mandatory in non diarrhea patients.⁹ The variations in shape and position of the spleen and kidneys and concomitant diseases expressing somatostatin receptors are further potential sources of false positive findings.^{1,24,25} Two patients with an enlargement of suprarenal glands on CT and negative SRS were excluded from the final analysis because the nature of the lesions had not been established yet. If these lesions were confirmed not to represent carcinoid spread, this would indicate that unrelated suprarenal masses in carcinoid patients could cause false positives on conventional imaging modalities.

Conclusion

¹¹¹In-octreotide scintigraphy encompasses the whole body and can be advocated as an imaging modality of choice in patients suspected of having carcinoid tumor, especially in the search for primary site and extrahepatic spread. In patients with documented disease high predictive value of positive and negative

scintigraphic findings justifies its use in the evaluation of the spread of the disease. Bowel preparation with laxatives before SRS is recommended. Further investigations on affinity for binding of somatostatin analogues, depending on carcinoid origin, can be proposed.

References

1. Krenning EP, Kwekkeboom DJ, Bakker WH, Breeman WAP, Kooij PPM, Oei HY, et al. Somatostatin receptor scintigraphy with [^{111}In -DTPA-D-Phe 1]- and [^{123}I -Tyr-3]-octreotide: the Rotterdam experience with more than 1000 patients. *Eur J Nucl Med* 1993; **20**: 716-31.
2. Lefebvre H, Jégou S, Leroux P, Dero M. Characterization of the somatostatin receptor subtype Ia in a bronchial carcinoid tumor responsible for Cushing's syndrome. *J Clin Endocrinol Metab* 1995; **80**: 1423-8.
3. John M, Meyerhof W, Richter D, Waser B, Schaefer J-C, Scherl H, et al. Positive somatostatin receptor scintigraphy correlates with the presence of somatostatin receptor subtype 2. *Gut* 1996; **38**: 33-9.
4. Nilsson O, Kölbly L, Wängberg B, Wigander A, Billib H, William-Olsson L, et al. Comparative studies on the expression of somatostatin receptor subtypes, outcome of octreotide scintigraphy and response to octreotide treatment in patients with carcinoid tumors. *B J Cancer* 1998; **77**: 632-7.
5. Reubi JC, Kvols KJ, Waser B, Nagorney DM, Heity PU, Charboneau JW, et al. Detection of somatostatin receptors in surgical and percutaneous needle biopsy samples of carcinoid and islet cell carcinomas. *Cancer Res* 1990; **50**: 5969-77.
6. Kisker O, Weinell RJ, Geks J, Zacara F, Joseph K, Rothmund M, et al. Value of somatostatin receptor scintigraphy for preoperative localization of carcinoids. *World J Surg* 1996; **20**: 162-7.
7. Kwekkeboom DJ, Krenning EP, Bakker WH, Oei HY, Kooij PPM, Lamberts SWJ. Somatostatin analogue scintigraphy in carcinoid tumors. *Eur J Nucl Med* 1993; **20**: 283-92.
8. Krenning EP, Kwekkeboom DJ, Reubi JC, Lamberts SWJ. Somatostatin receptor scintigraphy. In: Sandler MP, Coleman RE, Wackers FJT, editors. *Diagnostic nuclear medicine*. Baltimore: Williams & Wilkins; 1996. p. 1047-66.
9. Joseph K. Nuklearmedizinische Methoden zur Lokalisation von Tumoren des endokrinen und des neuroendokrinen Systems. *Nuklearmediziner* 1996; **19**: 287-303.
10. Krenning EP, Bakker WH, Kooij PPM, Breeman WAP, Oei HY, de Jong M, et al. Somatostatin receptor scintigraphy with indium-111-DTPA-D-Phe-1-octreotide in man: metabolism, dosimetry and comparison with 123I-Tyr-3-octreotide. *J Nucl Med* 1992; **33**: 652-8.
11. McNeil BJ. Guidelines for evaluating new tests. In: Rocha AFG, Harbert JC, editors. *Textbook of nuclear medicine: clinical applications*. Philadelphia: Lea & Febiger 1979. p. 473-84.
12. Kwekkeboom DJ, Lamberts SWJ, Habbema JDF, Krenning EP. Cost-effectiveness analysis of somatostatin receptor scintigraphy. *J Nucl Med* 1996; **37**: 886-92.
13. Lebtahi R, Cadiot G, Sarda L, Daou D, Faraggi M, Petegnief Y, et al. Clinical impact of somatostatin receptor scintigraphy in the management of patients with neuroendocrine gastroenteropancreatic tumors. *J Nucl Med* 1997; **38**: 853-8.
14. Jamar F, Fiasse R, Leners N, Pauwels S. Somatostatin receptor imaging with indium-111-pentetreotide in gastroenteropancreatic neuroendocrine tumors: safety efficacy and impact on patient management. *J Nucl Med* 1995; **36**: 542-9.
15. Krenning EP, Kwekkeboom DJ, Pauwels S. Somatostatin receptor scintigraphy. In: Freeman LM, editor. *Nuclear medicine annual* 1995. New York: Raven Press; 1995. p. 1-50.
16. Chiti A, Fanti S, Savelli G, Romeo A, Bellanova B, Rodari M, et al. Comparison of somatostatin receptor imaging, computed tomography and ultrasound in the clinical management of neuroendocrine gastro-entero-pancreatic tumors. *Eur J Nucl Med* 1998; **25**: 1396-403.
17. Schillaci O, Scorpino F, Angeletti S, Tavolaro R, Danieli R, Annibale B, et al. SPECT improves accuracy of somatostatin receptor scintigraphy in abdominal carcinoid tumors. *J Nucl Med* 1996; **37**: 1452-6.
18. Ahlman H, Wängberg B, Tisell LE, Nilsson O, Fjälling M, Forssell-Aronsson E. Clinical efficacy of octreotide scintigraphy in patients with midgut carcinoid tumors and evaluation of intraoperative scintillation detection. *B J Surg* 1994; **81**: 1144-9.
19. Meko JB, Doherty GM, Siegel BM, Norton JA. Evaluation of somatostatin-receptor scintigraphy

- for detecting neuroendocrine tumors. *Surgery* 1996; **120**: 975-84.
20. Dresel S, Tatsch K, Zachoval R, Hahn K. ^{111}In -Octreotide and ^{123}I -MIBG scintigraphy for imaging carcinoids and its metastases. Results of a comparative investigation. *Nuclearmedizin* 1996; **35**: 53-8.
21. Schillaci O, Annibale B, Scopinaro F, Delle Fave G, Colella AC. Somatostatin receptor scintigraphy of malignant somatostatinoma with indium-111 pentetreotide. *J Nucl Med* 1997; **38**: 886-7.
22. Briganti V, Manelli M, La Cava G, Peri A, Meldolesi U, Masi R, et al. Characterizing of ectopic secreting carcinoid with indium-111-DTPA-d-phe-pentetreotide. *J Nucl Med* 1997; **38**: 711-4.
23. Dörr U, Räh U, Sautter-Bihl ML, Guzman G, Bach D, Adrian HJ, et al. Improved visualization of carcinoid liver metastases by indium-111 pentetreotide scintigraphy following treatment with cold somatostatin analogue. *Eur J Nucl Med* 1993; **20**: 431-3.
24. Berní L, Chico A, Matúas-Guiu X, Mato E, Catafau A, Alosa A, et al. Use of somatostatin analogue scintigraphy in the localization of recurrent medullary thyroid carcinoma. *Eur J Nucl Med* 1998; **25**: 1482-8.
25. Lebtahi R, Cadiot G, Marmuse JP, Vissuzaine C, Petengnif Y, Courllion-Mallet A, et al. False-positive somatostatin receptor scintigraphy due to an accessory spleen. *J Nucl Med* 1997; **38**: 1977-81.

Adenocarcinoma skin metastases treated by electrochemo therapy with cisplatin combined with radiation

Gregor Serša, Maja Čemažar, Zvonimir Rudolf and Albert P. Fras

Institute of Oncology, Ljubljana, Slovenia

Background. The aim of this study was to determine the interaction between electrochemotherapy as a means of facilitated cisplatin delivery into the cells and irradiation of adenocarcinoma skin metastases.

Case report. A patient with progressive disease presenting skin metastases of tubal dedifferentiated papillary adenocarcinoma was enrolled in the study. Skin metastases were treated by electrochemotherapy with intratumoral injection of cisplatin. Its antitumor effectiveness was compared to that of combined treatment of irradiation with electrochemotherapy. After a two week observation time, the response to treatment was comparable between the electrochemotherapy and electrochemotherapy combined with irradiation. Both of these treatments were more effective than irradiation alone. Furthermore, antitumor effectiveness of the combined electrochemo- and radiotherapy was found to be quicker than that of electrochemotherapy alone.

Comment. This study shows that electrochemotherapy with cisplatin is also effective in the treatment of adenocarcinoma skin metastases. In spite of the short observation time, positive interaction between radiotherapy and electrochemotherapy with cisplatin was found.

Key words: skin neoplasms - secondary - therapy; adenocarcinoma; electric stimulation therapy; cisplatin; electrochemotherapy

Introduction

Cisplatin has been reported to enhance the cytotoxicity of radiation in many preclinical studies, *in vitro* on cells, as well as in tumor bearing animals.¹⁻⁶ In addition, cisplatin is used in combination with radiotherapy in treatment of a number of solid tumors.⁶

Since the presence of cisplatin during irradiation is essential for radiosensitization of tumor cells, several drug delivery systems were employed in order to increase intracellular accumulation of the drug.²⁻⁴ Among the drug delivery systems that have been tested *in vivo* is also electroporation.⁷ This is a physical method of drug delivery that temporarily and reversibly increases plasma membrane permeability and thereby facilitates intracellular accumulation of molecules such as drugs, dyes, antibodies and DNA.⁸ When electroporation is combined with chemotherapeutic drugs, the treatment is termed electrochemotherapy.⁸

Received 30 September 1999

Accepted 29 October 1999

Correspondence to: Gregor Serša, Ph.D., Institute of Oncology, Zaloška 2, SI-1000 Ljubljana, Slovenia. Tel./Fax: +386 61 133 74 10; E-mail: gswersa@onko-i.si

Electrochemotherapy is effective for drugs with a hampered transport through the plasma membrane, but are very cytotoxic once reaching their intracellular targets. Due to the increased accumulation of bleomycin and cisplatin in tumors, which were exposed to electric pulses, the potentiation of bleomycin and cisplatin antitumor effectiveness was demonstrated on several animal tumor models.⁸⁻¹² These two drugs also proved their clinical application in electrochemotherapy protocols both being very effective in the treatment of different cutaneous tumor nodules in cancer patients.¹³⁻¹⁹

Our previous report also indicates that the delivery of cisplatin into the cells by electroporation of tumors increases radiosensitizing effect of cisplatin.⁷ Therefore, the aim of this study was to determine the interaction between electrochemotherapy as a means of cisplatin delivery into the cells and irradiation of adenocarcinoma skin metastases.

Case report

In February 1993 a 53-year old woman was admitted to the Institute of Oncology. After diagnostic laparoscopy, where right adnexal mass was found together with elevated CA 125, she was initially surgically treated. Total abdominal hysterectomy and bilateral salpingo-oophorectomy (TAHBSO), appendectomy, subtotal resection of omentum, and resection of sigmoid colon were performed. No peritoneal implants were present at the time of surgery. Pathohistology of the resected tissue was tubal dedifferentiated papillary adenocarcinoma directly invading omentum, and resected colon. Postoperatively, she continued with cytoxan/paraplatin chemotherapy. On completion of six courses two months later, at second look laparoscopy no residual tumor was present.

Three years later, CA 125 was elevated to 284.6 U/ml. CT scan showed a mass in the

true pelvis left. An ultrasound guided aspiration biopsy was made, and in the bioptic material, malignant metastatic cells were present. A second line chemotherapy cytoxan/paraplatin was introduced. As after six courses of the second line chemotherapy CA 125 did not return to normal value, she was given high voltage irradiation of iliac and paraaortal lymphatic chain. Cumulative dose of 43.5 Gy was delivered in seven weeks. At the end of radiotherapy, CA 125 was still elevated to 108.0 U/ml. She continued with low dose chemotherapy for six months, when supraclavicular metastatic nodes appeared. This region was irradiated with cumulative dose 21 Gy in seven days.

Shortly after the irradiation of supraclavicular nodes, iliac and paraaortal lymphatic chain was irradiated again. The pain in the left leg, indicating on the progression of the disease diminished after 39 Gy irradiation given in three weeks. Three months later suprapubic skin metastases appeared. Skin metastatic spread was observed also in bilateral inguinal regions. Palliative treatment of skin metastases was planned. With progression of recidivant mass in true pelvis ureteral obstruction progressed and one month later the patient died.

Skin metastases were palliatively treated by electrochemotherapy with cisplatin combined with irradiation. Due to a large number of metastases which were up to 20 mm in diameter, it was possible to select groups of metastases that were treated by each modality of the combined treatment (Figure 1). National ethics committee approval and informed consent from the patient was obtained before the beginning of treatment.

Several metastases could not be treated, therefore served as control nodules. Since the observation time was only 11 days, some of them moderately increased in size, whereas in the rest there was no increase.

Electrochemotherapy was performed by the injection of cisplatin to the tumor nodule,

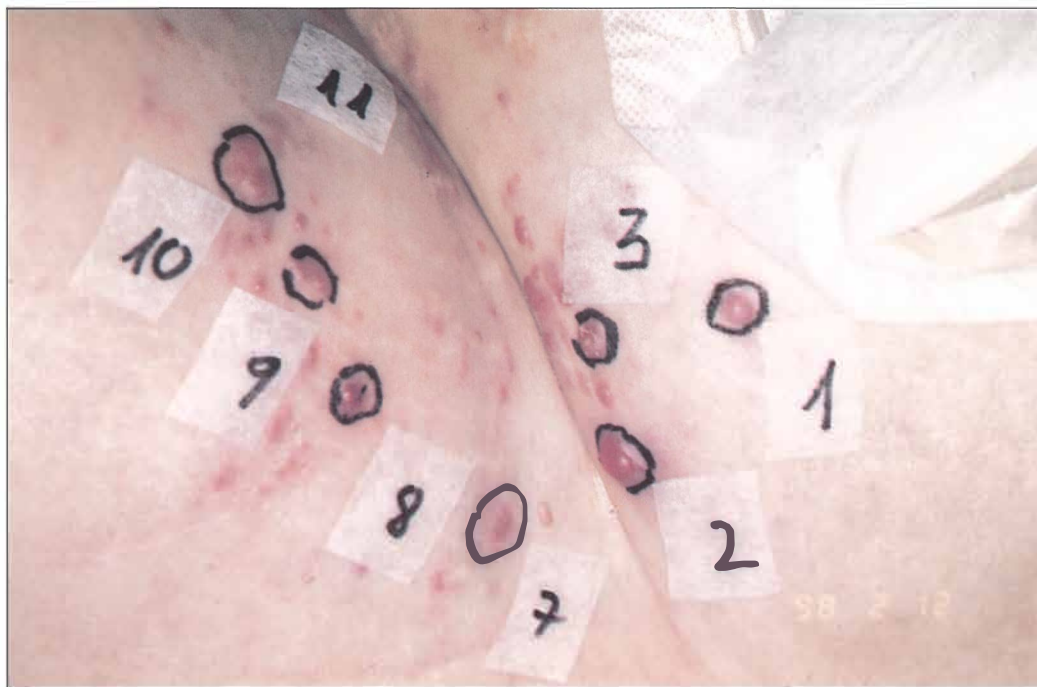


Figure 1. Photograph of tumor nodules on the leg before treatment. Nodules 1,2,3 were treated with electrochemotherapy combined with local tumor irradiation, nodule 7 was treated with electric pulses combined with irradiation, nodule 8 was treated with irradiation as single treatment, nodules 9 and 10 were treated with electrochemotherapy and nodule 11 with electric pulses alone. Several unmarked nodules are also present, that were not treated and served as controls.

one to two minutes thereafter electric pulses were applied to the tumor. Cisplatin (Platamine, Pharmitalia) was given at the dose of $1\text{mg}/100\text{ mm}^3$ tumor volume. Square wave electric pulses of $100\text{ }\mu\text{sec}$, 910 V amplitude (amplitude to electrode distance ratio 1300 V/cm), frequency 1 Hz were delivered through two parallel stainless steel electrodes (thickness, 1 mm ; width, 7 mm ; length, 14 mm , with rounded tips and inner distance between them 7 mm) with an electropulsator Jouan GHT 1287 (Jouan, France). Each run of electric pulses was delivered in two trains of four pulses, with one second interval in between the two trains, in two perpendicular directions. Good contact between the electrodes and skin was assured by conductive gel. Eleven days after the treatment, the metastases that were treated by cisplatin

alone or exposed to electric pulses alone, were the same size as before the treatment. When both treatments were combined in electrochemotherapy protocol, the treated nodules responded well. They reduced in size, so that under the scab no tumor tissue was palpable, and after 11 days the response to the treatment was evaluated as complete (Figure 2).

Irradiation of tumor nodules was performed by therapeutic X-ray. The dose of 15 Gy was moderated by the tubus of the suitable size. Irradiation of the tumor nodules, as single treatment, had no effect on the growth of the tumor nodules (Figure 2). No effect of the treatment was observed either when irradiation was combined with each of the modalities that were used in electrochemotherapy; cisplatin, and application of electric

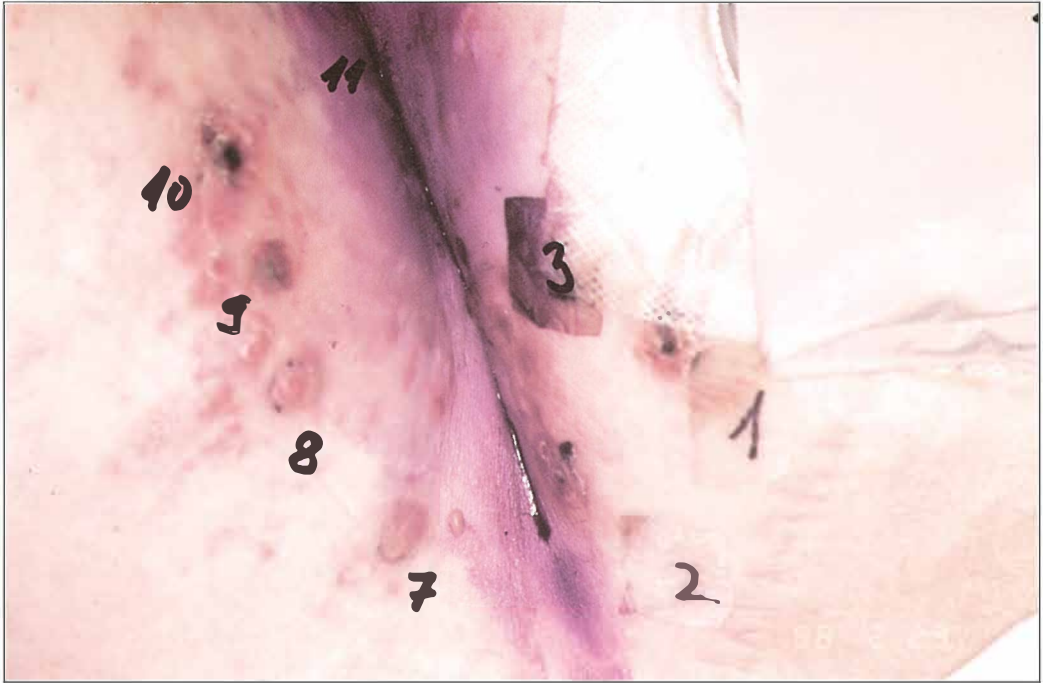


Figure 2. Photograph of the same tumor nodules 11 days after the treatment. Nodules that were treated with electrochemotherapy combined with irradiation responded to the treatment quick. The scab that was formed within two days after the treatment on the tumor nodule 2 and 3 fell off already before day 11. Nodules that were treated with electrochemotherapy (nodules 9,10) also responded well, however the scab is still present. No effect on growth of tumor nodules was observed after irradiation alone, or when combined with application of electric pulses (nodules 7,8).

pulses (Figure 2). Whereas, when electrochemotherapy was combined with irradiation, quick and complete reduction of the size of the treated nodules was observed, within the observation time (Figure 2). Although in both, electrochemotherapy alone and combined with irradiation, the response to the treatment was complete, the effect was found to be quicker after electrochemo-radiotherapy.

Comment

This case report demonstrates that electrochemotherapy with cisplatin is effective in treatment of adenocarcinoma skin metastases. In spite of the short observation time, positive interaction between electrochemotherapy with cisplatin and radiotherapy was found.

Electrochemotherapy has already proved to be effective in the treatment of cutaneous and subcutaneous tumor nodules of different tumor types. In several studies, it was shown that electrochemotherapy with bleomycin is effective in the treatment of adenocarcinoma, however this is the first report demonstrating antitumor effectiveness of electrochemotherapy with cisplatin on this tumor type.¹³

Electrochemotherapy combines electroporation as a drug delivery system with local or systemic drug administration. If the drug used is cytotoxic, when reaching its intracellular targets, increased cytotoxicity is observed. This was demonstrated in the electrochemotherapy with cisplatin *in vitro*, on experimental tumor models in mice and in patients with cutaneous tumor nodules.^{10-12,15,17}

If the drug used in electrochemotherapy is also radiosensitizer, its increased accumulation in tumor cells may lead to better antitumor effectiveness of radiotherapy. In our previous study, we demonstrated that electroporation of mouse tumors increases radiosensitizing effect of cisplatin by 20%. The number of complete responses was increased from 73% in the group of mice treated by cisplatin and irradiation to 92% when electroporation was used as drug delivery for cisplatin combined with irradiation.⁷ Treatment of this patient was planned on these preclinical data. Due to a large number of skin tumor nodules, it was impossible to treat them all, and this enabled us to have also pertinent control groups, treated as single or in combination of the two modalities.

This three modality treatment proved its effectiveness in the treatment of adenocarcinoma skin metastases, and form the basis for further studies elaborating electroporation as a nonspecific drug delivery for radiosensitizing and bioreductive drugs in radiotherapy.

Acknowledgement

This work was supported by research grant from the Ministry of Science and Technology of the Republic of Slovenia.

References

1. Britten RA, Evans AJ, Allalunis-Turner MJ, Pearcey RG. Effect of cisplatin on the clinically relevant radiosensitivity of human cervical carcinoma cell lines. *Int J Radiat Oncol Biol Phys* 1996; 34: 367-74.
2. Yapp DTT, Lloyd DK, Zhu J, Lehnert SM. Tumor treatment by sustained intratumoral release of cisplatin: Effects of drug alone and combined with radiation. *Int J Radiat Oncol Biol Phys* 1997; 39: 497-504.
3. Theon AP, Madewell BR, Ryu J, Castro J. Concurrent irradiation and intratumoral chemotherapy with cisplatin: A pilot study in dogs with spontaneous tumors. *Int J Radiat Oncol Biol Phys* 1994; 29: 1027-34.
4. Begg AC, Deurloo MJ, Kop W, Bartelink H. Improvement of combined modality treatment with cisplatin and radiation using intratumoral drug administration in murine tumors. *Radiother Oncol* 1991; 31: 129-33.
5. Geldof AA, Kruit A, Newling DW, Slotman BJ. Synergism between cisplatin and radiotherapy in an *in vitro* prostate tumor cell line. *Anticancer Res* 1999; 19: 505-8.
6. Dewitt L. Combined treatment of radiation and cis-diamminedichloroplatinum (II): A review of experimental and clinical data. *Int J Radiat Oncol Biol Phys* 1987; 13: 403-26.
7. Serša G, Kranjc S, Čemažar M. Improvement of combined modality therapy with cisplatin and radiation using electroporation of tumors. *Int J Radiat Oncol Biol Phys* 1999; in press.
8. Mir LM, Orlowski S. Mechanisms of electrochemotherapy. *Adv Drug Deliver Rev* 1999; 35: 107-18.
9. Mir LM, Orlowski S, Belehradek JrJ, Paoletti C. Electrochemotherapy potentiation of antitumor effect of bleomycin by local electric pulses. *Eur J Cancer* 1991; 27: 68-72.
10. Serša G, Čemažar M, Miklavčič D. Antitumor effectiveness of electrochemotherapy with cis-diamminedichloroplatinum(II) in mice. *Cancer Res* 1995; 55: 3450-5.
11. Čemažar M, Miklavčič D, Ščančar J, Dolžan V, Golouh R, Serša G. Increased platinum accumulation in SA-1 tumor cells after *in vivo* electrochemotherapy with cisplatin. *Br J Cancer* 1999; 79: 1386-91.
12. Čemažar M, Milačič R, Miklavčič D, Dolžan V, Serša G. Intratumoral cisplatin administration in electrochemotherapy: antitumoreffectiveness, sequence dependence and platinum content. *Anti-Cancer Drugs* 1998; 9: 525-30.
13. Mir LM, Glass LF, Serša G, Teissie J, Domenge C, Miklavčič D, et al. Effective treatment of cutaneous and subcutaneous malignant tumors by electrochemotherapy. *Br J Cancer* 1998; 77: 2336-42.
14. Rudolf Z, Štabuc B, Čemažar M, Miklavčič D, Vodovnik L, Serša G. Electrochemotherapy with bleomycin: The first clinical experience in malignant melanoma patients. *Radiol Oncol* 1995; 29: 229-35.

15. Serša G, Štabuc B, Čemažar M, Jančar B, Miklavčič D, Rudolf Z. Electrochemotherapy with cisplatin: Potentiation of local cisplatin antitumor effectiveness by application of electric pulses in cancer patients. *Eur J Cancer* 1998; **34**: 1213-18.
16. Heller R, Gilbert R, Jaroszeski MJ. Clinical applications of electrochemotherapy. *Adv Drug Deliver Rev* 1999; **35**: 119-29.
17. Serša G, Štabuc B, Čemažar M, Miklavčič D, Rudolf Z. Electrochemotherapy with cisplatin: Clinical experience in malignant melanoma patients. *Clin Cancer Res* in press
18. Panje WR, Harrell E, Hier M, Goldman A, Garman GR, Bloch I. Electroporation therapy of head and neck cancer. *Ann Oto Rhinol Laryn* 1998; **107**: 779-85.
19. Kubota Y, Mir LM, Nakada T, Sasagawa I, Suzuki H, Aoyama N. Successful treatment of metastatic skin lesions with electrochemotherapy. *J Urol* 1998; **160**: 1426.

Reorganization of microtubules in V-79 cells after treatment with cytohalasin B

Aleš Iglič¹, Urška Batista², Peter Veranič³

¹Faculty of Electrical Engineering, ²Institute of Biophysics and ³Institute of Cell Biology, Medical Faculty, University of Ljubljana, Slovenia

Background. The aim of this work was to study the configuration of the microtubules in the cytochalasin B treated V-79 cells in connection to the cell shape and to see whether there are any similarities to the phenomena taking place in phospholipid vesicles.

Subjects and methods. An experiment was performed where cytochalasin B was added to the V-79 cells (lung fibroblasts of Chinese hamster).

Results. The cell shape changed from an elongated one into the shape with a profile resembling the Greek letter ϕ . The microtubules were found to be organized into a rod within the symmetry axis of the cell.

Conclusion. As similar shapes were previously observed also in the phospholipid vesicles with entrapped microtubule rods, our results support the hypothesis that similar physical mechanisms may pertain in simple systems as well as in living cells.

Key words: cell culture - drug effects; cytochalasin B; microtubules -drug effects

Introduction

The cytoplasm of eucaryotic cells is spatially organized by a network of protein filaments - the cytoskeleton which contains three main types of filaments: microtubules, actin filaments, and intermediate filaments. Actin filaments are dynamic structures. They are organized into an actin cortex, a layer just beneath the plasma membrane, and thin stress fibers within the cells.¹ Actin-rich cortex as well as the cytoskeleton within the cytoplasm deter-

mine the mechanical properties of the cell and therefore control the shape of most animal cells.²

It was previously observed that the disintegration of the cytoskeleton affects the morphology of the fibroblasts grown in culture.³ Cytochalasin B prevents actin polymerization to actin filaments. By disrupting the equilibrium of depolymerization-polymerization, the addition of cytochalasin B causes disaggregation of the actin filaments while it has no direct effect on microtubules.⁴ However, upon disaggregation of the actin filaments, the microtubules may get reorganized as their interactions with the surrounding structures are changed. The reorganization of the cytoskeleton may affect the cell shape. In

Correspondence to: Assist Prof. Aleš Iglič, Ph.D. Faculty of Electrical Engineering, University of Ljubljana; Tržaška 25, SI-1000 Ljubljana, Slovenia; Tel: +386-61-1768-235; Fax: +386-61-1264-630; E-mail: ales.iglic@fe.uni-lj.si

cytochalasin B treated cells, the effect of the actin filaments on the cell shape is diminished while the effect of the microtubule configuration on the cell shape becomes pronounced.

The distortion of the shape by entrapped microtubules was studied on the phospholipid vesicles.^{5,6} The tubulin, encapsulated by the vesicles, polymerized and assembled into a rod within the vesicle. The rod grew and increased in length, causing initially a sphere-to-ellipsoid change in shape while, upon further growth of the rod, the vesicle developed regions of negative curvature and eventually transformed into a shape that had a profile resembling the Greek letter ϕ . The effect of the microtubule rod on the vesicle shape was also theoretically described by taking into account the elastic properties of the vesicle membrane.⁵⁻⁸

We observed that after addition of the cytochalasin B the shape of the body of the V-79 cells transformed from elongated to more globular while the cell took the ϕ shape. On the basis of the similarity with the observed morphology of the phospholipid vesicles with entrapped microtubule rods we assumed that the shape transformation of the V-79 cells is due to physical mechanisms similar to the ones taking place in phospholipid vesicles. Therefore, we wanted to determine whether the microtubules would get organized into a rod-like structure within the cell.

The aim of this work was to study the configuration of the microtubules in the cytochalasin B treated V-79 cells in connection to the cell shape and to see whether there are any similarities to the phenomena taking place in phospholipid vesicles.

Materials and methods

Cells

The V-79-379 A (diploid lung fibroblasts of Chinese hamster) were grown in Eagle MEM

(minimal essential medium - GIBCO) supplemented with 10% fetal calf serum (FCS - FLOW), penicillin (100U/ml) and streptomycin (100 μ g/ml) at 37°C in a CO₂ incubator.

Cytochalasin B treatment

The cells ($2 \cdot 10^5$) were seeded in 50mm plastic Petri dishes. After 24 hours, the cells were treated with cytochalasin B (SIGMA) (final concentration of 2 μ g/ml) for one hour. At first, the cells were observed with a phase contrast microscope and then prepared for tubulin staining. The cells were simultaneously fixed and permeabilized with a mixture of 4% formaldehyde, microtubule stabilizing buffer⁹ and 0.5% Triton at 37°C for 30 min. After washing in PBS and blocking an unspecific labelling with 1% BSA, the cells were immunolabelled with monoclonal anti β -tubulin (SIGMA) over night. The FITC-labelled secondary antibodies (SIGMA) were applied for 2 hours at 37°C. After washing the cells were mounted in vectashield with DAPI (VECTOR) and examined in fluorescent microscope (LEITZ Laborlux S).

Results and discussion

The morphological appearance of control V79 fibroblasts in cell culture was flat and mainly spread over the substrate while the microtubules were radially oriented within the cell body (Figure 1). After cytochalasin B treatment, the cell body became globular and the area of contact with the substrate diminished while the cell exhibited long cylindrical protrusions (Figure 2). With time, the cells more and more resembled the ϕ shape. The fluorescence microscope image showed that the microtubules were organized into rod-like structures emanating from the nuclear area (Figure 2).

While observing the ϕ shape of the cell in the phase contrast microscope, our assump-

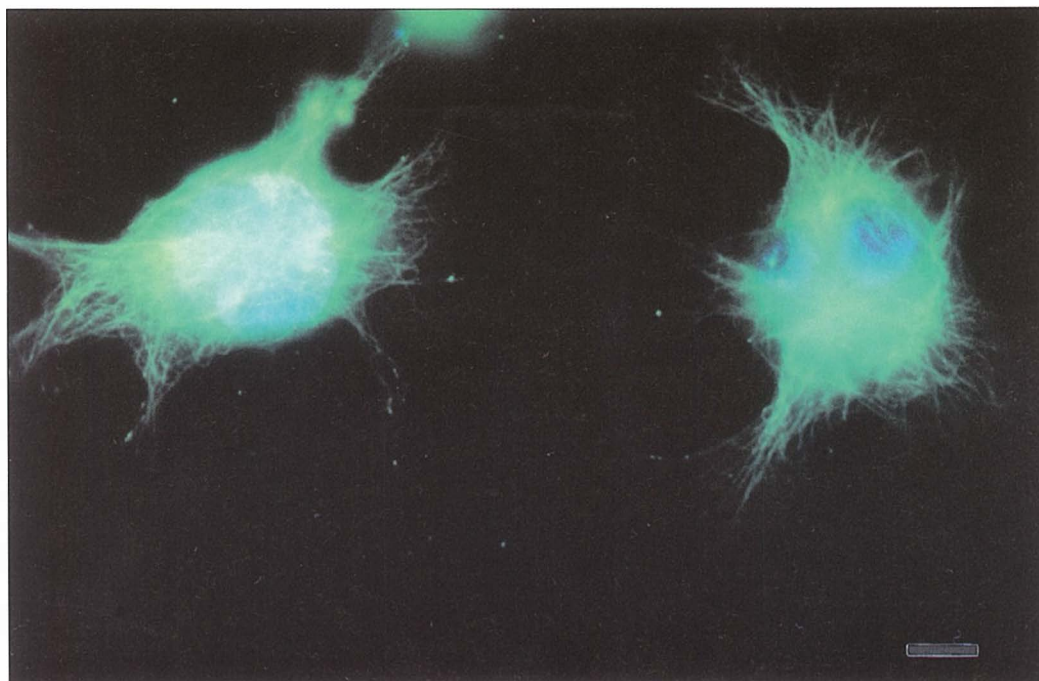


Figure 1. Control V-79 cells observed in fluorescence microscope showing the microtubules labelled with FITC (green) and nucleus with DAPI (blue). Bar - 10 μ m.

tion that there is a rod-like structure acting upon the membrane was therefore confirmed. A similarity can be drawn from the ϕ shape of V-79 cell with long tubular protrusions containing microtubule rod, and the shape of the phospholipid vesicle with a long entrapped microtubule rod.⁶ There is however a major difference in interpreting the origin of the stability of the shape in phospholipid vesicles and in V-79 cells. In the determination of the shape of the phospholipid vesicles, the membrane bending energy is minimized at relevant geometrical constraints.¹⁰ On the other hand, the fibroblasts are modelled as fluid drops bounded by actin cortex under persistent tension and possessing area elasticity.¹¹ The plasma membrane usually exhibits wrinkling, in contrast to the surface of the phospholipid vesicles where it is smooth.

There could be many possible reasons responsible for the microtubule reorganiza-

tion after disaggregation of the actin filaments. In the experiments with phospholipid vesicles, the microtubules spontaneously associated into rodlike structure indicating that such configuration is energetically favourable. These processes could also be present in the cytochalasin B treated cells. However, in intact cells, the microtubules in the cell body have radial orientation that is maintained by the integrity of the whole cytoskeleton. After the disaggregation of the actin filaments, the radial orientation of the tubules may become unfavourable as the surface structure would impose a force on the microtubules leading to the bending of the microtubules. The microtubules may redistribute as to avoid energetically unfavourable bending.

In order to explain the observed shape of V-79 cells treated by cytochalasin B in more detail, additional experimental evidence



Figure 2. V-79 cells after treatment with cytochalasin B for 60 min in fluorescence microscope. Bar - 10 μ m.

should first be collected. It should be established to what extent the membrane cortex has been preserved. Also, it would be of interest to see whether the wrinkling of the plasma membrane is increased with respect to untreated cells.

A related effect has been observed also in the erythrocytes of the patients with the sickle-cell disorder. These cells in the deoxygenated blood develop long protrusions of the membrane which apparently are caused by polymerized hemoglobin S in the cell interior.¹²

Conclusion

Based on the similarity of the shape of the cytochalasin B treated cells and phospholipid vesicles with entrapped rod-like structure, we suggest that the elastic properties of the surface structure determine the shape of the cytochalasin B treated cells as well as of the

phospholipid vesicles subject to tension. Our results also support the hypothesis¹³ that the shape of the intact cells is mainly determined by the configuration of the actin filaments.

References

1. Alberts B, Bray D, Lewis J, Raff M, Roberts K, Watson JD. *Molecular Biology of the Cell* (1994) Garland Publishing Inc., New York & London; p. 787-846.
2. Gupta PD, Nandini R, Rao KS. Hormone-induced changes in cell shape: role of cytoskeletal proteins. *Cytobios* 1996; **86**: 75-111.
3. Keller HU, Zimmermann A. Shape changes and chemokinesis of Walker 256 carcinosarcoma cells in response to colchicine, vinblastine, nocodazole and taxol. *Invasion Metastasis* 1986; **6**: 33-43.
4. Ostlund RE, Leung JT jr, Hajek SV. Regulation of microtubule assembly in cultured fibroblasts. *J Cell Biol* 1980; **85**: 386-91.
5. Fygenson DK, Marko JF, Libchaber A. Mechanics of microtubule-based membrane extension. *Phys Rev Lett* 1997; **79**: 4497-50.

6. Emsellem V, Cardoso O, Tabeling P. Vesicle deformation by microtubules: A phase diagram. *Phys Rev E* 1998; **58**: 4807-10.
7. Božič B, Svetina S, Žekš B. Theoretical analysis of the formation of membrane microtubes on axially strained vesicles. *Phys Rev E* 1997; **55**: 5834-42.
8. Umeda T, Nakajima H, Hotani H. Theoretical analysis of shape transformations of liposomes caused by microtubule assembly. *J Phys Soc Japan* 1998; **67**: 682-8.
9. Bell PB, Safiejko-Mroccka B. Improved methods for preserving macromolecular structures and visualizing them by fluorescence and scanning electron microscopy. *Scan Micro* 1995; **9**: 834-60.
10. Deuling HL, Helfrich W. The curvature elasticity of fluid membranes: A catalogue of vesicle shapes. *J Phys (Paris)* 1976; **37**: 1335-45.
11. Thoumine O, Cardoso O, Meister J. Changes in the mechanical properties of fibroblasts during spreading: a micromanipulation study. *Eur Biophys J* 1999; **28**: 222-34.
12. Bunn HF, Forget BG. *Hemoglobin: molecular, genetic and clinical aspects*. Philadelphia: Saunders Company; 1995.
13. Tsai MA, Waugh RE, Keng PC. Passive mechanical behavior of human neutrophils: Effects of colchicine and paclitaxel. *Biophys J* 1998; **74**: 3282-91.

Comparison of colorimetric MTT and clonogenic assays for irradiation and cisplatin treatment on murine fibrosarcoma SA-1 cells

Maja Čemažar, Darja Marolt, Mira Lavrič and Gregor Serša

Department of Tumor Biology, Institute of Oncology Ljubljana, Slovenia

Background. The aim of our study was to determine the relationship between cell survival of SA-1 tumor cells measured by clonogenic assay and MTT assay after irradiation and cisplatin treatment.

Materials and methods. Survival of SA-1 cells was measured after irradiation (2-8 Gy) and cisplatin treatment (0.05-0.5 μ g/ml) by clonogenic assay performed 7 days after treatment, and by MTT assay performed on day 3, 4, 5, and 7 after the treatment.

Results. The results showed good correlation between MTT assay and clonogenic assay for irradiation doses below 4 Gy. For higher doses good correlation between MTT and clonogenic assay was determined only when MTT assay was performed on day 5 and 7 after the treatment. In the case of cisplatin treatment, similar pattern was observed, good correlation between IC₅₀ values for MTT and clonogenic assay was found when MTT assay was performed on day 5 and 7 after the treatment.

Conclusion. Results of our study confirmed the results of previous studies addressing this topic and further support the use of MTT test as an alternative test for clonogenic test as a predictive assay of tumour response to the radio or chemotherapy.

Key words: sarcoma, experimental-radiotherapy-drug therapy; colony forming units assay; cisplatin; colorimetry-methods; triazoles

Introduction

The use of predictive assays in radio and chemotherapy is getting more and more attention in the last years, especially, because some clinical studies demonstrated good correlation between a predictive assays and clinical response to therapy.¹⁻⁸ Numerous different approaches, such as measurement of either survival or growth of cells, tumour cell kinetics, determination of chromosomal or DNA damage following gene expression and mea-

Received 25 August 1999

Accepted 4 October 1999

Correspondence to: Maja Čemažar, Ph.D., Institute of Oncology, Department of Tumor Biology, Zaloška 2, SI-1000 Ljubljana, Slovenia. Tel: +386 61 323 063 ext. 2933; Fax: +386 61 133 74 10; E-mail: mcemazar@onko-i.si

surement of tumour hypoxia, were tested in order to predict tumour or normal tissue response of particular patient to radio or chemotherapy.⁹⁻¹¹ The rationale of predictive assays is to identify patients before the commencement of therapy, in whom the dose could be either increased or decreased according to the sensitivity of tumour or normal tissue that is determined by predictive assay.⁹⁻¹¹

Clonogenic assay, which measures directly the ability of tumour cells to proliferate, is the predictive assay which has been most often tested in connection with tumour response to radiotherapy. Tumour cell sensitivity showed to be a good predictor of tumour response in some tumour types, however in others this relationship was not determined.¹⁻⁸ There are several drawbacks associated with this test, *i.e.* the non-ability of some tumour cell to form colonies and also quite big costs. Clonogenic assay can also be time consuming in the cases of cells with low plating efficiencies and long doubling times.⁹⁻¹¹

Therefore, several alternative non-clonogenic tests were developed, which measure either growth of the cells or DNA damage. Growth assays estimate survival by comparing the number of viable cells in treated and control groups. Several different methods are currently used for measuring growth of the cells *i.e.* measurements of cells number, dye exclusion, isotope precursor uptake, and measurement of cell metabolism.¹¹⁻¹⁵

One of the latter methods is the MTT (3-(4,5-dimethylthiazol-2-yl)-2,5-diphenyl-tetrazolium bromide) assay.¹² The MTT assay quantifies the ability of viable cells to reduce a yellow tetrazolium salt to purple formazan crystal using the mitochondrial enzyme succinate dehydrogenase. The MTT assay is rapid and semi-automated and was shown in some studies to be a good replacement for clonogenic assay.¹²⁻¹⁷

The aim of this study was to determine the relationship between cell survival of SA-1 tumour cells measured by clonogenic assay

and MTT assay after irradiation and cisplatin treatment.

Materials and methods

Cell line

Fibrosarcoma SA-1 cells (Jackson Laboratory, Bar Harbor, ME) were used in experiments. Cells were grown in Eagle's minimum essential medium (EMEM; Sigma Chemical Co., St. Louis, MO) supplemented with 10% heat-inactivated foetal calf serum (FCS; Sigma). Cells were routinely subcultured twice per week and were maintained in a humidified atmosphere with 5% CO₂ at 37°C. Doubling time of the SA-1 cells was 18 hours.

Determination of relationship between cell number and optical density

To determine the relationship between cell number and optical density exponentially-growing cells were trypsinized and suspended in EMEM supplemented with 10% FCS. The cells were diluted to final concentrations in EMEM and plated in round-bottomed 96-well microtiter plates (Costar, Badhoevedorp, The Netherlands). The cell densities used were 1×10³, 3×10³, 5×10³, 1×10⁴, 1.2×10⁴, 1.5×10⁴, 3×10⁴, 5×10⁴, 7.5×10⁴ and 1×10⁵ cells per well. MTT solution (5 mg/ml; 25 µl) was added to each well after 3 h, which was the time needed for cells to seed. The microtiter plates were then incubated for another 3 hours at 37°C in an incubator containing humidified atmosphere and 5% CO₂. At the end of incubation period the MTT test was performed (see below).

Irradiation

Cells from the exponential growth phase were trypsinized and suspended in EMEM supplemented with 10% FCS, counted and diluted to final concentrations. For clono-

genic assay cells were plated in 60 mm Petri dishes and for MTT assay cells were placed in 100 mm Petri dishes (Costar, Beovendorf, The Netherlands). Cells were irradiated using a 220 kV X-ray Machine (Darpac, Gulmay Medical Ltd, UK) filtered with 0.6 mm Cu and 3 mm Al at a dose rate of 2 Gy/min. After irradiation, 100 µl of cell in EMEM were plated in round-bottomed 96-well microtiter plates (Costar). Final cell densities at particular radiation doses for MTT assay were as follows: 100 cells per well at 0 Gy (control); 100 cells per well at 2.0 Gy; 250 and 300 cells per well at 4.0 Gy; 1000 cells per well at 6.0 Gy; and 1500 cells per well at 8.0 Gy. One column of eight wells was utilised for each irradiation dose. Cell densities at particular radiation doses for clonogenic assay were as follows: 200 cells per Petri dish at 0 and 2.0 Gy; 400 cells at 4.0 Gy; 1500 cells at 6.0 Gy; and 6000 cells per well at 8.0 Gy. The microtiter plates as well as 60 mm Petri dishes were incubated at 37°C in an incubator containing humidified atmosphere and 5% CO₂ for 3, 4, 5 and 7 days. On day 3 50 µl of EMEM and on day 5 25 µl of EMEM were added to each well to provide nutrition for the cells and to compensate media loss due to the evaporation.

MTT test was performed 3, 4, 5 and 7 days after irradiation. Clonogenic assay was performed on day 7. Experiments were repeated four times in duplicates for MTT assay and in triplicates for clonogenic assay.

Treatment with cisplatin

Exponentially growing cells were trypsinized and suspended in EMEM supplemented with 10% FCS at a concentration of 2.2×10^3 cells/ml for MTT assay. Ninety µl of cell suspension was seeded in well and 10 µl of medium containing different cisplatin concentration was added to each well. For clonogenic assay 300 cells were seeded in Petri dish containing 10 ml of medium with specific cisplatin concentration. The cisplatin concentra-

tions used were 0.05, 0.1, 0.2, 0.3 0.4, 0.5 µg/ml. Cells were incubated at 37°C in a humidified atmosphere containing 5% CO₂ for 3, 4, 5 and 7 days. At the end of incubation period MTT test or clonogenic assay were performed as described below.

MTT assay

Survival of SA-1 cells after irradiation and treatment with cisplatin was measured by 3-(4,5-dimethylthiazol-2-yl)-2,5-diphenyl-tetrazolium bromide (MTT) assay. At the end of incubation time (3, 4, 5, or 7 days) MTT solution (25 µl of 5 mg/ml solution) was added to each well and the microtiter plates were further incubated for 3 hours at 37°C. The microtiter plates were then centrifuged at 2000 rpm to collect the formed formazan crystals at the bottom of the rounded shaped wells. EMEM containing MTT solution was carefully removed with a pipette and then the formazan crystals were dissolved in 100 µl of dimethyl sulfoxide (Sigma). The microtiter plates were shaken for 99 seconds to ensure adequate solubilization and the absorbance of the resulting solution was measured at 540 nm using an Anthos microplate reader (Anthos, Austria).

Using the calibration curve, absorbance at different doses was converted to cell number. Plating efficiency (PE) was calculated by dividing the number of cell obtained with the number of cells seeded. Surviving fraction was calculated by dividing the PE of treated cells with PE of the control.

Clonogenic assay

Clonogenic assay was performed 7 days after irradiation or treatment with cisplatin. Colonies were fixed and stained with crystal violet (Sigma). Colonies of less than 50 cells were not counted. Plating efficiency and surviving fraction were calculated for each treatment group.

Statistical analysis

Linear regression was used to fit the experimental data of cell number with corresponding optical densities to obtain the calibration curve and Pearson correlation coefficient was calculated. One-way analysis of variance and Turkey-Keuls test were used to compare the data between clonogenic and MTT assay at different doses.

Results

Calibration

To calculate the surviving fraction after irradiation and cisplatin treatment using the MTT assay the calibration curve was constructed determining the correlation between cell number and optical densities. There was a good reproducibility between replicates and between the experiments with standard errors of the arithmetic mean below 10%. We found a linear relationship between cell number and optical densities (Figure 1). The correlation coefficient between the cell number and optical densities was 0.992. The equation, which described best the experimental data, was

$$y = 2.6 \cdot 10^{-5} x + 0.07.$$

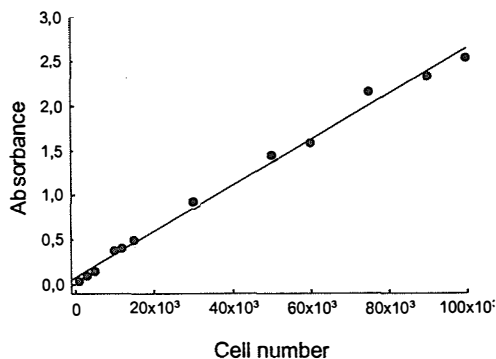


Figure 1. The calibration curve for absorbance against cell number of SA-1 tumour cells. Data represents $AM \pm SE$. Experiments were performed four times in duplicates.

This equation was therefore used in further irradiation and cisplatin treatment experiments to convert the optical density measured into cell number, which allowed us to calculate the surviving fraction of cells when MTT test was employed.

Comparison of assays after irradiation

To determine the correlation between MTT and clonogenic assay, MTT test was performed on day 3, 4, 5 and 7 after the irradiation (Figure 2). Up to 4 Gy dose of irradiation the survival curves were almost identical for all tested groups. However, when MTT test was performed on day 3 the cell kill was not detected for higher doses. Nevertheless, when MTT test was performed on day 5 or 7 very good correlation with clonogenic test was obtained ($r=0.984$ and 0.997 , respectively).

Comparison of assays after cisplatin treatment

To determine the correlation between MTT and clonogenic assay, MTT test was per-

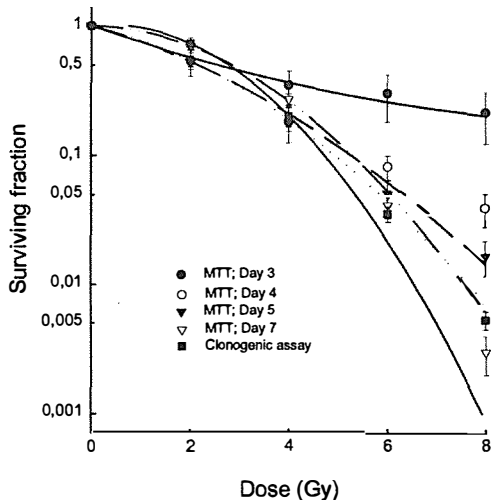


Figure 2. Comparison of cell survival after irradiation measured by clonogenic assay and MTT assay. Data represents $AM \pm SE$. Experiments were performed four times in duplicates.

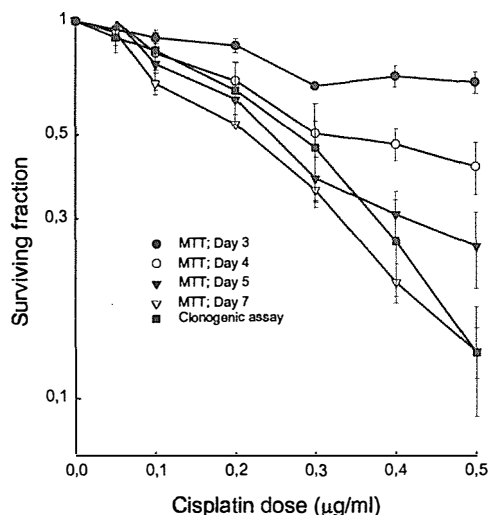


Figure 3. Comparison of cell survival after treatment with cisplatin measured by clonogenic assay and MTT assay. Data represents AMISE. Experiments were performed four times in duplicates.

formed on day 3, 4, 5 and 7 after the cisplatin treatment. MTT assay gave higher IC_{50} value when performed on day 3 or on day 4 ($IC_{50} > 0.5 \mu\text{g/ml}$ and $0.4 \mu\text{g/ml}$, respectively), but good correlation was found between IC_{50} values of MTT assay performed on days 5, and 7 and clonogenic assay ($IC_{50} = 0.25, 0.22$, and $0.28 \mu\text{g/ml}$, respectively).

Discussion

This study shows good correlation between MTT assay and clonogenic assay for irradiation for doses below 4 Gy. For higher irradiation doses the good correlation between MTT and clonogenic assay was determined only when MTT assay was performed on day 5 and 7 after the treatment. In the case of cisplatin treatment, similar pattern was observed, good correlation between IC_{50} values between MTT and clonogenic assay was determined, when MTT assay was performed on day 5 and 7 after the treatment.

The use of MTT assay to measure the number of viable cells depends on the assumption

that the production of formazan crystals and the resultant absorbance is proportional to the number of cells. Linear relationship between absorbance and cell number was previously reported for low cell number up to 1×10^5 .^{13-15,17} For higher cell inoculum the relationship was not linear and therefore surviving fraction could not be calculated by comparing the absorbance with cell number.¹⁸ In our study, we also found a linear relationship between absorbance and cell number. We used low cell inoculum in both, irradiation and chemotherapy experiments therefore, cell number at the end of incubation period did not exceed linearity of the calibration curve. This experimental protocol enabled us to calculate the surviving fraction and thus direct comparison of MTT test with clonogenic assay.

In our experiments on SA-1 tumour cells we found a very good correlation of MTT assay and clonogenic assay when cell were irradiated at 2 Gy. For higher doses, results between both assays correlated well only for longer incubation times in MTT assay. Similar results were published previously testing correlation between MTT and clonogenic assay on different cell lines.^{12,13,18,19} In these studies, some of the tested cell lines did not show good correlation at 2 Gy, but at higher doses, indicating that use of MTT assay can sometimes be restricted by radiation dose ranges.

Use of MTT assay in determining chemosensitivity of tumours was already established.⁵⁻⁷ In a study of Carmichel *et al.* four chemotherapeutic drugs were tested in three cell lines to determine the correlation between MTT and clonogenic assay.¹⁷ They found excellent agreement between the IC_{50} values for melphalan, adriamycin and cisplatin, whereas for vinblastine, MTT assay appeared more sensitive.¹⁷ In this study MTT assay was performed 4 days after the treatment. In our study, good agreement between MTT and clonogenic assay was obtained only when at least 5 days incubation was used in MTT assay, demonstrating that for reliable results incubation time for MTT

assay should be adjusted with regard to the doubling time of tested cells. It should be long enough to allow chemotherapeutic drugs to exert their cytotoxic potential.

In conclusion, results of our study confirmed the results of previous studies addressing this topic and further support the use of MTT test as an alternative test to clonogenic test as a predictive assay of tumour response to the radio or chemotherapy.

Acknowledgement

This work was supported by research grant from the Ministry of Science and Technology of the Republic of Slovenia.

References

1. West CM, Davidson SE, Roberts SA, Hunter RD. The independence of intrinsic radiosensitivity as a prognostic factor for patient response to radiotherapy of carcinoma of the cervix. *Br J Cancer* 1997; **76**: 1184-90.
2. Eschwege F, Bourhis J, Girinski T, Lartigau E, Guichard M, Deble D, et al. Predictive assays of radiation response in patients with head and neck squamous cell carcinoma: A review of the Institute Gustave Roussy experience. *Int J Radiat Oncol Biol Phys* 1997; **39**: 849-53.
3. Brock WA, Baker FL, Peters LJ. Radiosensitivity of human head and neck squamous cell carcinomas in primary culture and its potential as a predictive assay of tumor radiocurability. *Int J Radiat Biol* 1989; **56**: 751-60.
4. Brock WA, Baker FL, Wike JL, Sivon SL, Peters LJ. Cellular radiosensitivity of primary head and neck squamous cell carcinomas and local tumor control. *Int J Radiat Oncol Biol Phys* 1990; **18**: 1283-6.
5. Shaw GL, Gazdar AF, Phelps R, Steinberg SM, Linnoila RI, Johnson BE, et al. Correlation of the in vitro drug sensitivity testing results with response to chemotherapy and survival: Comparison of non-small cell lung cancer and small cell lung cancer. *J Cell Biochem Suppl* 1996; **24**: 173-85.
6. Elledge RM, Clark GM, Hon J, Thant M, Belt R, Maguire YP, et al. Rapid *in vitro* assay for predicting response to fluorouracil in patients with metastatic breast cancer. *J Clin Oncol* 1995; **13**: 419-23.
7. Klumper E, Pieters R, Kaspers GJ, Huismans DR, Loonen AH, Rottier MM, et al. *In vitro* chemosensitivity assessed with the MTT assay in childhood acute non-lymphoblastic leukemia. *Leukemia* 1995; **9**: 1864-9.
8. Strausbol-Gron B, Overgaard J. Relationship between tumour cell in vitro radiosensitivity and clinical outcome after curative for suamous cell carcinoma of the head and neck. *Radiother Oncol* 1999; **50**: 47-55.
9. Peters LJ, Brock WA, Chapman JD Wilson G. Predictive assay of tumor radiocurability. *Am J Clin Oncol*; 1988; **11**: 275-87.
10. West CML: Invited review: Intrinsic radiosensitivity as a predictor of patient response to radiotherapy. *Br J Radiol* 1995; **68**: 827-37.
11. Begg AC. Individualization of radiotherapy. In: Steel GG, editor. *Basic Clinical Radiobiology*. New York: Arnold, London & Oxford University Press; 1997. p. 234-45.
12. Carmichael J, DeGraff WG, Gazdar AF, Minna JD, Mitchell JB. Evaluation of a tetrazolium-based semiautomated colorimetric assay: Assessment of radiosensitivity. *Cancer Res* 1987; **47**: 943-6.
13. Wasserman TH, Twentyman P. Use of colorimetric microtiter (MTT) assay in determining the radiosensitivity of the cells from a murine tumours. *Int J Radiat Oncol* 1988; **15**: 699-702.
14. Plumb JA, Milroy R, Kaye SB. Effects of the pH dependence of 3-(4,5-dimethylthiazol-2-yl)-2,5-diphenyl-tetrazolium bromide-formazan absorption on chemosensitivity determined by a novel tetrazolium-based assay. *Cancer Res* 1989; **49**: 4435-40.
15. Price P, McMillan TJ. The use of non-clonogenic assays in measuring the response of cells in vitro to ionising radiation. *Eur J Cancer* 1994; **30**: 838-41.
16. Watts ME, Roberts IJ, Woodcock M. A comparison of colorimetric and clonogenic assay for hypoxic-specific toxins with hamster and human cells. *Int J Radiat Oncol Biol Phys* 1989; **16**: 939-42.
17. Carmichael J, DeGraff WG, Gazdar AF, Minna JD, Mitchell JB. Evaluation of a tetrazolium-based semiautomated colorimetric assay: Assessment of chemosensitivity testing. *Cancer Res* 1987; **47**: 936-42.
18. Price P, McMillan TJ. Use of the tetrazolium assay in measuring the response of human tumor cells to ionizing radiation. *Cancer Res* 1990; **50**: 1392-6.
19. Slavotinek A, McMillan TJ, Steel CM. Measurement of radiation survival using the MTT assay. *Eur J Cancer* 1994; **30**: 1376-82.

Comparison of four models for calculation of collimator scatter factors of linac photon beams

Dario Faj¹, Matija Bistrovic²

¹Department of Oncology, University Hospital Osijek, 31000 Osijek

²University Hospital for Tumors, Ilica 197, Zagreb, Croatia.

Background. Two approaches for approximation of collimator scatter correction factors of rectangular fields can be found in recent publications. One is based on empirical equations or some more sophisticated physical models using certain parameters which have to be adjusted for a specific machine. The other is based on an earlier proposed idea of decomposition of collimator scatter correction factor function of two variables - into the product of two functions of one variable. In this work four models, based on the decomposition, are compared. All these models are based on the measurement of the output variation while opening one of the two collimator blocks, the other being opened at some fixed value.

Material and methods. The measurements were carried out using nominal 6 MV and 15 MV X-ray beams of a Siemens linac and nominal 6 MV and 18 MV X-ray beams of a Varian linac.

Results and conclusions. It was shown that better approximation can be achieved with a suitable choice of basic measurements and normalisation of data.

Key words: radiotherapy dosage; scattering radiation; photons; collimator scatter, rectangular fields

Introduction

From a review of tumor control dose-response curves a standard requirement of 3.5% has been proposed for the accuracy of the dosimetry of radiotehrapy units.¹ In order to provide this level of accuracy it was recommended to separate collimator (head) and phantom scatter. Namely, as shown by sever-

al authors,²⁻⁵ the collimator scatter correction factor Sc for rectangular fields and, therefore, the total scatter correction factor Scp will differ if the upper and lower collimator jaws are interchanged. The magnitude of this, so called collimator exchange effect (CEE), depends on the construction of the treatment unit head and will be defined as

$$CEE = Sc(x,y) - Sc(y,x).$$

Then the maximum difference is expected as

$$CEE_{max} = Sc(x_{max}, y_{min}) - Sc(x_{min}, y_{max}),$$

where indices min and max indicate the largest and the smallest openings, and x is the opening of the upper, y of the lower collimator jaw. Sc is usually normalised so that

Received 4 October 1999

Accepted 14 October 1999

Corresponding author: Dario Faj, Physicist, Department of Oncology, University Hospital Osijek, J. Huttlera 4, 31000 Osijek, Croatia; Phone: +385 31 511 496; Fax: +385 31 512 222; E-mail: dario_faj@hotmail.com

$Sc(x_{ref}, y_{ref})=1$, while $x_{ref}=y_{ref}=10$ cm at nominal distance.

Determining a two-dimensional table for Sc factors of rectangular fields is time consuming. Therefore, various models were proposed, based on a significantly smaller amount of data. The application of Sterling's formula can cause even a 3% deviation from real data. The model proposed by Karlsson et al.⁶ decomposes the function $Sc(x,y)$ of two independent variables into the product of two one-variable functions

$$Sc(x,y)=Sc(x_{max},y) \cdot Sc(x,y_{max}),$$

when two decomposing functions are normalised so that they are a unity at $y=y_{ref}$ or $x=x_{ref}$, respectively. This model requires measurements for various y 's at x_{max} , thus significantly reducing the number of measurements. Using this model we also obtained deviations up to 3% from the actually measured $Sc(x,y)$.

In this work we shall compare three various models also based on the idea of the decomposition of $Sc(x,y)$ into the product of two one-variable functions, trying to get a better approximation using various types of normalisation and limitation.

Materials and methods

The measurements were carried out using nominal 6 MV and 15 MV X-ray beams of a Siemens linac (Mevatron MD installed in Osijek) and nominal 6 MV and 18 MV X-ray beams of a Varian linac (Clinac 1800 installed in Zagreb).

The total scatter correction factor (Scp) is defined as the ratio of the doses at an arbitrary collimator opening and at the reference opening, in the precisely defined reference point at the reference source scin distance (SSD). The reference data in our measurements were: SSD=100cm, reference point is on the central axes at $d_{ref}=10$ cm and the reference opening was defined as field size 10cmx10cm at SSD=100cm.

Total scatter correction factor is the product of the collimator scatter correction factor Sc and phantom scatter correction factor Sp :

$$Scp=Sc \cdot Sp.$$

Collimator scatter correction factors of rectangular fields were measured using a mini-phantom described in ESTRO booklet No 3. A Farmer tape 0.6 ccm ionization chamber, placed into the mini phantom, was always perpendicular to the elongated field size in order to reduce the cable effect as much as possible. The response of the dosimeter should reflect the change of the photon fluence due to the variation of collimator setting. Sc was determined in the same way as prescribed for Scp , except that the above mentioned mini-phantom was used for the measurements instead of a large water phantom.

For every of the four X-ray beams we measured a table of 8x8 values of $Sc(x_i, y_j)$, where x_i and y_j are discrete openings assuming values $x_i, y_j = 4, 6, 8, 10, 15, 20, 30, 40$ cm at indices $i, j=1..8$. For the sake of clarity let us simplify the notation by using the symbol $Sc(i,j) \equiv Sc(x_i, y_j)$. At our choice of discrete openings, index $i, j=4 \equiv ref$ means reference value of x_i, y_j and similarly $i, j=1 \equiv min$ and $i, j=8 \equiv max$ mean minimum and maximum openings, respectively. The $Sc(i,j)$ values were normalized in the standard way, so that $Sc(ref, ref)=Sc(4,4)=1$.

We compared four models to calculate $Sc(i,j)_{calc}$ from partial set of measured data $Sc(i,j)$ consisting of one column and one row (models 1 and 2) or two columns and two rows (models 3 and 4):

Model 1

This model was proposed by Karlsson et al.⁶ The only measured row and column are $Sc(max, j)$ and $Sc(i, max)$, with $i, j=1..8$, respectively. In our notation Sc is calculated as

$$Sc(i,j)_{calc} = Sc(i, max) \cdot Sc(max, j) / [Sc(ref, max) \cdot Sc(max, ref)].$$

Model 2

The only measured row and column are $Sc(ref,j)$ and $Sc(i,ref)$, with $i,j=1..8$, respectively. Sc is calculated as

$$Sc(i,j)_{calc} = Sc(i,ref) \cdot Sc(ref,j).$$

No additional normalization is necessary due to the fact that both, row $Sc(i,ref)$ and column $Sc(ref,j)$ are already normalized by $Sc(ref,ref)=1$.

Model 3

The two measured rows and columns are $Sc(min,j)$, $Sc(max,j)$ and $Sc(i,min)$, $Sc(i,max)$, with $i,j=1..8$, respectively. This model of calculation is given with three expressions which define the function $Sc(i,j)_{calc}$ within three separated ranges, namely

$$\text{for } x < y: \quad Sc(i,j)_{calc} = Sc1 = Sc(min,j) \cdot Sc(i,max) / Sc(min,max),$$

$$\text{for } x > y: \quad Sc(i,j)_{calc} = Sc2 = Sc(max,j) \cdot Sc(i,min) / Sc(max,min),$$

$$\text{for } x = y: \quad Sc(i,j)_{calc} = (Sc1 + Sc2) / 2.$$

It is easy to see that following equations are valid:

$$Sc(min,j)_{calc} = Sc(min,j) \text{ for } j=1..8,$$

$$Sc(i,max)_{calc} = Sc(i,max) \text{ for } i=1..8,$$

$$Sc(max,j)_{calc} = Sc(max,j) \text{ for } j=1..8,$$

$$Sc(i,min)_{calc} = Sc(i,min) \text{ for } i=1..8.$$

These equations express the fact that all calculated values on the border of the table are identical to the measured data. Therefore, the maximum deviations of calculated data could be expected in the middle of the table.

Model 4

The two measured rows and columns are the same as for Model No. 3.

This model of calculation is also given by three expressions, with somewhat different normalization, namely

$$\text{for } x < y: \quad Sc(i,j)_{calc} = Sc1 = Sc(min,j) \cdot Sc(i,max) / [Sc(min,ref) \cdot Sc(ref,max)],$$

$$\text{for } x > y: \quad Sc(i,j)_{calc} = Sc2 = Sc(max,j) \cdot Sc(i,min) / [Sc(max,ref) \cdot Sc(ref,min)],$$

$$\text{for } x = y: \quad Sc(i,j)_{calc} = (Sc1 + Sc2) / 2.$$

The possibility to calculate other Sc values by linear interpolation is implied for all four models.

Results and discussion

A sample of measured data versus data processed by model 3 and for Clinac 1800 18MV X-rays is shown in Table 1. Similar

Table 1. Measured and calculated data for Clinac 1800 18MV X-rays, according to model 3

\ upper jaw:		4cm	6cm	8cm	10cm	15cm	20cm	30cm	40cm
lower jaw:	measured	0.950	0.958	0.971	0.977	0.982	0.989	0.994	1.001
	calculated	0.950	0.958	0.971	0.977	0.982	0.989	0.994	1.001
	deviation%	0.00	0.00	0.00	0.00	0.00	0.00	0.00	0.00
4cm	measured	0.959	0.973	0.982	0.989	0.997	1.004	1.007	1.016
	calculated	0.959	0.975	0.986	0.992	0.997	1.004	1.009	1.016
	deviation%	0.00	0.21	0.36	0.26	-0.03	-0.02	0.19	0.00
6cm	measured	0.961	0.978	0.991	0.996	1.008	1.012	1.019	1.027
	calculated	0.961	0.980	0.994	1.002	1.008	1.015	1.020	1.027
	deviation%	0.00	0.20	0.31	0.64	-0.05	0.27	0.08	0.00
8cm	measured	0.961	0.980	0.992	1.000	1.010	1.016	1.025	1.032
	calculated	0.961	0.980	0.992	1.005	1.012	1.020	1.025	1.032
	deviation%	0.00	0.00	0.00	0.51	0.24	0.36	-0.02	0.00
10cm	measured	0.961	0.980	0.992	1.000	1.010	1.016	1.025	1.032
	calculated	0.961	0.980	0.992	1.005	1.012	1.020	1.025	1.032
	deviation%	0.00	0.00	0.00	0.51	0.24	0.36	-0.02	0.00

\ upper jaw:		4cm	6cm	8cm	10cm	15cm	20cm	30cm	40cm
lower jaw:									
15cm	measured	0.962	0.981	0.993	1.001	1.013	1.020	1.030	1.038
	calculated	0.962	0.981	0.993	1.004	1.018	1.026	1.031	1.038
	deviation%	0.00	0.00	0.00	0.30	0.46	0.56	0.07	0.00
20cm	measured	0.962	0.981	0.993	1.002	1.016	1.022	1.032	1.041
	calculated	0.962	0.981	0.993	1.004	1.017	1.026	1.034	1.041
	deviation%	0.00	0.00	0.00	0.20	0.10	0.38	0.17	0.00
30cm	measured	0.962	0.981	0.993	1.003	1.017	1.023	1.033	1.043
	calculated	0.962	0.981	0.993	1.004	1.017	1.023	1.035	1.043
	deviation%	0.00	0.00	0.00	0.10	0.10	0.00	0.19	0.00
40cm	measured	0.962	0.981	0.993	1.004	1.017	1.023	1.034	1.044
	calculated	0.962	0.981	0.993	1.004	1.017	1.023	1.034	1.044
	deviation%	0.00	0.00	0.00	0.00	0.00	0.00	0.00	0.00
RMS= 0.187%									
E_{max} =0.64%									
CEE_{max} =3.9%									

tables, not shown here, were elaborated for various beam qualities and the summarized results are given in Table 2.

The results are shown in Table 2. In addition to other methods the results of Sterling formula are also represented for comparison. From Table 2, following conclusions may be

drawn. The first two models are based on the measurement of one row and one column. Better results obtained by model 2 mean that, if we measure only one row and one column, the better choice is to use that column and row which correspond to the fixed reference opening, instead of the row and column

Table 2. The roots of mean squares (RMS's) and the maximum deviations (Emax) obtained for various methods and the maximum collimator exchange effects (CEE_{max}) for various beams

BEAM	Model 1	Model 2	Model 3	Model 4	Sterling
Mevatron 6MV					
RMS%	0.63	0.68	0.20	0.37	1,11
E_{max} %	2.1	1.1	0.72	0.98	3,03
Mevatron 15MV					
RMS%	0.63	0.61	0.19	0.39	1,14
E_{max} %	2.1	1.14	0.62	0.97	2,95
Mevatron 6MV wedge 30°					
RMS%	1.33	0.96	0.39	0.61	1,19
E_{max} %	3.33	1.58	1.19	1.69	2,56
Mevatron 15MV wedge 30°					
RMS%	1.15	0.79	0.39	0.53	1,03
E_{max} %	3.32	1.39	1.12	1.53	2,71
Clinac 6MV					
RMS%	1.42	0.33	0.32	0.65	1,26
E_{max} %	2.66	0.56	1.05	2.1	3,00
Clinac 18MV					
RMS%	0.69	0.47	0.19	0.37	1,28
E_{max} %	2.06	0.78	0.64	1.11	3,2

which correspond to the fixed maximum opening of the collimator. Models 3 and 4 are based on measured data of two rows and two columns (i.e. double amount of measured data) and, therefore, superior in results as compared with the first two models. The model 3 is obviously the most accurate in spite of the fact that Sc is not exactly equal to a unity under reference conditions.

References

1. Dutreix A, Bjärngard BE, Bridier A, Muijnheer B, Shaw JE, Svensson H. Monitor unit calculation for high energy photon beams. ESTRO booklet no. 3, Leuven: Garant Publishers N.V; 1997.
2. Vadash P, Bjärngard BE. An equivalent square formula for head scatter factors. *Med Phys* 1993; **20**: 733-4.
3. van Gasteren JJM, Heukelom S, Jager HN, Muijnheer BJ, van der Laarse R, van Kleffens HJ, et al. Determination and use of scatter correction factors of megavoltage photon beams. Report 12 of the Netherlands Commission on Radiation Dosimetry, March 1998.
4. Tathcher M, Bjärngard BE. Head scatter factors in rectangular photon fields. *Med Phys* 1993; **20**: 205-6.
5. Kim S, Zhu TC, Palta JR. An equivalent square field formula for determining head scatter factors of rectangular fields. *Med Phys* 1997; **24**: 1770-4.
6. Karlsson Magnus, Karlsson Mikael, Svensson H. A simple way to calculate head scatter factors for an arbitrary fieldsize at reference depth. Teaching course on dose and monitor unit calculations for high energy photon beams, Santorini - Greece, 26 - 30 April, 1998.

Pomen klasične radiološke diagnostike pri majhnih plevralnih izlivih

Kocijančič I, Vidmar K

Namen. Ugotoviti uporabnost dveh posnetkov v bočnem položaju v različnih fazah dihanja (v globokem vdihu in v izdihu) pri diagnostiki majhnih plevralnih izlivov.

Materiali in metode. Bolnikom, ki so bili na UZ pregledu trebuha zaradi različnih vzrokov, smo rutinsko pregledovali tudi plevralni prostor in iskali izlive. Od novembra 1994 do maja 1996 smo pri 36 bolnikih našli mali plevralni izliv do širine 15 mm bazalno in jih vključili v študijo. Slikali smo jim prsne organe v PA in stranski smeri. Nato so 5 min ležali na boku, nakar smo jim napravili posnetek v izdihu in vdihu leže na boku. Ob tem so imeli za 10° dvignjeno medenico, centralni žarek pa je bil usmerjen na stranico prsnega koša.

Rezultati. Pri 22 od 36 bolnikov (61%) na PA in stranskih posnetkih ni bilo znakov plevralnega izliva. Zato pa je bil ta jasno viden pri 35 od 36 bolnikov na posnetku leže na boku, napravljenem v izdihu. Povprečna širina tekočinske plasti je znašala 4,3 mm na posnetku leže na boku v vdihu in 7,9 mm na posnetku v izdihu. Pri 31 od 36 bolnikov (86%) sta se širini tekočinske plasti, izmerjeni na posnetkih leže na boku v vdihu in izdihu razlikovali. V 16% tekočine na posnetku leže na boku v inspiriju ni bilo videti.

Zaključek. Izkazalo se je, da so rentgenski posnetki prsnih organov v ustreznih smereh ravno tako občutljiva metoda za ugotavljanje malih plevralnih izlivov kot pregled z ultrazvokom. Rezultati naše študije kažejo tudi, da posnetek leže na boku, napravljen v izdihu, ključno prispeva k občutljivosti metode.

Računalniški sistem za določanje porazdelitve tlaka v kolčnem sklepu s pomočjo antero-posteriornega rentgenograma okolčja

Iglič A, Kralj-Iglič V

Izhodišča. V članku je opisan računalniški sistem HIPSTRESS, s katerim lahko določimo porazdelitev tlaka v kolčni sklepni površini. Pri tem moramo poznati težo telesa in nekatere karakteristične geometrijske parametre medenice in kolka, ki jih lahko določimo neposredno iz antero-posteriornega rentgenograma.

Zaključki. Sistem je uporaben v klinični praksi za določanje optimalne porazdelitve kolčnega sklepnega tlaka pri operativnem posegu v kolku.

Ultrazvok kot pomoč pri diagnostiki in zdravljenju analnih fistul

Košorok P

Izhodišča. Endoanalni ultrazvok (EUZ) je koristna preiskavna metoda v diagnostiki anorektalnih fistul in abscesov. Z uporabo radialne UZ sonde dobimo kvalitetno sliko visoke ločljivosti in dobro anatomsko orientacijo. Ta vrsta informacije je ključna v sledenju uspeha zdravljenja. Začetna EUZ slika narejena pred posegom je potrebna zaradi primerjave rezultatov pred in po posegu. EUZ med operacijo je v pomoč, če je lezija visoko nad mišičjem medeničnega dna, kar bi med operacijo morda spregledali.

Boljše EUZ slike perianalnih fistul lahko dobimo, če uporabimo kot kontrastno sredstvo vodikov peroksid.

Dodatna prednost kontrastnega EUZ slikanja z vodikovim peroksidom je odkrivanje morebitnih pričakovanih ali tudi nenadejanih poškodb mišice zapiralke.

Vsekakor je potrebno upoštevati individualnost ocen posameznih preiskovalcev in tudi večjo zanesljivost rezultatov z rastočimi izkušnjami preiskovalcev.

Zaključki. Endoanalni UZ je varna, ekonomična in zanesljiva preiskava za odkrivanje paraanalnih fistul, ki nudi več podatkov kot sam klinični pregled.

Akutna subarahnoidna krvavitev. Odkrivanje anevrizem na intrakranialnih arterijah z računalniškotomografsko angiografijo

Milošević Z

Izhodišče. Namen študije je bil oceniti diagnostično zanesljivost, občutljivost in specifičnost ter prednosti in slabosti računalniškotomografske preiskave arterij (CTA) intrakranialnih žil glede na digitalno subtrakcijsko angiografsko preiskavo (DSA) (zlati standard) pri bolnikih z akutno subarahnoidno krvavitvijo (SAK).

Bolniki in metode. V prospektivno študijo smo vključili 52 bolnikov z akutno subarahnoidno krvavitvijo, pri katerih smo takoj, ko smo krvavitev dokazali s konvencionalno računalniško tomografijo (CT) glave, naredili še CTA preiskavo intrakranialnih arterij, tako da rezultati DSA preiskave niso mogli vplivati na rezultate CTA preiskave. Glede na rezultate DSA preiskave in nevrokirurške rezultate smo ocenili diagnostično zanesljivost, senzitivnost in specifičnost CTA preiskave intrakranialnih arterij.

Analizirali smo primere, kjer se rezultati CTA preiskave in DSA preiskave niso ujemali. Opredelili smo prednosti in slabosti CTA preiskave.

Rezultati. Diagnostična zanesljivost CTA preiskave je bila 95%, občutljivost 93% in specifičnost 98%. Pri treh bolnikih je bila CTA preiskava lažno negativna. Pri dveh bolnikih z lažno negativnim izvidom CTA preiskave je bila manjša anevrizma v področju kavernoznega sinusa, pri enem pa ob razcepišču perikalozne in kalozomarginalne arterije. Pri bolniku z lažno pozitivnim izvidom CTA preiskave smo z DSA preiskavo pokazali, da gre za infundibularno razširjenje posteriorne komunikantne arterije. Pri vseh sedmih bolnikih, ki so bili operirani samo na podlagi rezultatov CTA preiskave, smo dobro prikazali anevrizmo in intrakranialne arterije.

Zaključek. Pri bolnikih z akutno SAK ima lahko CTA preiskava pomembno vlogo pri odkrivanju in preoperativni evalvaciji intrakranialnih anevrizem, ker dobimo rezultate hitro in na minimalno invaziven način. CTA preiskava intrakranialnega žilja ima visoko diagnostično zanesljivost, občutljivost in specifičnost.

Scintigrafija z indij-111-DTPA-oktreotidom pri bolnikih s karcinoidom

Težak S, Ostojić R, Perković Z, Rustemović N, Car N, Papa P, Poropat M, Dodig D

Izhodišča. Študijo smo izvedli z namenom, da ocenimo klinično uporabnost scintigrafije somatostatinskih receptorjev z indij-111-DTPA-oktreotidom (SRS) ter jo primerjamo s konvencionalnimi načini slikovne preiskave pri bolnikih s karcinoidom.

Bolniki in metode. Štirinajst bolnikov s patohistološko potrjenim karcinoidom in enega bolnika s klinično ugotovljenim karcinoidom smo preiskali s SRS. Preiskavo SRS smo izvedli po konvencionalni slikovni preiskavi in z njo poskušali lokalizirati primarni tumor in ugotoviti ponovitev ali razsoj bolezni. Scintigrafijo celotnega telesa in računalniško tomografijo z emisijo posameznih elektronov (SPECT) smo opravili 6 in 24 ur po vbrizganem radiofarmacevtskem sredstvu. Intenzivnost nespecifičnega kopičenja radiofarmacevtskega sredstva v črevesu smo ocenili semikvantitativno s scintigrafijo celotnega telesa.

Rezultati. Intenzivnost kopičenja smo ocenili glede na bolnike in glede na lokalizacijo tumorja. Pri bolnikih je občutljivost znašala 89%, specifičnost 100%, pozitivne in negativne napovedne vrednosti pa so bile 100% in 80% tako pri konvencionalnem načinu slikovne preiskave kot pri SRS. Pri ocenjevanju lokalizacije tumorja so bili zgornji parametri naslednji: slikanje celotnega telesa: občutljivost 69%, specifičnost 100%, pozitivne in negativne napovedne vrednosti 100% in 82%; SRS: občutljivost 88%, specifičnost 100%, pozitivne in negativne napovedne vrednosti 100% in 92%. Intenzivnost nespecifičnega kopičenja 111-indija-oktreotida v črevesju je bila pri slikah, posnetih po 6. urah 0,92 in pri slikah, posnetih po 24 urah, 2,01 ($p < 0,01$).

Zaključki. SRS bi morala biti vključena v diagnostični algoritem pri bolnikih, pri katerih je bil karcinoid ugotovljen le klinično in tudi pri bolnikih s potrjeno diagnozo karcinoida.

Radiol Oncol 1999; 33(4): 291-96.

Kombinirano zdravljenje kožnih metastaz adenokarcinoma z elektrokemoterapijo in obsevanjem

Serša G, Čemažar M, Rudolf R, Fras AP

Izhodišča. Študijo smo opravili z namenom, da bi ugotovili medsebojni vpliv med elektrokemoterapijo, s katero smo pospešili vnos cisplatina v celice, in obsevanjem kožnih metastaz adenokarcinoma.

Poročilo o primeru. Študija poroča o bolnici z napredovnajem boleznijo in ugotovljenimi kožnimi metastazami tubularnega dediferenciranega papilarnega adenokarcinoma. Kožne metastaze smo zdravili z elektrokemoterapijo in vbrizgavanjem cisplatina v tumor. Učinek zdravljenja smo primerjali z učinkom kombiniranega zdravljenja z obsevanjem in elektrokemoterapijo. Obe metodi sta bili učinkovitejši od zdravljenja samo z obsevanjem. Ugotovili smo tudi, da je kombinirano zdravljenje z elektrokemoterapijo in radioterapijo hitreje učinkovalo na tumor kot zdravljenje samo s kemoterapijo.

Zaključek. Študija potrjuje, da je elektrokemoterapija s cisplatinom uspešna tudi pri zdravljenju metastaz kožnega adenokarcinoma. Navzlic kratkemu opazovalnem času smo ugotovili ugoden medsebojen vpliv radioterapije in elektrokemoterapije s cisplatinom.

Radiol Oncol 1999; 33(4): 297-301.

Prerazporejanje mikrotubulov v celicah V-79 po delovanju citohalazina B

Iglič A, Batista U, Veranič P

Izhodišča. V tej raziskavi smo proučevali razporeditev mikrotubulov celicah V-79 po delovanju citohalazina B. Poleg njihove oblike smo poskušali ugotoviti, ali je ta pojav v čemer koli podoben dogajanju v fosfolipidnih mehurčkih.

Material in metode. Opravili smo preiskus s citohalazinom B, ki smo ga dodali celicam V 79 (pljučni fibroblasti kitajskega hrčka).

Rezultati. Oblika celice se je spremenila iz podolgovate v obliko, katere profil je podoben grški črki ϕ . Mikrotubuli so se uredili v palico v simetrijski osi celice.

Zaključek. Ker so podobne oblike pred tem opazili tudi pri fosfolipidnih mehurčkih, ki so vsebovali paličasto strukturo iz mikrotubulov, prikazani rezultati podpirajo hipotezo, da so podobni fizikalni mehanizmi prisotni v preprostih sistemih kot tudi v živih celicah.

Radiol Oncol 1999; 33(4): 315-20.

Primerjava kolorimetričnega testa MTT in testa klonogenosti na mišjih fibrosarkomskih SA-1 celicah po obsevanju in zdravljenju s cisplatinom

Čemažar M, Marolt D, Lavrič M, Serša G

Izhodišče. Namen naše raziskave je bil določiti povezavo med testom MTT in testom klonogenosti z merjenjem preživetja SA-1 tumorskih celic po obsevanju in po terapiji s cisplatinom.

Materiali in metode. Preživetje SA-1 celic smo določali po obsevanju celic (2-8 Gy) ali po terapiji s cisplatinom (0.05 - 0.5 µg/ml) s testom klonogenosti, ki smo ga izvedli 7 dan po terapiji, ter testom MTT, ki smo ga izvedli 3., 4., 5., in 7. po terapiji.

Rezultati. Ugotovili smo, da testa dobro korelirata, ko smo celice obsevali z dozami pod 4 Gy. Pri višjih dozah obsevanja sta test MTT in test klonogenosti dobro korelirala samo v primeru, ko smo merili preživetje celic z testom MTT 5. in 7. dan po obsevanju. Po terapiji s cisplatinom smo dobili podobne rezultate; korelacija med testom MTT in testom klonogenosti je bila dobra v primeru, ko smo izvedli test MTT 5. in 7. dan po terapiji.

Zaključki. Rezultati naše raziskave so potrdili ugotovitve predhodnih študij, ter podpirajo uporabo testa MTT kot alternativo testu klonogenosti pri napovedovanju izida zdravljenja tumorjev z radio- in kemoterapijo.

Primerjava štirih modelov izračunavanja kolimatorskih sipalnih faktorjev pri fotonjskih žarkih linearnega pospeševalnika

Faj D, Bistrović M

Izhodišča. V novejši literaturi najdemo dva pristopa za približno določanje korekcijskih faktorjev za pravokotna polja zaradi sipanja na kolimatorjih. Prvi temelji na empiričnih enačbah ali na nekoliko zapletenejših fizikalnih modelih, pri katerih se uporabljajo parametri, ki so specifični za določen obsevalni aparat. Drugi temelji na že predlagani zamisli o razstavitvi korekcijskega faktorja zaradi sipanja na kolimatorjih, ki je funkcija dveh spremenljivk, v zmnožek dveh funkcij ene same spremenljivke. V članku primerjamo štiri modele, ki temeljijo na takšni razstavitvi. Vsak od teh modelov temelji na meritvah osnovnih izhodnih karakteristik žarka, pri čemer je en par kolimatorjev stalno odprt do določene mere, položaj drugega para pa spreminjamo.

Material in metode. Meritve so bile opravljene na Siemensovem linearnem pospeševalniku z energijama žarkov X 6 MV in 15 MV ter na Varianovem linearnem pospeševalniku z nominalnima energijama žarkov X 6 MV in 18 MV.

Rezultati in zaključki. Pokazali smo, da lahko s primernim izborom osnovnih meritev in z normalizacijo podatkov dosežemo boljši približek.

Notices

Notices submitted for publication should contain a mailing address, phone and/or fax: number and/or e-mail of a Contact person or department.

Breast cancer

December, 1999

The ESO training course "Breast Reconstructive and Cancer Surgery" will take place in Paris, France.

Contact ESO Office, Viale Beatrice d'Este 37, 20122 Milan, Italy; or call +39 0258317850; or fax +39 0258321266; or e-mail esomi@tin.it

Cancer and genetics

December 2-4, 1999

The ESO training course will take place in Athens, Greece.

Contact ESO office for Balkans and Middle East, N. Pavlidis, E. Andreopoulou Medical School, Department of Medical Oncology, University Hospital of Ioannina, 45110 Ioannina, Greece; or call +30 651 99394 or +30 953 91083; or fax +30 651 97505

Lung cancer

December 3-4, 1999

International Symposium on Staging of Lung Cancer: New Perspectives for the New Century will take place in Madrid, Spain.

Contact Dr. A López Encuenera, Servicio Neumología, Hospital Universitario 12 de Octubre, Carretera Andalucía 5.4, 284041 Madrid, Spain; or call +3491 3908335; or fax +34 91 39083558

Radiotherapy

February 13-17, 2000

The ESTRO teaching course on "Radiotherapy Treatment Planning: Principles and Practice" will take place in Rotterdam, the Netherlands.

Contact Mieke Akkers, ESTRO office, Av. E. Mounierlaan, 83/4, B-1200 Brussels, Belgium; or call +32 7759347; or fax +32 2 7795494; or e-mail mieke.akkers@estro.be; or see internet <http://www.estro.be>

Lung cancer

March, 2000

The ESO training course will take place in Nicosia, Cyprus.

Contact ESO office for Balkans and Middle East, N. Pavlidis, E. Andreopoulou Medical School, Department of Medical Oncology, University Hospital of Ioannina, 45110 Ioannina, Greece; or call +30 651 99394 or +30 953 91083; or fax +30 651 97505

Liver tumours

March 12-14, 2000

The ESO training course will take place in Cairo, Egypt.

Contact ESO office for Balkans and Middle East, N. Pavlidis, E. Andreopoulou Medical School, Department of Medical Oncology, University Hospital of Ioannina, 45110 Ioannina, Greece; or call +30 651 99394 or +30 953 91083; or fax +30 651 97505

DCIS (ductal carcinoma in situ)

March 16, 2000

The ESO training course will take place in Athens, Greece.

Contact ESO office for Balkans and Middle East, N. Pavlidis, E. Andreopoulou Medical School, Department of Medical Oncology, University Hospital of Ioannina, 45110 Ioannina, Greece; or call +30 651 99394 or +30 953 91083; or fax +30 651 97505

As a service to our readers, notices of meetings or courses will be inserted free of charge.

Please sent information to the Editorial office, Radiology and Oncology, Vrazov trg 4, 1000 Ljubljana, Slovenia.

Brachytherapy

March 26-30, 2000

The ESTRO teaching course on "Modern Brachytherapy Techniques" will take place in Venezia-Mestre, Italy.

Contact ESTRO office, Av. E. Mounierlaan, 83/4, B-1200 Brussels, Belgium; or call +32 7759344; or fax +32 2 7795494; or e-mail gemeine.heeren@estro.be; or see internet <http://www.estro.be>

Thoracic tumours

April, 2000

The ESO training course will take place in Nicosia, Cyprus.

Contact ESO office for Balkans and Middle East, N. Pavlidis, E. Andreopoulou Medical School, Department of Medical Oncology, University Hospital of Ioannina, 45110 Ioannina, Greece; or call +30 651 99394 or +30 953 91083; or fax +30 651 97505

Radiation oncology

April 2-6, 2000

The ESTRO teaching course on "Clinical Research in Radiation Oncology" will take place in York, United Kingdom.

Contact ESTRO office, Av. E. Mounierlaan, 83/4, B-1200 Brussels, Belgium; or call +32 7759344; or fax +32 2 7795494; or e-mail martine.dansercoer@estro.be; or see internet <http://www.estro.be>

Radiotherapy

April 9-13, 2000

The ESTRO teaching course on "Imaging for Target Volume Determination in Radiotherapy" will take place in Como, Italy.

Contact ESTRO office, Av. E. Mounierlaan, 83/4, B-1200 Brussels, Belgium; or call +32 7759340; or fax +32 2 7795494; or e-mail info@estro.be; or see internet <http://www.estro.be>

Head and neck

May, 2000

The ESO training course "Head and Neck Pathology - Oncology" will take place in Ioannina, Greece.

Contact ESO office for Balkans and Middle East, N. Pavlidis, E. Andreopoulou Medical School, Department of Medical Oncology, University Hospital of Ioannina, 45110 Ioannina, Greece; or call +30 651 99394 or +30 953 91083; or fax +30 651 97505

Radiophysics

May 7-11, 2000

The ESTRO teaching course on "Dose and Monitor Unit Calculations for High Energy Photon Beams. Basic Principles and Application to Modern Techniques" will take place in Santorini, Greece.

Contact ESTRO office, Av. E. Mounierlaan, 83/4, B-1200 Brussels, Belgium; or call +32 7759340; or fax +32 2 7795494; or e-mail info@estro.be; or see internet <http://www.estro.be>

Clinical oncology

May 20-23, 2000

The 36th ASCO Annual Meeting will take place in New Orleans, Louisiana, USA.

Contact ASCO Office, 225 Reinekers Lane, Suite 650, Alexandria, VA 22314, USA; or call +1 703 299 0150; or fax +1 703 299 1044; or e-mail asco@asco.org; or see internet <http://www.asco.org>

Radiation therapy

May 22-25, 2000

The 13th International Conference on the Use of Computers in Radiation Therapy will take place in Heidelberg, Germany.

Contact Ms. Karin Beinert, call +49 6621 422551; or fax +49 6621 422561; or e-mail iccr@dkfz-heidelberg.de; or see internet <http://www.dkfz-heidelberg.de/iccr/>

Imaging, oncology and science

May 22-25, 2000

The congress "Imaging, Oncology and Science 2000 (IOS 2000) will take place in Birmingham, UK.

Contact IOS Secretariat, PO Box 2895; London, UK; or call +44 (0)20 7307 1410/20; or fax +44 (0)20 7307 1414; or e-mail ios@diap.pipex.com; or see internet <http://www.ios.org.uk>

Breast cancer

June, 2000

The ESO training course will take place in New York, USA.

Contact ESO US Office, R. Boschi-Belgin, American-Italian Cancer Foundation (AICF), 872 Madison Avenue - 2B, New York - NY 10021, USA; or call +1 212 6289090; or fax +1 212 5176089; or e-mail aicfny@aol.com

Urological cancer

June, 2000

The ESO training course will take place in Athens, Greece.

Contact ESO office for Balkans and Middle East, N. Pavlidis, E. Andreopoulou Medical School, Department of Medical Oncology, University Hospital of Ioannina, 45110 Ioannina, Greece; or call +30 651 99394 or +30 953 91083; or fax +30 651 97505

Oncology

June 4-8, 2000

The ESTRO teaching course on "Molecular Oncology for Radiotherapy" will take place in Innsbruck, Austria.

Contact ESTRO office, Av. E. Mounierlaan, 83/4, B-1200 Brussels, Belgium; or call +32 7759340; or fax +32 2 7795494; or e-mail info@estro.be; or see internet <http://www.estro.be>

Radiotherapy

June 4-8, 2000

The ESTRO teaching course on "IMRT and Other Conformal Techniques in Practice" will take place in Amsterdam, The Netherlands.

Contact ESTRO office, Av. E. Mounierlaan, 83/4, B-1200 Brussels, Belgium; or call +32 7759340; or fax +32 2 7795494; or e-mail info@estro.be; or see internet <http://www.estro.be>

Radiophysics

August 27-31, 2000

The ESTRO teaching course on "Physics for Clinical Radiotherapy" will take place in Leuven, Belgium.

Contact ESTRO office, Av. E. Mounierlaan, 83/4, B-1200 Brussels, Belgium; or call +32 7759340; or fax +32 2 7795494; or e-mail info@estro.be; or see internet <http://www.estro.be>

Myelodysplastic syndromes

September, 2000

The ESO training course will take place in Patras, Greece.

Contact ESO office for Balkans and Middle East, N. Pavlidis, E. Andreopoulou Medical School, Department of Medical Oncology, University Hospital of Ioannina, 45110 Ioannina, Greece; or call +30 651 99394 or +30 953 91083; or fax +30 651 97505

Lung cancer

September 11-15, 2000.

The "9th World Conference on Lung Cancer" will be offered in Tokyo, Japan.

Contact Dr. Yoshihiro Hayata, The 9th World Conference on Lung Cancer, Tokyo Medical College Cancer Center, 6-7-1 Nishishinjuku, Shinjuku-ku, Tokyo 160-0023, Japan; or fax +81 3 3342 0893

Radiation therapy

September 19-23, 2000

The 19th Annual ESTRO Meeting will take place in Istanbul, Turkey.

Contact ESTRO office, Av. E. Mounierlaan, 83/4, B-1200 Brussels, Belgium; or call +32 7759340; or fax +32 2 7795494; or e-mail info@estro.be; web: <http://www.estro.be>

Colorectal cancer

October, 2000

The ESO training course will take place in Milan, Italy.

Contact ESO Office, Viale Beatrice d'Este 37, 20122 Milan, Italy; or call +39 0258317850; or fax +39 0258321266; or e-mail esomi@tin.it

Radiation oncology

October 8-12, 2000

The ESTRO teaching course on "Evidence-Based Radiation Oncology: Principles and Methods" will be offered in Lleida, Spain.

Contact ESTRO office, Av. E. Mounierlaan, 83/4, B-1200 Brussels, Belgium; or call +32 7759340; or fax +32 2 7795494; or e-mail info@estro.be; or see internet <http://www.estro.be>

Radiobiology

October 8-12, 2000

The ESTRO teaching course on "Basic Clinical Radiobiology" will be offered in Bratislava, Slovakia.

Contact ESTRO office, Av. E. Mounierlaan, 83/4, B-1200 Brussels, Belgium; or call +32 7759340; or fax +32 2 7795494; or e-mail info@estro.be; or see internet <http://www.estro.be>

Radiation therapy

October 21-25, 2001

The ESTRO 20 / ECCO 11 Meeting will take place in Lisbon, Portugal.

Contact ESTRO office, Av. E. Mounierlaan, 83/4, B-1200 Brussels, Belgium; or call +32 7759340; or fax +32 2 7795494; or e-mail info@estro.be; web: <http://www.estro.be>

Radiation therapy

October 22-25, 2000

ASTRO Annual meeting will be held in Boston, Massachusetts, USA.

Contact American Society for Therapeutic Radiology and Oncology Office, 1891 Preston White Drive, Reston, VA 20191, USA.

Paediatric oncology

November 12-18, 2000

The training course under the auspices of the International Society of Paediatric Oncology will be held in Chandigarh, India.

Contact P.A. Voûte, call +31 20 5665655; or fax +31 20 6912231

Paediatric oncology

November 16-20, 2000

The training course under the auspices of the International Society of Paediatric Oncology will be held in Sao Paulo, Brazil.

Contact P.A. Voûte, call +31 20 5665655; or fax +31 20 6912231

Radiation morbidity

December 10-12, 2000

The ESTRO workshop on radiation morbidity will be held in Brussels, Belgium.

Contact ESTRO office, Av. E. Mounierlaan, 83/4, B-1200 Brussels, Belgium; or call +32 7759340; or fax +32 2 7795494; or e-mail info@estro.be; or see internet <http://www.estro.be>

Radiation therapy

November 4-7, 2001

ASTRO Annual meeting will be held in San Francisco, California, USA.

Contact American Society for Therapeutic Radiology and Oncology Office, 1891 Preston White Drive, Reston, VA 20191, USA.

Radiation therapy

May 15-19, 2002

The 7th International Meeting on Progress in Radio-Oncology ICRO/±GRO 7 will take place in Salzburg, Austria.

Contact Prof. D.H. Kogelnik, Salzburg, Austria; call +43 662 44823900; or fax +43 662 4482887; or e-mail d.kogelnik@lkasbg.gv.at

Radiation therapy

September 15-19, 2002

The 21st Annual ESTRO Meeting will take place in Prague, Czech Republic.

Contact ESTRO office, Av. E. Mounierlaan, 83/4, B-1200 Brussels, Belgium; or call +32 7759340; or fax +32 2 7795494; or e-mail info@estro.be; web: <http://www.estro.be>

Radiation therapy

October 6-9, 2002

ASTRO Annual meeting will be held in New Orleans, Louisiana, USA.

Contact American Society for Therapeutic Radiology and Oncology Office, 1891 Preston White Drive, Reston, VA 20191, USA.

Reviewers in 1999

Bartenjev I, Ljubljana - Berden P, Ljubljana - Brenčič E, Ljubljana - Brkljačić B, Zagreb, Budihna M, Ljubljana - Budihna N, Ljubljana - Budja M, Murska Sobota - Casar B, Ljubljana - Cvitković Kuzmić A, Zagreb - Čufer T, Ljubljana - Fidler V, Ljubljana - Golouh R, Ljubljana - Grmek M, Ljubljana - Jevtić V, Ljubljana - Kadivec M, Ljubljana - Knific J, Ljubljana - Kocijančič I, Ljubljana - Kotnik V, Ljubljana - Kovač V, Ljubljana - Kozak P, Ljubljana - Kragelj B, Ljubljana - Lešničar H, Ljubljana - Lindtner J, Ljubljana - Miklavčič D, Ljubljana - Novaković S, Ljubljana - Osmak M, Zagreb - Pirnat E, Ljubljana - Renner M, Ljubljana - Robar V, Ljubljana - Roić G, Zagreb - Rudolf Z, Ljubljana - Sterle M, Ljubljana - Strojani P, Ljubljana - Škrk J, Ljubljana - Šuštaršič J, Ljubljana - Umek B, Ljubljana - Vargazon T, Ljubljana - Vidmar D, Ljubljana - Vidmar K, Ljubljana - Volavšek Č, Ljubljana - Zwitter M, Ljubljana

Editors greatly appreciate the work of the reviewers who significantly contributed to the improved quality of our journal.

Radiol Oncol 1999; 33(4): 325-7.

Author Index 1999

Ahčan U: **Suppl 1/86-91**

Argenziano G: **Suppl 1/27-34**

Arnež ZM: Suppl 1/40-4, Suppl 1/86-91

Balatoni Zs: **2/159-62**

Barsnick P: 1/55-8

Bartenjev I: **Suppl 1/Foreword I**, Suppl 1/24-6,

Suppl 1/35-7, Suppl 1/38-9, Suppl 1/80-5

Batista U: 4/297-301

Beeke E: 1/55-8

Benedičič-Pilih A: **Suppl 1/80-5**

Benk U: 3/189-92

Benulić T: **1/87**, 2/181, 3/257, 4/329

Bistrović M: 4/309-13

Bleckmann Ch: 2/111-7

Buhoslavizki KH: **1/15-21**; 2/111-7; **3/207-13**

Borštnar S: **1/43-53**

Božikov V: 3/179-87

Boyomo A-B: 2/153-7

Brenner W: 2/111-7

Brkljačić B: 2/87-94; **3/179-87**

Bubić-Filipi Lj: 3/215-20

Buchert R: 1/15-21; 3/207-13

Budihna M: 2/143-51

Bumči I: 3/189-92

Car N: 4/283-90

Carli P: Suppl 1/27-34

Cindro V: 3/237-44

Cizej TE: 2/119-26

Chimenti S: Suppl 1/106-11

Clausen M: 1/15-21; 2/111-7; 3/207-13

Crnković S: 3/215-20

Curtin-Savard AJ: **2/163-8**

Cvitković-Kuzmić A: **2/87-94**

Czembirek H: 2/101-9

Čemažar M: **2/127-36**; 3/221-5; 4/291-6, **4/303-8**;
Suppl 1/55-63

Čop S: 3/189-92

Čufer T: 1/43-53; Suppl 1/55-63

De Giorgi V: Suppl 1/27-34

Delfino M: Suppl 1/27-34

Dodig D: 3/215-20; 4/283-90

Élő J: 2/159-62

Ercegović S: 3/189-92

Evans MDC: **3/227-35**

- Fabbrocini G: Suppl 1/27-34
 Faj D: **4/309-13**
 Fickert P: 3/199-205
 Fras AP: **3/221-5**; 4/291-6
 Freeman C: 3/227-35
 Fuchshuber PR: **1/59-61**
- Galešić K: 2/87-94
 Garaj-Vrhovac V: 1/35-41
 Garbe C: **Suppl 1/1-13**
 Gibbs JF: 1/59-61, 1/63-8
 De Giorgi V: Suppl 1/27-34
 Glamocanin S: 1/23-6
 Glavina K: 1/9-14
 Glumac B: 1/69-75
 Gornik T: Suppl 1/35-7
 Gosselin M: 3/227-35
 McGrath B: 1/59-61
 Groell R: **3/199-205**
 Grošev D: 3/215-20
- Hadjiev J: **1/1-8**
 Hajdinjak T: 2/119-26
 Hebrang A: 3/179-87
 Henze E: 2/111-7
 Hertl H: Suppl 2/13-23, **Suppl 2/30-8**
 Hitzelhammer H: 2/101-9
 Hodl S: **Suppl 1/103-5**
 Horváth L: 1/1-8
 Huben R: 1/63-8
 Huić D: **3/215-20**
- Iglić A: **4/263-6**, **4/297-301**
 Ihan A: **1/27-33**
 Ilić D: **1/23-6**
- Jančar Boris: Suppl 1/55-63
 Jančar Breda: 3/237-44
 Janevska V: 1/23-6
- Kadivec M: **Suppl 2/Foreword II**
 Kansky A: **Suppl 1/69-74**
 Kansky AA Jr: **Suppl 1/96-102**
 Kašuba V: **1/35-41**
 Klutmann S: **2/111-7**; 3/207-13
 Kocijančič I: **4/257-61**
 Koren A: 3/193-89
 Kos J: 2/143-51
 Košorok P: 467-74
 Kótai ZS: 2/159-62
 Kovačič D: 1/9-14
 Kralj-Iglić V: 4/263-6
 Kranjc S: 3/221-5
 Kraybill WS: 1/59-61
 Kristek B: 1/9-14
 Krištof E: 1/69-75
 Kröger S: 2/111-7
 Kugler CH: 3/199-205
- Kurbel S: **1/9-14**
 Kusić Z: 1/35-41
- Lavrič M: 4/303-8
 Lee RJ: 1/59-61, 1/63-8, **2/137-42**
- Mali T: **3/237-44**
 Marolt D: 4/303-8
 Maučec M: **1/69-75**
 McGarath B: 1/59-61
 Mester J: 1/15-21; 2/111-7; 3/207-13
 Mezőfi B: 1/1-8
 Middleton AW Jr: 2/137-42
 Middleton GW: 2/137-42
 Miklavčič D: Suppl 1/55-63
 Miklavčič L: **Suppl 2/24-9**
 Mikuž M: 3/237-44
 Milošević D: **4/275-82**
- Nestle FO: **1/64-8**
- Olivares M: 3/227-35
 Orel A: Suppl 1/35-7
 Ostojić A: 4/283-90
- Papa B: 4/283-90
 Parker W: 2/163-8
 Perković Z: 4/283-90
 Planinšek F: **Suppl 1/40-4**
 Plesničar A: 1/87; 2/181; 3/257; 4/329
 Podgoršak EB: 2/163-8; 3/227-35
 Pompe-Kirn V: **Supl 1/14-9**
 Popović B: Suppl 1/24-6, Suppl 1/75-9
 Poropat M: 3/215-20; 4/283-90
 Preidler KW: 2/101-9
 Proulx GM: 1/59-61, **1/63-8**
 Puretić Z: 3/215-20
- Radmard A: 2/153-7
 Rainer S: **Suppl 2/39-41**, **Suppl 2/42-6**
 Rant J: 1/69-75
 Renner M: **Suppl 2/13-23**, Suppl 2/30-8
 Repše S: 2/95-9
 Rienmüller R: 3/199-205
 Roić G: **3/189-92**
 Rudolf Z: 1/43-53; 4/291-6; **Suppl 1/Foreword I**,
Suppl 1/50-4, Suppl 1/55-63
 Rustemović N: 4/283-90
- Samardžinski M: 1/23-6
 Sammarco E: Suppl 1/27-34
 Sause WT: 2/137-41
 Schaeffer CS: 2/137-41
 Serša G: 3/221-5; **4/291-6**, 4/303-8; **Suppl 1/55-63**
 Šimova N: 1/23-6
 Snoj M: **Suppl 1/45-9**
 Sotošek B: Suppl 1/96-102
 Soyer PH: **Suppl 1/24-6**, Suppl 1/35-7, **Suppl 1/75-9**

Stauber RE: 3/199-205
 Steiner E: 2/101-9
 Stiskal M: **2/101-9**
 Stolz W: **Suppl 1/20-3**
 Strojan P: **2/143-51**
 Sučić M: 3/179-87
 Svetić B: 2/143-51
 Szalai G: 1/1-8
 Szolar D: 2/101-9

Škrk J: 2/143-51
 Šmid L: 2/143-51
 Štabuc B: **2/119-26**; Suppl 1/55-63; 1/87, **2/181**,
3/257, **4/329**

Težak S: **4/283-90**
 Tolevska C: 1/23-6

Uggowitz MM: 3/199-205

Vaskova O: 1/23-6
 Velagapudi S: 1/63-8

Veranič P: 4/297-301
 Vidmar D: **2/95-9**
 Vidmar K: 4/257-61
 Višnar-Perovič A: **3/193-8**
 Višnjić S: 3/189-92
 Vlahović T: 3/189-92
 Vrhovec I: 1/43-53; 2/143-51
 Vuong T: 2/163-8

Wagner W: **1/55-8**; **2/153-7**
 Werner JA: 3/207-13
 Worret W: **Suppl 1/38-9**

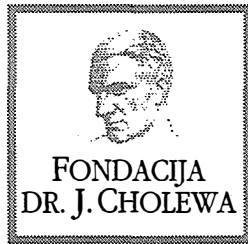
Zafirovski G: 1/23-6
 Zagoričnik B: **Suppl 1/92-5**
 Zdešar U: 3/237-44; **Suppl 2/1-8**, **Suppl 2/9-12**
 Zizovski N: 1/23-6

Žgavec B: Suppl 1/24-6, Suppl 1/75-9

Subject Index 1999

- absces: 4/267-74
adenocarcinoma: 4/291-6
adjuvants, immunologic: Suppl 1/50-4
amifostine: 2/153-7
antero - posterior radiograph: 4/263-6
arterial occlusive diseases - drug therapy: 1/1-8
autonomous adenoma: 3/179-87
- bladder neoplasms - drug therapy - radiotherapy - surgery: 1/63-8
bleomycin: Suppl 1/55-63
bone neoplasms - radionuclide imaging: 1/23-6
boron neutron capture therapy: 1/69-75
breast neoplasms: 1/43-53; Suppl 2/1-8
- breast neoplasms - diagnosis: Suppl 2/30-8
- breast neoplasms - radiotherapy: 3/227-35
- cancer: Suppl 1/64-8
carcinoid tumor - radionuclide imaging: 4/283-90
carcinoma: Suppl 1/86-91; Suppl 1/92-102
- carcinoma basal cell - diagnosis: suppl 1/92-5
- carcinoma, squamous cell - diagnosis - pathology: Suppl 1/75-9
- carcinoma, verrucous - surgery: Suppl 1/103-5
cathepsins, cathepsins H: 2/143-51
cerebral aneurysm - diagnosis: 4/275-82
cisplatin: 4/291-6; 4/303-8
chemotherapy, cisplatin: 2/119-26
child: 2/87-94; 3/189-92; Suppl 1/38-9
cholelithiasis, intestinal obstruction - ultrasound, gallstone ileus: 2/95-9
collimator scatter, rectangular fields: 4/309-13
colony forming units assay: 4/303-8
color Doppler imaging: 2/87-94
colorimetry - methods: 4/303-8
computed tomographic angiography, digital subtraction angiography: 4/275-82
computer communication networks: Suppl 1/35-7
cryosurgery: 3/221-5
cytochalasin B: 4/297-301
- dendritic cells: Suppl 1/64-8
diagnosis: 4/257-61
- diagnosis differential: Suppl 1/92-5
diagnostic imaging: 1/15-21
- economics, cost-effectiveness: 2/111-7
electric stimulation therapy: 4/291-6
electrochemotherapy: 4/291-6
electroporation: Suppl 1/55-63
ethanol: 3/179-87
exocytosis, cell degranulation: 1/27-33
- family practice: Suppl 1/35-7
foreign bodies - ultrasonography: 3/189-92
- glomerular filtration rate, creatinine clearance, renal function: 2/119-26
graft rejection: 3/215-20
- head and neck neoplasms, carcinoma, squamous cell: 2/143-51
head and neck neoplasms - radiotherapy: 2/153-7
hip joint contact stress: 4/263-6
¹¹¹In - octreotide scintigraphy, diagnosis: 4/283-90
hyperthyroidism - radiotherapy: 1/35-41
- immunohistochemistry: Suppl 1/75-9
incidence: Suppl 1/14-9
indium radioisotopes, octreotide, DTPA: 4/283-90
interferon - alpha: Suppl 1/50-4
interstitial obstruction - ultrasonography: 3/193-8
intestinal obstruction - ultrasound, gallstone ileus: 2/95-9
iodine radioisotopes - adverse effects: 1/35-41
iron overload: 1/9-14
- kidney transplantation: 3/215-20
kidney tubular necrosis, acute, kidney - blood supply - radionuclide imaging: 3/215-20
killer cells, natural: 1/27-33
- larynx - surgery: 2/159-62
liver cirrhosis: 1/9-14
liver diseases: 1/9-14
luminiscence: Suppl 1/20-3; Suppl 1/24-6; Suppl 1/27-34
lymphatic metastasis: 1/23-6
- lymphatic metastasis, CUP-syndrome: 3/207-13
lymph node excision: Suppl 1/40-4; Suppl 1/45-9
lymphocytes: 1/35-41
lymphoma - classification: Suppl 1/106-11
- macular degeneration - radiotherapy, visual acuity: 1/55-8
magnetic resonance (MR) imaging, image enhancement, paramagnetic contrast media, morphology: 2/101-9
mammography: 3/237-44; Suppl 2/1-8; Suppl 2/13-23; Suppl 2/24-9
- mammography - instrumentation: Suppl 2/30-8
- mammography - methods: Suppl 2/30-8
Meckel's diverticulum - complications: 3/193-21
medical records - standards: 1/15-21
melanoma: Suppl 1/45-9
- melanoma - diagnosis: Suppl 1/38-9

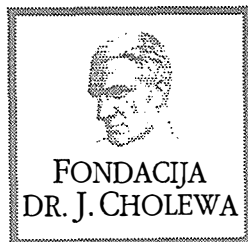
- melanoma - diagnosis - pathology: Suppl 1/20-3; Suppl 1/27-34
- melanoma - drug therapy: Suppl 1/50-4
- melanoma - epidemiology - mortality: Suppl 1/1-13
- melanoma - surgery: Suppl 1/40-4
- melanoma - therapy: Suppl 1/55-63
- melanoma - therapy- immunology: Suppl 1/64-8
- mice: 3/221-5
- micronucleus test: 1/35-41
- microtubules - drug effects: 4/297-301
- minimal requirements: 1/15-21
- mouth neoplasms: Suppl 1/96-102
- multileaf collimator: 2/163-8
- neoplasms - drug therapy - radiotherapy: 2/127-36
- neoplasms - radiotherapy: 1/69-75
- neoplasms, second primary: 1/59-61
- neoplasms staging: 2/137-42
- neoplasm, unknown primary: 3/207-13
- nerve sheath tumor: 1/59-61
- nevus, pigmented: Suppl 1/24-6; Suppl 1/38-9
- nevus pigmented - diagnosis: Suppl 1/35-7
- non-specific bowel accumulation: 4/283-90
- nuclear medicine: 1/15-21
- nuclear reactors: 1/69-75
- organ sparing - methods: 2/159-62
- oropharyngeal neoplasms - surgery: 2/159-62
- osteosarcoma: 1/23-6
- pelvis: 4/263-6
- photons: 4/309-13
- plasminogen activator inhibitor 1: 1/43-53
- plasminogen activator inhibitor 2: 1/43-53
- pleural effusion - radiology: 4/257-61
- positron emission tomography, F-18-FDG: 2/111-7
- prognosis: 1/43-53; 2/143-51; Suppl 1/40-4; Suppl 1/102-5
- prostatectomy: 2/137-42
- prostate - specific antigen: 2/137-42
- prostatic neoplasms - radiotherapy, oncology: 2/137-42
- quality assurance: Suppl 2/24-9
- quality control: Suppl 2/13-23
- quantitative analysis: 3/215-20
- radiation - adverse effects: 2/153-7
- radiation dosage: Suppl 2/1-8
- radiation injuries: 2/127-36
- radiographic image enhancement: 3/237-44
- radioisotope renography, iodohippuric acid, ¹³¹I hippuran renography: 2/119-26
- radiotherapy - adverse effects: 1/59-61; 2/153-7
- radiotherapy dosage: 2/163-8; 3/227-35; 4/309-13
- radiotherapy - methods: 2/163-8
- radiotherapy planning, computer assisted: 2/163-8
- rectal diseases - ultrasonography: 4/267-74
- rectal fistula - ultrasonography: 4/267-74
- registries: Suppl 1/1-13
- renal artery - ultrasonography: 2/87-94
- risk factors: Suppl 1/1-13
- rotating half - block, CT simulation, beam matching: 3/227-35
- sarcoma: 1/63-8
- sarcoma, experimental - radiotherapy - drug therapy: 4/303-8
- sarcoma, experimental - surgery - radiotherapy: 3/221-5
- scattering radiation: 4/309-13
- seminoma - radiotherapy: 1/59-61
- silicon: 3/237-44
- Sjogren(s syndrome, parotid diseases: 2/101-9
- skin melanoma: Suppl 1/14-19
- skin neoplasms: Suppl 1/20-3; Suppl 1/27-34; Suppl 1/92-5; Suppl 1/103-5; Suppl 1/106-11
- skin neoplasms - diagnosis: Suppl 1/24-6
- skin neoplasms - diagnosis surgery: Suppl 1/86-91
- skin neoplasms - epidemiology - mortality: Suppl 1/1-13
- skin neoplasms - etiology: Suppl 1/69-74
- skin neoplasms - preventive and control: Suppl 1/80-5
- skin neoplasms - secondary - therapy: 4/291-6
- Slovenia: Suppl 1/14-9
- soft tissue sarcoma: 1/59-61
- splenomegaly, liver cirrhosis: 3/199-205
- squamous cell - diagnosis - therapy: Suppl 1/96-102
- subarachnoid haemorrhage - diagnosis: 4/275-82
- survival: Suppl 1/14-9
- technetium Tc 99m medronate: 1/23-6
- technology, radiologic: Suppl 2/13-23; Suppl 2/24-9; Suppl 2/30-8
- thoracic radiography - methods: 4/257-61
- thrombolytic therapy - methods: 1/1-8
- thyroid neoplasms - radiotherapy: 1/35-41
- thyroid neoplasms - ultrasonography: 3/179-87
- thyroid nodule - drug therapy: 3/179-87
- T - lymphocytes, cytotoxic: Suppl 1/64-8
- tomography, emission - computed: 2/111-7
- tomography, emission - computed, fluorine radioisotopes, F-18-FDG PET: 3/207-13
- tomography, x-ray computed: 4/275-82
- tomography, x-ray computed, electron - beam, enhancement: 3/199-205
- tomography, x-ray computed, Fourier analysis: 1/9-14
- treatment outcome: 2/127-36
- triazoles: 4/303-8
- tumor cells cultured - drug effects: 4/297-301
- ultrasound, quality assurance: Suppl 2/42-6
- ultrasound systems, technical requirements: Suppl 2/39-41
- ultraviolet rays - adverse effects: Suppl 1/69-74
- urokinase: 1/43-53
- utilization, cardiology, neurology, oncology: 2/111-7
- visual acuity: 1/55-8



FONDACIJA "DOCENT DR. J. CHOLEWA"
JE NEPROFITNO, NEINSTITUCIONALNO IN NESTRANKARSKO
ZDRUŽENJE POSAMEZNIKOV, USTANOV IN ORGANIZACIJ, KI ŽELIJO
MATERIALNO SPODBUJATI IN POGLABLJATI RAZISKOVALNO
DEJAVNOST V ONKOLOGIJI.

MESESNELOVA 9
1000 LJUBLJANA
TEL 061 15 91 277
FAKS 061 21 81 13

ŽR: 50100-620-133-05-1033115-214779



Activity of "Dr. J. Cholewa" Foundation for Cancer Research and Education - A Report for the Second Quarter of 1999

In the second quarter of 1999 the „Dr. J. Cholewa“ Foundation for cancer research and education continued with its activities, as already outlined in previous reports. The activity of the Foundation is slowly adapting itself to the summer recess. World-wide financial crisis left its impact on the willingness of the donors to contribute to the Foundation, and the need for the reassessment of the strategies concerning financial contributions from private and constitutional donors is therefore obvious, making the summer recess even more welcome.

Despite the problems mentioned in the first paragraph, the Foundation continues to support the regular publication of „Radiology and Oncology“ international scientific journal, and the regular publication of the „Challenge ESO Newsletter“, the newsletter of the European School of Oncology from Milan, Italy. Both medical journals mentioned are edited and published in Ljubljana, Slovenia. It is also worth mentioning the educational grants awarded to three oncologists for their training in foreign countries, as well as the support the Foundation granted to the Organising Committee of the 1st. Slovenian Congress of Surgery, held in the city of Maribor. All of this in addition to the grants and support mentioned before in the previous reports in „Radiology and Oncology“ journal.

In the plan for the activity of the Foundation submitted to the members of its Executive board seven major points were presented. As such, the proposal also constitutes a viable framework for the activity of the Foundation for years to come. Besides editorial activity mentioned above, the Foundation will additionally concentrate on bestowing educational and study grants for the research work in oncology. Some of this research and educational work will probably be carried out in the clinical and research facilities in Ljubljana. Contrary to the research and education performed abroad that will continue to be financed by the Foundation, this grants will be of shorter duration of one or two months, thus benefiting a larger number of applicants in a shorter period of time. The Foundation will also try to sponsor a larger number of educational meetings and congresses in Slovenia than until recently, especially those with oncology as the main subject. In addition to those mentioned above, special attention will continue to be given to the requests coming from the regions of Slovenia outside Ljubljana, and the Foundation will especially try to help in the process of choosing and financing the visits of renowned lecturers on such meetings. The Foundation will also continue to provide grants for the participation of Slovenian oncologists and others interested in this subject on various educational meetings organised by the European School of Oncology from Milan, Italy, thus enhancing the collaboration with this internationally recognised educational and research organisation.

The Foundation continues to pursue its stated goals, as outlined at the meetings of its Executive and Advisory Boards.

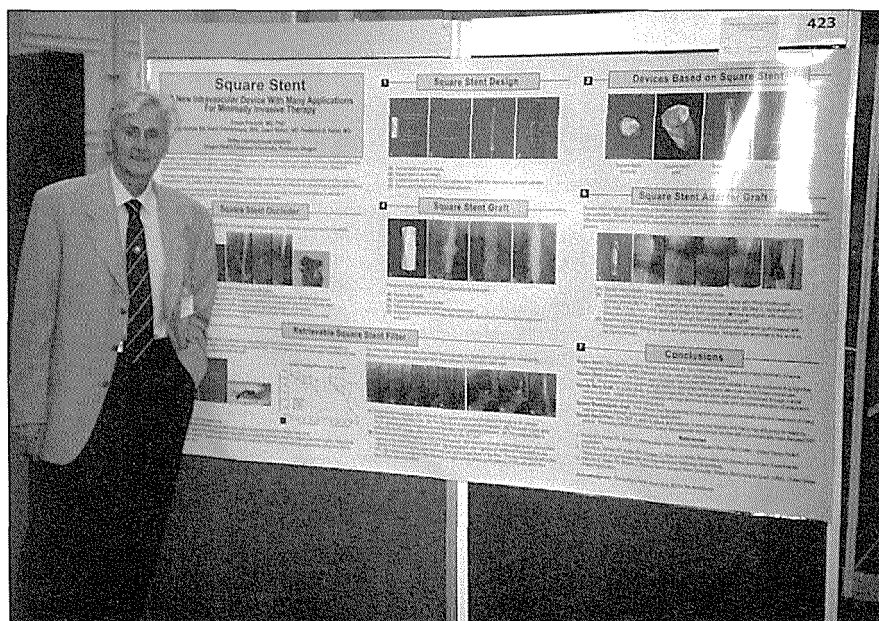
Borut Štabuc, MD, PhD
Andrej Plesničar, MD
Tomaž Benulič, MD

Former Institute of Radiology faculty member wins CIRSE award

Dr. Dušan Pavčnik, research professor at Dotter Interventional Institute, won First Prize in the 1999 Scientific Poster Competition during the Annual Meeting and post graduate Course of the Cardiovascular and Interventional Radiological Society of Europe. The meeting was held last September in Prague.

Dr. Pavčnik received the first prize for his research on Square Stent, A New Intravascular Device with Many Applications for Minimally Invasive Therapy, which basic idea was developed in Ljubljana in 1992.

Prof. Dušan Pavčnik served as interventional radiologist in the Institute of radiology at the Clinical Center Ljubljana until 1995, when he moved to Portland to continue contribution to the field of research in minimally invasive therapy.



Sporočamo, da je pri Tehniški založbi Slovenije izšel

NUKLEARNOMEDICINSKI SLOVAR

avtorja **prim. Janeza Šuštaršiča, dr. med.**

Cena: 3990 SIT

Naročite ga lahko:

- *po telefonu:* 061 17 902 11
- *po faksu:* 061 17 902 30
- *po pošti:* TZS, Lepi pot 6, 1000 Ljubljana
- *po elektronski pošti:* tzs-lj@siol.net

Več informacij o naših publikacijah boste našli na internet
knjigarni: <http://www.tehniska-zalozba.si>

Sporočamo, da je pri Tehniški založbi Slovenije
izšla knjiga avtorja:

prim. Janeza Šuštaršiča, dr.med

NUKLEARNA MEDICINA

Cena: 3560 SIT

Naročite jo lahko:

- *po telefonu:* 061 17 902 11
- *po faksu:* 061 17 902 30
- *po pošti:* TZS, Lepi pot 6, 1000 Ljubljana
- *po elektronski pošti:* tzs-lj@siol.net

Več informacij o naših publikacijah boste našli na internet
knjigarni: <http://www.tehniska-zalozba.si>



Diagnostics

Elecsys, Reaching New Heights



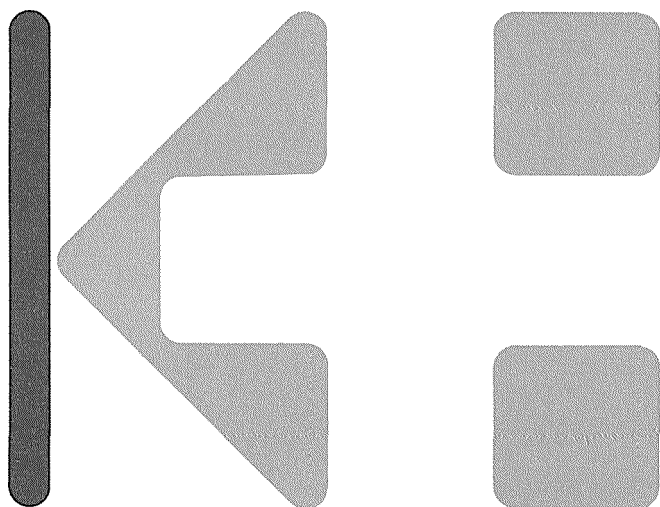
Roche and Boehringer Mannheim, two of the most experienced innovators in diagnostics, have joined forces to create a new, fully-integrated approach to health management worldwide.

There are no limits to innovation at Roche Diagnostics.

Roche Diagnostics
Info Office Ljubljana

Parmova 53
1000 Ljubljana
Slovenia

tel.: * 386 61 133 60 24
* 386 61 133 63 31
fax: * 386 61 130 92 02



KEMOFARMACIJA


Lekarne, bolnišnice, zdravstveni domovi in
veterinarske ustanove večino svojih
nakupov opravijo pri nas.

Uspeh našega poslovanja temelji na
kakovostni ponudbi, ki pokriva vsa
področja humane medicine in veterine, pa
tudi na hitrem in natančnem odzivu na
zahteve naših kupcev.

KEMOFARMACIJA – VAŠ ZANESLJIVI DOBAVITELJ!



Veletrgovina za oskrbo zdravstva, d.d. / 1000 Ljubljana, Cesta na Brdo 100
Telefon: 061 12-32-145 / Telefax: 271-588, 271-362



**Zdravljenje pomenopavzalnih bolnic z
napredovalo ali ponovljeno obliko raka dojk
je bolj uspešno z novim, selektivnim
zaviralcem aromataz:**

Arimidex
anastrozol

**bolnica vzame eno tableto enkrat dnevno
hitro zmanjšanje koncentracij estradiola
povečanje telesne teže ni izrazito
nadomeščanje steroidov ni potrebno
dobro prenašanje**

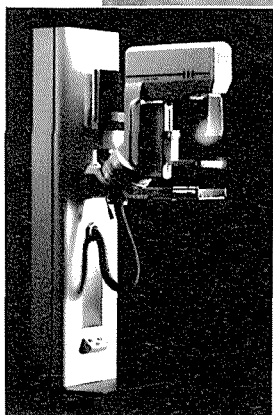
**Podrobnejše informacije
so na razpolago pri:**

ZENECA

**Zeneca International Ltd
Podružnica v Sloveniji
Einspielerjeva 6, Ljubljana
tel.: 061 136 97 13
061 136 24 71
faks: 061 136 97 02
el. pošta: zeneca@eunet.si**

SIEMENS

Rešitve po meri



Mammomat 3000 modular

- univerzalni sistem za vse vrste mamografije
- optimizacija doze in kompresije z OPDOSE in OPCOMP sistema
- modularna zgradba zagotavlja posodabljanje sistema
- servis v Sloveniji z zagotovljenimi rezervnimi deli in garancijo
- izobraževanje za uporabnike

SIEMENS d.o.o.
Dunajska 22
1511 Ljubljana
Telefon 061/1746 100
Telefaks 061/1746 135

A woman with blonde hair, wearing a white lab coat, is shown in profile, looking down at a control panel of a medical device. The panel is white with a black display screen and various buttons and knobs. The background is a solid blue color.

Think what you'd gain by giving
your radiologists a free hand.

Are your radiographers' hands tied by equipment that slows them down? And what can you do about it? Nearly 70% of X-rays are made at a Bucky. A fact that has influenced the design of Philips' Bucky systems. It's led to technology without gadgetry, for uncomplicated, speedy work. Control units operated one-handed.

A display that eliminates trips to the generator. Tomography functions activated via a single button. All to speed patient throughput, for improved cost-efficiency. It's one way in which Philips Medical Systems is working with you to meet today's changing healthcare needs. For more information call 061 177 88 50.

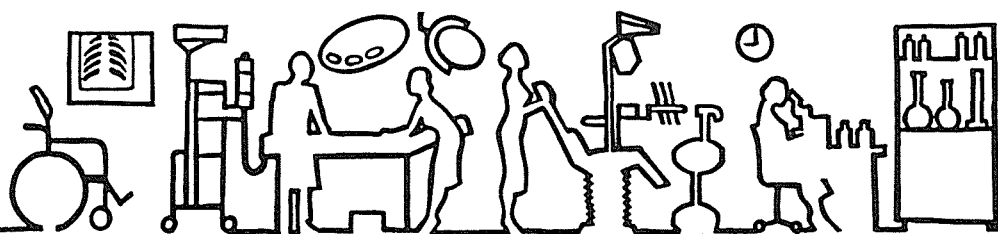
website: www.philips.com/ms



PHILIPS

Let's make things better.

SANOLABOR



Pri nas dobite vse za rentgen!

- KODAK • SIEMENS • GENERAL ELECTRIC •
- PHILIPS • BENNETT • HITACHI • POLAROID •
- XENOLITE • MAVIG • CAWO •

- rentgenski filmi in kemikalije
- kontrastna sredstva
- rentgenska zaščitna sredstva
- rentgenski aparati, aparati za ultrazvočno diagnostiko, stroji za avtomatsko razvijanje, negatoskopi in druga oprema za rentgen

SANOLABOR, Leskoškova 4, 1103 Ljubljana

Tel.: 061 185 42 11

Fax: 061 140 13 04

iflazon®

kapsule flukonazol

*v svetu največ predpisovani sistemski
antimikotik*

*edini peroralni sistemski antimikotik
za zdravljenje vaginalne kandidoze,
ki ga je odobril FDA*

Skrajšano navodilo

Flukonazol je sistemski antimikotik iz skupine triazolov.

Odmerjanje pri različnih indikacijah:

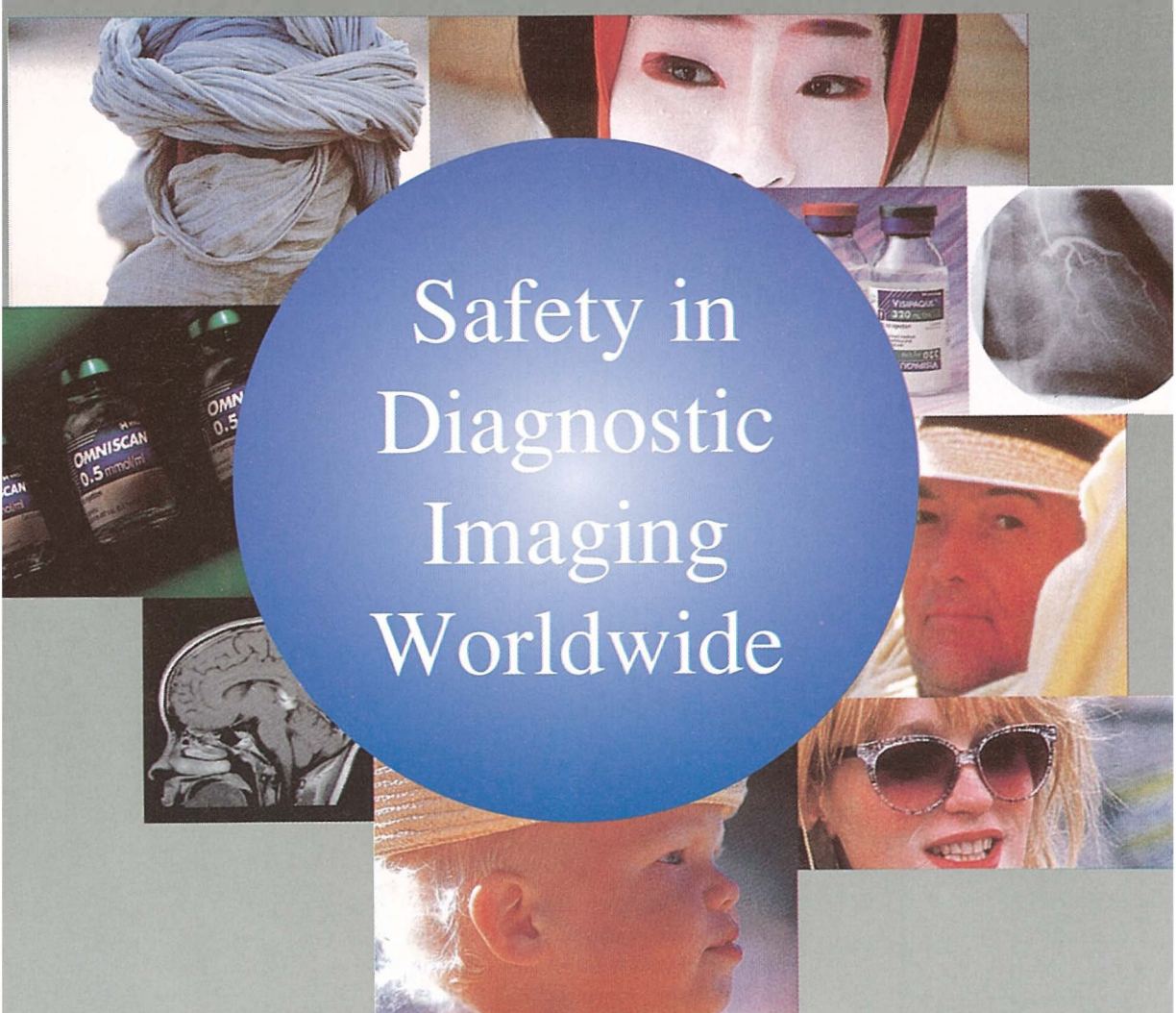
vaginalna kandidoza	150 mg v enkratnem odmerku
mukozna kandidoza	50 do 100 mg na dan
dermatomikoze	50 mg na dan ali 150 mg na teden
sistemska kandidoza	prvi dan 400 mg, nato od 200 do 400 mg na dan Največji dnevni odmerek je 800 mg.
preprečevanje kandidoze	50 do 400 mg na dan
kriptokokni meningitis	prvi dan 400 mg, nato od 200 do 400 mg na dan
vzdrževalno zdravljenje	200 mg na dan

Kontraindikacije: Preobčutljivost za zdravilo ali sestavine zdravila. **Interakcije:** Pri enkratnem odmerku flukonazola za zdravljenje vaginalne kandidoze klinično pomembnih interakcij ni. Pri večkratnih in večjih odmerkih so možne interakcije s terfenadinom, cisapridom, astemizolom, varfarinom, derivati sulfonilureje, hidroklortiazidom, fenitoinom, rifampicinom, ciklosporinom, teofilinom, indinavirom in midazolamom. **Nosečnost in dojenje:** Nosečnica lahko jemlje zdravilo le, če je korist zdravljenja za mater večja od tveganja za plod. Doječe matere naj med zdravljenjem s flukonazolom ne dojijo. **Stranski učinki:** Povezani so predvsem s prebavnim traktom: slabost, napenjanje, bolečine v trebuhu, driska; zelo redko se pojavijo preobčutljivostne kožne reakcije, anafilaksija in angioedem – v tem primeru takoj prenehamo jemati zdravilo. Pri bolnikih s hudimi glivičnimi obolenji lahko pride do levkopenije in trombocitopenije in do povečane aktivnosti jetrnih encimov. **Oprema in način izdajanja:** 7 kapsul po 50 mg, 28 kapsul po 100 mg, 1 kapsula po 150 mg. Na zdravniški recept. 1/99.

Podrobnejše informacije so na voljo pri proizvajalcu.



Krka, d. d. Novo mesto
Šmarješka cesta 6
8501 Novo mesto



Safety in Diagnostic Imaging Worldwide

*Nycomed Imaging is proud
of its role in providing
for the early, accurate
diagnosis of disease,
thus improving patients'
quality of life and
prospect for effective
treatment. The company is
committed to the continuous
development of innovative
imaging product to enhance
diagnostic procedures.*

ZASTOPA
HIGIEA d.o.o., Trzin
tel.: (061) 1897 225
fax: (061) 1897 226

Nycomed
Amersham

DISTRIBUCIJA
SALUS d.d. Ljubljana
tel.: (061) 1899 100
fax: (061) 1681 420

LABORMED

laboratory & medical equipment

LABORMED d.o.o. · SLO-1215 Medvode · Zg. Pirniče 96/c
Telefon 061 / 621 098 · Telefax 061 / 621 415

Labormed v Sloveniji ekskluzivno zastopa naslednje firme:

KÖTTERMANN

laboratorijsko pohištvo, varnostne omare za kisline, luge, topila, pline in strupe, ventilacijska tehnika in digestoriji

EHRET

laminar flow tehnika, inkubatorji, sušilniki, suhi sterilizatorji in oprema za laboratorijsko vzrejo živali - kletke

DAKO

testi za aplikacijo v imunohistokemiji, patologiji, mikrobiologiji, virologiji, mono- in poliklonalna protitelesa...

GFL

laboratorijski aparati, omare in skrinje za globoko zamrzovanje

ROSYS ANTHOS

fotometri, avtomatski pralni sistem za mikrotitrne plošče

CHARLES ISCHI Pharma-Prüftechnik

specialna oprema za testiranje izdelkov v farmacevtski industriji; aparati za procesno kontrolo in kontrolo kvalitete

NOVODIRECT BIOBLOCK

kompletna oprema in pripomočki za delo v laboratoriju

ANGELANTONI SCIENTIFICA

hladilna tehnika in aparati za laboratorije, transfuziologijo, patologijo in sodno medicino

INTEGRA BIOSCIENCES

laboratorijska oprema za mikrobiologijo, biologijo celic, molekularno biologijo in biotehnologijo

CORNINGCostar

specialna laboratorijska plastika za aplikacijo v imunologiji, mikrobiologiji, virologiji, ipd., mehanske eno- in večkanalne pipete ter nastavki

BIOMERICA

hitri testi za diagnostiko, EIA / RIA testi

Advanced BIOTECHNOLOGIES

PCR tehnologija, potrošni material, reagenti, encimi

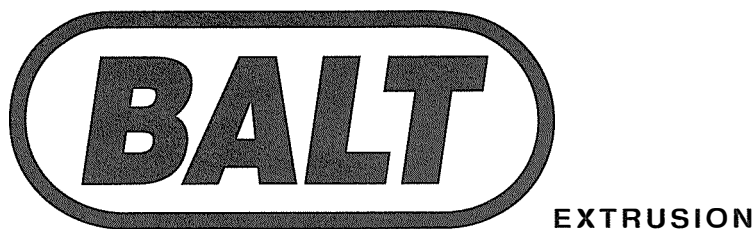
SVANOVA Biotech

Elisa testi za diagnostiko v veterini

HÜRNER

ventilacijska tehnika

ARROW®
INTERNATIONAL INC.



DISTRIBUTED
BY
SIRION s.r.l.
34170 GORIZIA - ITALY
Corso Italia 112
Tel. (0481) 32073-32074
Fax. (0481) 534753

Instructions for authors

Editorial policy of the journal *Radiology and Oncology* is to publish original scientific papers, professional papers, review articles, case reports and varia (editorials, reviews, short communications, professional information, book reviews, letters, etc.) pertinent to diagnostic and interventional radiology, computerized tomography, magnetic resonance, ultrasound, nuclear medicine, radiotherapy, clinical and experimental oncology, radiobiology, radiophysics and radiation protection. The Editorial Board requires that the paper has not been published or submitted for publication elsewhere: the authors are responsible for all statements in their papers. Accepted articles become the property of the journal and therefore cannot be published elsewhere without written permission from the editorial board. Papers concerning the work on humans, must comply with the principles of the declaration of Helsinki (1964). The approval of the ethical committee must then be stated on the manuscript. Papers with questionable justification will be rejected.

Manuscript written in English should be submitted to the Editorial Office in triplicate (the original and two copies), including the illustrations: *Radiology and Oncology*, Institute of Oncology, Vrazov trg 4, SI-1000 Ljubljana, Slovenia; (Phone: +386 61 132 00 68, Tel./Fax: +386 61 133 74 10, E-mail: gsera@onko-i.si). Authors are also asked to submit their manuscripts on a 3.5" 1.44 Mb formatted diskette. The type of computer and word-processing package should be specified (Word for Windows is preferred).

All articles are subjected to editorial review and review by independent referee selected by the editorial board. Manuscripts which do not comply with the technical requirements stated

herein will be returned to the authors for correction before peer-review. Rejected manuscripts are generally returned to authors, however, the journal cannot be held responsible for their loss. The editorial board reserves the right to ask authors to make appropriate changes in the contents as well as grammatical and stylistic corrections when necessary. The expenses of additional editorial work and requests for reprints will be charged to the authors.

General instructions • Radiology and Oncology will consider manuscripts prepared according to the Vancouver Agreement (*N Engl J Med* 1991; **324**: 424-8, *BMJ* 1991; **302**: 6772; *JAMA* 1997; **277**: 927-34.). Type the manuscript double spaced on one side with a 4 cm margin at the top and left hand side of the sheet. Write the paper in grammatically and stylistically correct language. Avoid abbreviations unless previously explained. The technical data should conform to the SI system. The manuscript, including the references may not exceed 15 typewritten pages, and the number of figures and tables is limited to 4. If appropriate, organize the text so that it includes: Introduction, Material and methods, Results and Discussion. Exceptionally, the results and discussion can be combined in a single section. Start each section on a new page, and number each page consecutively with Arabic numerals.

Title page should include a concise and informative title, followed by the full name(s) of the author(s); the institutional affiliation of each author; the name and address of the corresponding author (including telephone, fax and e-mail), and an abbreviated title. This should be followed by the *abstract page*, summarising in less than 200 words the reasons for

the study, experimental approach, the major findings (with specific data if possible), and the principal conclusions, and providing 3-6 key words for indexing purposes. Structured abstracts are preferred. If possible, the authors are requested to submit also slovenian version of the title and abstract. The text of the report should then proceed as follows:

Introduction should state the purpose of the article and summarize the rationale for the study or observation, citing only the essential references and stating the aim of the study.

Material and methods should provide enough information to enable experiments to be repeated. New methods should be described in detail. Reports on human and animal subjects should include a statement that ethical approval of the study was obtained.

Results should be presented clearly and concisely without repeating the data in the tables and figures. Emphasis should be on clear and precise presentation of results and their significance in relation to the aim of the investigation.

Discussion should explain the results rather than simply repeating them and interpret their significance and draw conclusions. It should review the results of the study in the light of previously published work.

Illustrations and tables must be numbered and referred to in the text, with appropriate location indicated in the text margin. Illustrations must be labelled on the back with the author's name, figure number and orientation, and should be accompanied by a descriptive legend on a separate page. Line drawings should be supplied in a form suitable for high-quality reproduction. Photographs should be glossy prints of high quality with as much contrast as the subject allows. They should be cropped as close as possible to the area of interest. In photographs mask the identities of the patients. Tables should be typed double spaced, with descriptive title and, if appropriate, units of numerical measurements included in column heading.

References must be numbered in the order in which they appear in the text and their corresponding numbers quoted in the text. Authors are responsible for the accuracy of their references. References to the Abstracts and Letters to the Editor must be identified as such. Citation of papers in preparation, or submitted for publication, unpublished observations, and personal communications should not be included in the reference list. If essential, such material may be incorporated in the appropriate place in the text. References follow the style of Index Medicus. All authors should be listed when their number does not exceed six; when there are seven or more authors, the first six listed are followed by "et al.". The following are some examples of references from articles, books and book chapters:

Dent RAG, Cole P. *In vitro* maturation of monocytes in squamous carcinoma of the lung. *Br J Cancer* 1981; 43: 486-95.

Chapman S, Nakielny R. *A guide to radiological procedures*. London: Bailliere Tindall; 1986.

Evans R, Alexander P. Mechanisms of extracellular killing of nucleated mammalian cells by macrophages. In: Nelson DS, editor. *Immunobiology of macrophage*. New York: Academic Press; 1976. p. 45-74.

Page proofs will be faxed to the corresponding author whenever possible. It is their responsibility to check the proofs carefully and fax a list of essential corrections to the editorial office within 48 hours of receipt. If corrections are not received by the stated deadline, proof-reading will be carried out by the editors.

Reprints: Fifty reprints are free of charge, for more contact editorial board.

For reprint information in North America Contact:
International Reprint Corporation 968 Admiral Callaghan Lane, # 268 P.O. Box 12004, Vallejo; CA 94590, Tel: (707) 553 92 30, Fax: (707) 552 95 24.

Za mirno potovanje skozi kemoterapijo

Navoban
tropisetron

- preprečevanje slabosti in bruhanja pri emetogeni kemoterapiji
- učinkovito zdravilo, ki ga odrasli in otroci dobro prenašajo
- vedno 1-krat na dan
- vedno 5 mg

Skrajšano navodilo za uporabo: Navoban® kapsule, Navoban® raztopina za injiciranje 2 mg in 5 mg. Serotoninski antagonist. **Oblika in sestava:** 1 trda kapsula vsebuje 5 mg tropisetronovega hidroklorida. 1 ampula po 2 ml vsebuje 2 mg tropisetronovega hidroklorida. 1 ampula po 5 ml vsebuje 5 mg tropisetronovega hidroklorida. **Indikacije:** Preprečevanje slabosti in bruhanja, ki sta posledici zdravljenja s citostatiki. Zdravljenje pooperativne slabosti in bruhanja. Preprečevanje pooperativne slabosti in bruhanja pri bolnicah, pri katerih je načrtovana ginekološka operacija v trebušni votlini. **Odmerjanje in uporaba:** Preprečevanje slabosti in bruhanja, ki sta posledici zdravljenja s citostatiki. **Odmerjanje pri otrocih:** Otroci starejši od 2 let 0,2 mg/kg telesne mase na dan. Največji dnevni odmerek ne sme preseči 5 mg. Prvi dan kot intravenska infuzija ali kot počasna intravenska injekcija. Od 2. do 6. dne naj otrok jemlje zdravilo oralno (raztopino v ampuli razredčimo s pomarančnim sokom ali koka kolo). **Odmerjanje pri odraslih:** 6-dnevna kura po 5 mg na dan. Prvi dan kot intravenska infuzija ali počasna intravenska injekcija. Od 2. do 6. dne 1 kapsula na dan. **Zdravljenje in preprečevanje pooperativne slabosti in bruhanja:** **Odmerjanje pri odraslih:** 2 mg Navobana z intravensko infuzijo ali kot počasna injekcija. Glej celotno navodilo! **Kontraindikacije:** Preobčutljivost za tropisetron, druge antagoniste receptorjev 5-HT₃ ali katerokoli sestavino zdravila. Navobana ne smemo dajati nosečnicam; izjema je preprečevanje pooperativne slabosti in bruhanja pri kirurških posegih, katerih del je tudi terapevtska prekinitev nosečnosti. **Previdnostni ukrepi:** Bolniki z nenadzorovano hipertenzijo; bolniki s prevodnimi ali drugimi motnjami srčnega ritma; ženske, ki dojijo; bolniki, ki upravljajo s stroji ali vozili. **Medsebojno delovanje zdravil:** Rifampicin ali druga zdravila, ki inducirajo jetrne encime. Glej celotno navodilo! **Stranski učinki:** Glavobol, zaprtje, redkeje omotica, utrujenost in prebavne motnje (bolečine v trebuhu in driska), preobčutljivostne reakcije. Zelo redko kolaps, sinkopa ali zastoj srca, vendar vzročna zveza z Navobanom ni bila dokazana. **Način izdajanja:** Kapsule: uporaba samo v bolnišnicah, izjemoma se izdaja na zdravniški recept pri nadaljevanju zdravljenja na domu ob odpustu iz bolnišnice in nadaljnjem zdravljenju. Ampule: uporaba samo v bolnišnicah. **Oprema in odločba:** Zloženska s 5 kapsulami po 5 mg; številka odločbe 512/B-773/97 z dne 10. 11. 1997. Zloženska z 1 ampulo po 2 ml (2 mg/2 ml); številka odločbe 512/B-772/97 z dne 10. 11. 1997. Zloženska z 10 ampulami po 5 ml (5 mg/5 ml); številka odločbe 512/B-771/97 z dne 10. 11. 1997. **Izdovalec:** NOVARTIS PHARMA AG, Basel, Švica. **Imetnik dovoljenja za promet z zdravilom:** NOVARTIS PHARMA SERVICES INC., Podružnica v Sloveniji, Dunajska 22, 1511 Ljubljana, kjer so na voljo informacije in literatura. **Preden predpišete Navoban, prosimo preberite celotno navodilo.**

 **NOVARTIS**

